Friction modeling for dynamic system simulation

Ej Berger

Friction modeling for dynamic system simulation

EJ Berger

CAE Laboratory, Department of Mechanical, Industrial, and Nuclear Engineering,
University of Cincinnati, PO Box 210072, Cincinnati, OH 45221-0072; ed.berger@uc.edu

Friction is a very complicated phenomenon arising at the contact of surfaces. Experiments indicate a functional dependence upon a large variety of parameters, including sliding speed, acceleration, critical sliding distance, temperature, normal load, humidity, surface preparation, and, of course, material combination. In many engineering applications, the success of models in predicting experimental results remains strongly sensitive to the friction model. Further-more, a broad cross section of engineering and science disciplines have developed interesting ways of representing friction, with models originating from the fundamental mechanics areas, the system dynamics and controls fields, as well as many others. A fundamental unresolved question in system simulation remains: what is the most appropriate way to include friction in an analytical or numerical model, and what are the implications of friction model choice? This review article draws upon the vast body of literature from many diverse engineering fields and critically examines the use of various friction models under different circumstances. Special focus is given to specific topics: lumped-parameter system models (usually of low order)—use of various types of parameter dependence of friction; continuum system models—continuous interface models and their discretization; self-excited system response—steady-sliding stability, stick/slip, and friction model requirements; and forced system response—stick/slip, partial slip, and friction model requirements. The conclusion from this broad survey is that *the system model and friction model are fundamentally coupled*, and they cannot be chosen indepen-dently. Furthermore, the usefulness of friction model and the success of the system dynamic model rely strongly on each other. Across disciplines, it is clear that multi-scale effects can dominate performance of friction contacts, and as a result more research is needed into com-putational tools and approaches capable of resolving the diverse length scales present in many practical problems. There are 196 references cited in this review-article.

1 INTRODUCTION

1.1 Motivation

Friction plays a central, controlling role in a rich variety of physical systems, and as such has been the topic of focused research for more than 500 years. Indeed, the fundamental experiments of Coulomb [1] have evolved into very sophisticated surface and interface characterization techniques seen today. In parallel to the experimental efforts, friction models—both phenomenological and empirical—have emerged to provide predictive capabilities and design tools. However, far too frequently the predicted performance of a system dynamic model is undermined by an inappropriate friction model, or the accuracy of the friction model is limited by the system dynamic model. This can occur in a number of ways; for example, the friction literature is replete with examples of *velocity-dependent friction models*, and clearly single-coefficient friction models cannot account for this parameter dependence. As a result, predictions of friction using a *correct* dynamic model but highly simplified friction will be of limited value. On the other hand, consider a friction model which accurately captures the interface shear behavior of two components. If the system dynamic model does not have the ability to represent variations in, say, normal force, then once again the performance predictions for the system, despite the correctness of the friction model, will be of limited value. This strong coupling must be carefully considered when building a system model, but how can the best combination of friction and dynamic model be defined? What are the modeling choices available for friction? What are their strengths and limitations? What are the implications on computations and what are the likely computational obstacles?

For the moment, it suffices to say that much of the confusion and controversy in friction modeling is attributable to the diversity of friction-related problems, and in order to understand friction modeling more completely it will be necessary to examine some typical problems from each of the areas described above. Friction modeling and simulation are important tools across a wide variety of engineering disci-

plines: contact mechanics, system dynamics and controls, aeromechanics, geomechanics, fracture and fatigue, structural dynamics, and many others. Each of these areas possesses its own view of friction and its importance. In addition, the required degree of sophistication for friction models varies widely across these areas, and the reason for this is related to the nature of the problems themselves. For cases in which the sensitivity of the solution to changes in the friction model is small, the friction models are rightly considered in their simplest form. On the other hand, much more sophisticated models are required in other resesarch areas. Finally, within each broad category defined above, there exist specific problems for which friction modeling is critical, and some of these problems will be explored throughout this review.

This paper reviews the literature on friction modeling for dynamic systems across a wide range of engineering and science disciplines. Here we focus strictly on sliding contact; see the book by Kalker [2] for a discussion of rolling contact issues. The intent is to present the full variety of viewpoints, to identify their commonalities, and to appreciate their differences. As such, a complete bibliographic survey of the full literature is not presented; rather, literature representative of the variety of applications and relevant problems is cited. In addition, a key point which is explored in detail in this paper is the relationships between system dynamic parameters and friction description. Developing an appropriate and ultimately useful system model—including sufficient levels of detail in both the dynamic and friction models—remains a very difficult task. This paper aims to present researchers across disciplines with a better understanding of the available modeling tools and techniques, along with some insight about each, so that they can make informed decisions in friction and system dynamic modeling.

This paper is distinct from other recent reviews in the literature. Ibrahim [3,4] examines the literature and presents a thorough bibliographic survey which emphasizes mechanics of contact and parameter dependence of friction [3], as well as important nonlinear dynamics problems and their modeling tools [4]. There is also a related web site at:

http://www.mi.uni-koeln.de/mi/Forschung/Kuepper/English/friction.html.

Ferri [5] examines the literature related to friction damping, focusing on nominally-stationary contacts such as joints, stranded cables, and various passive damping treatments. Feeny, Guran, Hinrichs, and Popp [6] present a historical review of the evolution of friction research from antiquity forward. Back, Burdekin, and Cowley [7] describe relevant research for the machine tool industry, including implications of joint stiffness, damping, and wear, and their relationship to friction. Beards has frequently updated his review of passive damping mechanisms for built-up structures (eg, [8]). Previously Goodman [9] and then Ungar [10] both examined joint slip damping in structures. Each of these articles presents valuable information about friction modeling. This review distinguishes itself from those mentioned above by critically examining the friction models available across a wide variety of engineering disciplines, and drawing specific conclusions about their similarities and differences, including multiple length scale effects and their implications on friction system simulation.

Table 1. Notation used throughout this article for various system parameters and friction features. Variables are illustrated schematically in Fig. 1.

Feature	Notation
relative velocity	V_{rel}
contact normal load	F_n
contact friction force	F_f
applied normal load	F_p
applied tangential load	F_q
velocity dependence	$g(v)$
memory dependence	time lag: Δt
	critical slip distance: d_c
multi-valued sticking friction	$F_f \leqslant F_s$
time-dependent sticking friction	$F_s = F_s(t; t_\infty, \gamma)$
pre-slip displacement	x_{pre}, k_t

1.2 Experimental observations and preliminary discussion

This section links key experimental observations of friction to a general framework of notation that will be used consistently throughout this article. The notation used here may depart somewhat from that used by the original authors of the references cited, but a unified notation will help highlight similarities and differences in approaches across disciplines. Where appropriate, specific notations will be introduced and defined as we examine unique features within the literature.

Key experimental observations that will be examined in more detail over the following sections are:

- velocity dependence of friction
- memory dependence, time lag, or critical slip displacement of friction response
- multi-valued friction at zero relative velocity
- dwell time dependence of static friction
- pre-slip displacement

The mathematical descriptions of these phenomena are summarized in Table 1, and a consistent approach is taken here to define the friction constitutive behavior as follows for discrete contacts:

$$F_f = \mu F_n \tag{1}$$

or for continuous contacts:

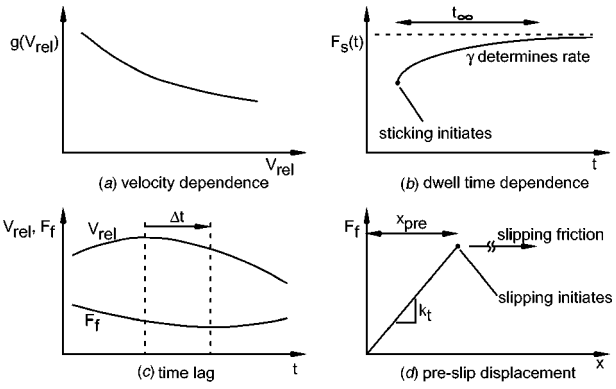

Fig. 1 Notation for parameter-dependent friction: *a*) velocity dependence, *b*) dwell time dependence, *c*) time lag, *d*) pre-slip displacement

Table 2. Common friction-related problems, analysis methods, and friction models

Engineering Field	Relevant Analysis	Typical Friction Model
contact mechanics	quasi-static sliding	$\tau_f = \mu\sigma_n$ + partial slip
dynamics and controls	steady-sliding stability	$\mu = \mu(V_{\text{rel}})$
aeromechanics	forced response of frictionally-damped structures	$F_f = \mu F_n$ + partial slip
geomechanics	steady-sliding stability	$\tau_f = \tau_f(V_{\text{rel}}, \theta_1, \theta_2, \ldots)$
fracture and fatigue	forced response of frictionally-damped structures	$\tau_f = \mu\sigma_n$ + partial slip
structural dynamics	forced response and energy dissipation (joints)	$F_f = \mu F_n$ + partial slip

$$\tau_f = \mu\sigma_n \tag{2}$$

where τ_f is the friction shear traction and σ_n is the contact stress normal to the surface. The general parameter dependence of friction is captured via variations in coefficient μ or changes in contact force/stress.

The notations shown in Table 1 are demonstrated in the diagrams of Fig. 1, and the key variables are defined. Parts a, b, c, and d of the figure indicate the velocity dependence, dwell time dependence, time lag, and pre-slip displacement of friction, respectively. There are clearly a number of important parameters to identify for accurate friction simulations, and we will see throughout this article that these friction modeling parameters operate in concert with system dynamic parameters to govern the overall behavior of the system.

2 FRICTION AND DYNAMICS MODELS ACROSS ENGINEERING AND SCIENCE DISCIPLINES

The friction-related literature consists of somewhat disjointed contributions spanning many important engineering fields. Friction plays an important role in each of the problems listed in Table 2, where the notation has been described previously, and *partial slip* problems are clearly defined and given special attention in Section 2.6.2. Note the broad distinctions drawn out in the table. There are two broad approaches to friction interface modeling: continuous (mechanics-type problems) and discrete (dynamics and control problems). There are three classes of parameter dependence: none (quasi-static problems), velocity dependence (steady-sliding and forced response problems), and general rate and state dependence (steady-sliding stability problems). There are two classes of contact: point contact (dynamics and control, some geomechanics problems) and distributed contact (including partial interfacial slip). With so many choices in modeling procedures, and so many possible foci of friction and system dynamic analysis, the selection of appropriate models can be difficult.

2.1 Preview

Across the literature presented in this section, several important themes will be explored:

- Appropriate tuning between friction parameters and system dynamic parameters can result in undesirable system behavior, including a variety of self-excited instabilities.
- Highly localized details of contact interactions often dictate component performance, efficiency, or durability; the relevant contact length scale is often much smaller than the relevant structural length scale.
- Both of these observations have important implications on friction and system dynamic modeling, including coupled structure-interface problem formulation, analytical tractability, appropriate discretization approaches, or efficient numerical solution.

The remainder of this section examines some of the literature across a variety of engineering and science fields, with an emphasis on the diversity of applications for which careful consideration of friction and system dynamic modeling is important. Some rigor and detail of individual research efforts is neglected in favor of a more global view supportive of the three items listed above.

2.2 Friction and system dynamics

In order to develop a meaningful understanding of friction experiments, and to predict dynamic system response and performance, a robust friction model must be employed. As such, parameter dependence of friction becomes an important issue, and a large number of researchers have investigated friction from a variety of viewpoints. In this section, friction experiments and models typically used for dynamic systems are introduced and reviewed.

Two key ideas have emerged over the past half century concerning the nature of system dynamics and friction, and they are: i) system dynamics can have a profound influence on friction measurements, and ii) normal-tangential coupling effects play an important role in friction oscillations. Indeed, in many engineering applications, we find that the synergy of the system dynamics and interface friction dominates system performance, as in brake squeal for example. An unfavorable combination of dynamics and friction behavior results in noise generation, consumer dissatisfaction, increased warranty costs, etc. Furthermore, because of a variety of weight and packaging constraints, alterations to the system dynamics (using very thick brake rotors, for example) are often not feasible. So the design of the dynamic system must explicitly include consideration of friction, and a goal of designers is always to tune the system dynamics to minimize the impact of friction; as consideration of the substantial literature in this area shows, this design task is usually easier said than done.

2.2.1 Role of velocity and acceleration

Early work considering the role of dynamics in friction contacts includes Sampson, Morgan, Reed, and Muskat [11] and also Rabinowicz [12], both of which observed not only velocity dependence of friction, but also apparent acceleration dependence. These two works in particular highlight an early appreciation for the complicated nature of dynamic interface

contact. A key observation in both cases, and one which has gone on to be perhaps the most celebrated and oft-cited culprit in friction-excited vibrations, is the negative slope of the friction-velocity curve. Alternately referred to as *rate weakening*, this condition is illustrated schematically in Fig. 1*a* and expressed mathematically as:

$$\frac{\partial g(V_{\text{rel}})}{\partial V_{\text{rel}}} < 0 \tag{3}$$

It will be shown in subsequent sections how this negative friction curve slope manifests itself in dynamic systems as a negative viscous damping term, which has a destabilizing effect. The difference between the accelerating and decelerating branches of the friction-velocity curve allowed Rabinowicz [12] to first assert the idea of memory-dependent friction, in which a time lag Δt of friction response is observed. He proposed the physical mechanism that only after sliding a critical distance d_c would friction evolve to its *steady-state* value at that particular system sliding speed. He suggested that this critical length was on the scale of the asperity spacing on the surfaces, perhaps 10 μm or slightly more. This idea then suggests that memory effects will be more pronounced during rapid changes in system state than for quasi-static state changes, because rapid state changes do not allow for stabilization of friction force and quasi-static state changes do. As a result, the instantaneous slope of the friction curve from Eq. (3) is actually a *multi-valued* function which depends upon the previous sliding history. This is precisely the experimental finding of a number of other researchers [11,13,14]. A simple time-lag model can be proposed as:

$$F_f(\dot{x}(t);\Delta t) = F_f(\dot{x}(t-\Delta t)) \tag{4}$$

where Δt is the characteristic time lag in the system, and is in general an empirically-determined parameter. Hess and Soom [14] measure this time lag for a variety of load and lubricant combinations, and find $\Delta t \approx 3-9$ ms, which over the sliding velocities they investigate (near zero to about 0.5 m/s) translates into a length scale d_c ranging from 30–4500 μm. In order for Rabinowicz's critical *length* scale related to asperity spacing to come into play here, it seems that the sliding velocity must be small. And it should be recognized that there are a variety of lubrication-related effects contributing to the observations of Hess and Soom which may not be fully explained by the critical length scale or time scale argument. For example, viscous friction increases linearly with sliding velocity, even for fairly thin films, and the contribution of hydrodynamic effects may play a role here. However, their basic conclusion is supportive of Rabinowicz' observations, that a time lag or critical slip distance is responsible for multi-valued sliding friction.

Hunt, Torbe, and Spencer [15] performed detailed experiments on steady sliding of machine tools and concluded that velocity dependence of friction alone could not account for all observed effects; they used phase plane tools to examine the experimental results. A 1-dof dynamic model is used to support the analysis and aid interpretation of the experimental results. Pavelescu and Tudor [16] present an informative history of the friction coefficient, tracing its development from the origins of scientific investigation (da Vinci, Amontons, Coulomb) through its use for non-dry and three-body contacts (thin films, boundary lubrication, EHL). Both mechanics and empirical models are presented, as are connections to wear, stick-slip, and other interface phenomena. Energy approaches are cited as well. Lin and Wang [17] use a drill string application as a candidate system for stick-slip vibration analysis. Modeled as a single-dof torsional pendulum, the drill string dynamic response is shown to be sensitive to torsional natural frequency, driving velocity, and torsional (viscous) damping. The friction is modeled as an exponential function of sliding velocity. A parameter study indicates the existence of a critical natural frequency above which stick-slip is precluded. An interesting connection to observations of a beating phenomena in real drill strings is proposed, although the explanation of beating as a stick-slip response was not conclusively validated. The central impact of these works relates to the observations of sophisticated velocity and acceleration dependence of friction, and in fact in a variety of applications tuning between friction parameters and system dynamics parameters provides insight about overall system performance.

Popp [18] reviews some model problems for stick-slip oscillations and chaotic response in dry sliding. He uses four different friction laws with four different system dynamic models (two discrete and two continuous), and reports on the nonlinear response and bifurcation behavior under various operating conditions. In addition, Bengisu and Akay [19,20] describe friction-induced vibrations in multiple-dof systems, described by a linear structural model and a nonlinear friction force input at only one of the lumped masses. In addition to a stability analysis for steady sliding, a bifurcation process is described for changes in friction curve slope at the steady-sliding equilibrium point. The total number of bifurcations observed is equal to the number of dofs in the problem, and as each bifurcation is passed the system response becomes more dynamically rich and includes more fundamental frequencies. The conclusion is that even (structurally) linear systems can demonstrate a nonlinear response due to the nonlinear friction force.

de Velde and Baets [21] develop a mathematical and computational approach for exploring existence of stick-slip response under *decelerative* motion. This is one of the very few articles in the literature which considers non-constant reference velocity, and their results indicate that stick-slip can occur under deceleration for systems which exhibit no stick-slip under steady sliding. Furthermore, a (numerical) parameter study of the single-dof dynamic model indicates that stick-slip under deceleration is only possible for a *sufficiently high system stiffness*, a conclusion in stark contrast to other work which finds quite the opposite ([22], for example). The difference is the deceleration, and in particular inertial forces play an important role in the overall force balance. Also, in the presence of a very large negative friction curve slope, increasing system damping actually has a destabilizing effect and can induce stick-slip.

Lim and Chen [23] describe the results of a numerical

investigation of stick-slip behavior in a single-dof system with state-dependent friction. They explore the roles of system stiffness and driving velocity on existence of stick-slip, and the phase plane results compare favorably with analytical predictions put forth by Rice and colleagues [24,25] across a wide velocity range. The model captures both creep (low velocity) and inertia (high velocity) dominated response, and the transition across the two response regimes is characterized by either a Hopf bifurcation (as stiffness increases) or an inverted Hopf bifurcation (as velocity increases).

2.2.2 *Role of normal-tangential-angular coupling*

In addition to velocity/acceleration-dependent friction, coupling in the system dynamics has been examined as a contributor to friction-related problems such as steady-sliding instability or stick-slip oscillations. The first profound impact in this area was made by Tolstoi [26], who completed delicate experiments which measured both the in-plane (tangential) motion as well as the out-of-plane (normal) motion of a slider against a countersurface. He constructed a test rig to determine the influence of small normal vibrations (including impacts) upon break-away behavior. He noticed two key points: i) tangential slip events were invariably accompanied by simultaneous upward normal motion, and ii) a normal contact resonance condition could be observed under which apparent friction was reduced. The argument here is that in order for friction to change, the real area of contact must change, and therefore the mean normal separation of the surfaces must also change.[1] Nayak [28] and Gray and Johnson [29] have also studied contact normal vibration problems from both analytical [Nayak] and experimental [Gray and Johnson] points of view. In particular, Gray and Johnson examine the effects of surface roughness on normal vibrations in rolling contact.

One of the early efforts in this area, about the same time as Tolstoi, is the work of Godfrey [30], who demonstrates an apparent friction reduction due to normal vibrations. The idea is similar to Tolstoi's: normal vibrations influence the mean surface separation, and therefore the real area of contact. With the measured frictional shear being a function of real contact area, there is an apparent reduction in friction force with normal vibration. This was experimentally verified with contact resistance measurements as well, and implications on wear are also considered. This work reinforces the close connection between friction measurements and out-of-plane system dynamics.

Antoniou, Cameron, and Gentle [31] used a simple dynamic model along with a reverse Lienard's construction to develop a bifurcating friction description for stick-slip data. They conclude that a fundamentally important event is the *triggering* oscillation, a normal vibration which signals the onset of a friction jump from one branch to the other of the characteristic curve. Both their experimental and analytical work further support the role of the normal dof. Sakamoto [32] used a pin-on-disk configuration to carefully examine normal separation effects in sliding contacts; he emphasizes the *slip portion only* of the stick-slip cycle. Clockwise friction-velocity loops are observed, and the variation in friction is interpreted as a change in the real area of contact during sliding (as inferred from contact resistance measurements).

Bo and Pavelescu [33] propose a two-exponential-curve model for sliding friction, one for accelerating motion and the other for deceleration. Each branch of the model is a function only of sliding velocity. They further report the results of experiments under oscillating sliding velocity that mean normal separation increases during acceleration and decreases during deceleration. Simplified friction equations for the two branches are developed and used to approximately solve (via the method of slowly varying parameters) for the system motion during the slip phase of a stick-slip cycle. Further, D'Souza and Dweib [34,35] show that normal-tangential coupling plays an important role in self-excited oscillations, and that increasing frequency *mistuning* between normal and torsional modes helps suppress self-excited system response.

The work of Soom and colleagues has recently contributed significantly to our understanding of system dynamics (and specifically the role of out-of-plane response) in friction contact. This group [36–38] examined roughness-induced normal vibrations in a pin-on-disk friction test. The earlier work uses frequency-domain tools to examine friction and normal force variations in time. One important conclusion is that the transfer function between normal and friction force is independent of frequency (a scalar with value roughly 0.33 for the results reported), and the forces essentially respond in phase. Moreover, peaks in the frequency spectra are observed near the normal contact resonance. The later work uses simulation tools and a simple, 2–dof dynamic system to investigate the effect of surface texture on normal vibrations. The result is that the effect of small surface features can be amplified by the normal contact resonance, resulting in relatively large fluctuations in normal force (including potential loss of contact) during start-up. Soom and Chen [39] perform a similar analysis for steady-sliding conditions with a Hertzian contact and nonlinear contact stiffness.

Polycarpou and Soom [40,41] demonstrate, in this two-part paper, that low-order linear dynamic models of the normal motion of a lubricated sliding system could be used to interpret experimental data and develop predictive models for dynamic friction. The 2D friction model is capable of capturing transients in friction force due to impacts, in addition to any mean normal load effects. They further conclude that the instantaneous normal separation plays a greater role in determining the instantaneous dynamic friction force than the normal load does, once again reinforcing the importance of understanding the normal dof in sliding contact. They also [42] examine the effects of normal surface separation in an empirical dynamic friction model using contact resistance. They develop two-parameter models to describe dynamic contact situations, and demonstrate that indeed explicitly including normal oscillation effects (through contact resistance

[1] Micromechanical views of friction and asperity-based contact models are not covered in detail here; the interested reader should refer to [3], where surface roughness effects, adhesion, and contact models such as Greenwood and Williamson [27] are described.

measurements) allows a better fit to experimental data for unsteady lubricated contact across a wide operating parameter range.

Rice, Moslehy, and Elmi [43] developed a pin-on-disk apparatus and an accompanying modeling framework for studying tribodynamic contact. In particular, the effect of test rig dynamic parameters on friction and wear measurements is the focus. The authors propose a detailed dynamic model including properties of both the pin and disk *sides* of the contact, as well as a nonlinear contact stiffness. Near-surface plastic deformation is considered for its role in reducing stiffness locally near the contact. Normal direction excitation is provided by either asperity contact or debris between the surfaces. The authors conclude that models of this sort, with sufficient detail of the test rig dynamics and interface behavior, can be useful in interpreting experimental data or understanding the role of normal contact oscillations in friction or wear tests.

Further work in the dynamic modeling area comes from Streator and Bogy [44], who examine the role of transducer dynamics in friction measurements. By modeling a pin-on-disk arm as a cantilevered beam with discrete end mass, and developing a transfer function to describe the beam/mass dynamics, they back-calculate the friction force from either a strain gage response (mounted near the beam root) or a displacement response of the end mass. The authors conclude that over a large frequency range, a single-dof transducer model based upon beam strain is inadequate for accurate interpretation of the measured data.

The idea of an angular contact degree of freedom has been introduced by a number of researchers ([45,46], others). The inherent asymmetry of *continuous* friction contact is shown schematically in Fig. 2, which demonstrates that the normal and angular contact conditions are coupled through the geometry of the component. As the friction force acts on only one side of the component, a net twisting moment acts on the body and an angular deflection results. Further, a consequent change in normal deflection (and normal contact pressure) must occur due to the kinematics of the contact. This normal-angular coupling (also referred to as geometric or kinematic coupling) has been investigated and found to play a significant role in contact dynamics.

One of the seminal works in the area of geometric coupling of deformation modes is by Jarvis and Mills [47], who present a thorough analysis of dry friction-induced vibrations

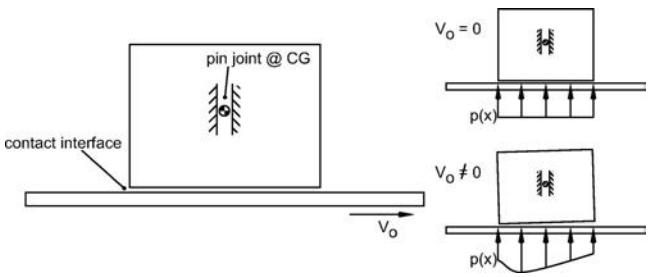

Fig. 2 Contact system showing angular deflection for $V_o \neq 0$ (due to friction asymmetry)

for a pin-on-disk-type experiment and a 2−dof dynamic model for analysis. The generalized coordinates in the model correspond to modal amplitudes of the pin (tangential) and disk (normal) deflections, and the model parameters are tuned from experimental measurements. Two important conclusions are given: i) velocity-dependent friction alone is *insufficient* to maintain an instability, and ii) geometric coupling of the motion of the two components can drive an instability under constant friction coefficient. Also referred to as a *kinematic constraint instability* in the paper's discussion, this mechanism can be controlled or suppressed by appropriate design of the system, including control of, in this case, pin length or contact radius on the disk.

Earles and Lee [48] developed a system dynamic model including rotation to explain noise generation in pin-on-disk experiments. The pin dynamic model consists of two translational (tangential, normal) and one rotational dof, while the disk model is composed of a single translational dof in the normal direction. They conclude that a geometrically-induced instability (ie, one which relates to coupling of the rotational dof to another system dof) is responsible for the noise generation. Other related work [49] indicates that squeal noise is most prominent when the pin vibrates in the rotational mode, and that geometric coupling of the components promotes response in the rotational mode. Similar results concerning the geometric coupling as an instability mechanism were found using a more sophisticated dynamic model [50].

Swayze and Akay [51] use a 1−dof oscillator, with coupled normal and angular motion, to demonstrate the coupling between friction and system dynamics. Motion of the rigid mass is excited by sliding friction, and phase plane results indicate stability of equilibrium points. For undamped systems, the friction coefficient determines a) the number of equilibrium points, and b) their stability. As μ varies from 0 to 0.6, the number of stable equilibria changes from three to one; for the damped case, stable centers become stable nodes.

Oden and colleagues have returned to the question of normal-tangential-angular coupling on several occasions [45,52,53]. They use a continuum approach to deriving interface constitutive laws, and establish two power law expressions for normal and tangential interface traction; the expression for normal stress is:

$$\sigma_n = c_n a^{m_n} - b_n a^{l_n} \dot{a} \tag{5}$$

where σ_n is normal stress, a is the normal approach of the surfaces, c_n, b_n are traction coefficients, and m_n, l_n are the exponents. This form includes both recoverable and non-recoverable components, through the dissipation term $b_n a^{l_n} \dot{a}$, and is therefore able to capture energy dissipation due to normal approach [54]. Tangential stress is expressed as:

$$|\tau_f| = \begin{cases} \leqslant c_f a^{m_f} & \text{stick} \\ = c_f a^{m_f} & \text{slip} \end{cases} \tag{6}$$

These power law expressions allow versatility in friction modeling in that by careful choice of parameters, a variety of

other friction laws can be recovered. For example, the authors point out that Coulomb friction is modeled using $m_f = m_n$ and $b_n = 0$. Subsequently, in order to ease the computational demands of solving the problem, a friction regularization approach of the $\tan^{-1}(...)$ form (Section 4.2) is used.

Several key accomplishments can be extracted from these works:

- normal-angular coupling plays an important role in self-excited oscillations, and their occurance is most likely when normal and rotational natural frequencies are tuned, and
- observations of static and kinetic friction are not intrinsic properties of the materials/surfaces in contact, but are influenced strongly by the dynamics of the measurement device.

Each of these conclusions has ample support in the literature, and in particular, the second has been substantiated in both the dry friction [13,55] and wet friction areas [56].

2.2.3 Role of normal force variations

It is difficult to envision a contact scenario in which the contact normal force F_n is truly constant, independent of the motion of the system. Similarly, for continuous contacts, it is reasonable to ascribe some spatial variation to interface normal pressure, and in fact contact mechanics presents many straightforward solutions. These two factors combine to spur interest in general analyses of normal force variations in dynamic systems. Once again, it has been found that normal force variations can play a significant role in friction contact.

Anderson and Ferri [57] demonstrate the behavior of a single-dof system under a generalized friction law including amplitude-dependent friction. Their generalized friction law of the form:

$$F_f = \mu(F_{n,o} + F_{n,1}|x| + F_{n,2}|\dot{x}|)\mathrm{sgn}(\dot{x}) \tag{7}$$

consists of a *constant* coefficient μ along with amplitude and velocity *gains* $F_{n,1}$ and $F_{n,2}$; $F_{n,o}$ is the constant part of the normal force. Note that the gains effectively model displacement-dependent or velocity-dependent normal force variations, while other velocity dependence could be implicitly accounted for (eg, the more common velocity-dependent sliding friction coefficient). The authors first examine solutions using a one-term harmonic balance, although they correctly note that this solution is increasingly in error as the percentage of stick over one forcing period increases. They map sticking regions in the position-time phase space and conclude that the interface *stiffness* (ie, the gain $F_{n,1}$) plays an important governing role in a sticking response and pre-slip displacement schematically shown in Fig. 1*d*. They also note that percent sticking increases monotonically with increasing gain $F_{n,1}$, an observation supported across the friction damping literature as well (Section 2.6). Other authors considering the role of normal force variations include Menq *et al* [58], Dupont and Bapna [59], and Berger *et al* [60]. Each of these works found an important role can be played by normal force variations, whether in forced response or self-excited oscillations. Finally, in addition to dynamic stability analyses, variations in normal force play a key role in determining frictional energy dissipation, the kinematic state of the interface (sticking or slipping), as well as influencing the overall structural integrity of jointed and built-up structures, as discussed in Section 2.6.

2.2.4 Stick-slip oscillations

One of the more vexing problems of friction and dynamics is stick-slip oscillations. Early studies of stick-slip date back to den Hartog [61], who developed a piecewise analytical solution to the nonlinear, piecewise equations of motion for a single-dof, harmonically forced oscillator undergoing stick-slip. Subsequently, a linearized analysis was developed by Blok [62] to predict a critical system damping value to suppress stick-slip oscillations. The critical damping was related to the slope of the friction-velocity relation. Rabinowicz [12] later noted that stick-slip is extinguished under sufficiently high sliding velocity, a conclusion no doubt coupled to the general characteristic of lower friction curve slope at higher sliding velocity. Subsequently, Derjaguin, Push, and Tolstoi [63] developed an expression for this critical speed, which is a function of the sliding velocity and therefore the friction curve slope. In a series of articles, Brockley and colleagues developed further quantitative understanding of stick-slip oscillations. First, Brockley, Cameron, and Potter [64] describe a critical velocity expression for the suppression of stick-slip vibrations, and this expression is a function of system damping, normal load, and friction characteristic. In addition, the system stiffness plays a role in the calculation. Brockley and Ko [65] use phase-plane tools to carefully examine the stick-slip limit cycles resulting from a variety of friction laws, including a non-monotonic *humped* law showing net rate strengthening as sliding velocity increases. The authors note the existence of quasi-harmonic vibrations under certain friction conditions. In fact, a non-stick-slip limit cycle can be observed with the humped friction law mentioned above, and the mechanism of this is again related to the friction curve slope. When the oscillator operates on a portion of the friction-velocity curve with negative slope, energy is inserted into the system; when it operates on a positive slope portion, energy is dissipated from the system. The negative/positive slope mechanism, in concert with the overall system damping, can produce a pure slipping solution which has a net energy change over one cycle of zero. This isolated, closed trajectory in the phase plane is therefore a non-sticking limit cycle, and its existence is critically dependent upon the nature of the friction curve and the system dynamics. A variety of other important results have been reported in the literature, notably the contributions of Popp, Pfeiffer, and colleagues [66–68]. These authors in particular have played an important role in the development of analytical formulations for stick-slip friction oscillators, as described next.

Stick-slip problems have recently been addressed as members of the broad class of non-smooth dynamic systems. Similarities between the stick-slip problem and the impact oscillator problem (which itself possesses a large literature base-see for example Budd [69] or Bishop [70,71]) have been explored in detail by Hinrichs, Oestreich, and Popp [72,73], and Popp [74]. In particular, [72] reviews a wide

variety of approaches relevant to non-smooth dynamic system analysis, and emphasizes the rich bifurcation behavior presented by such systems. The analysis tools include bifurcation maps, Lyapunov exponents, as well as a variety of time histories and phase portaits. The authors conclude that non-smooth system analysis tools are maturing and the smoothing procedures (see also Section 4.2) used previously for these sorts of problems are becoming less necessary.

The dynamics literature in general points to the critical role of both parameter dependence of friction and system dynamics response—particularly out-of-plane response–in governing overall performance of systems with friction. It seems clear that both the friction model and the system dynamic model must be chosen carefully, because their synergy dictates existence of self-excited responses.

2.3 Friction and control strategies

Friction presents a variety of obstacles to effective control of machines. Compensation schemes must deal with the inherent nonlinearity of friction problems under both sticking and slipping conditions. Surveillance of friction contacts is difficult, so estimators for friction force are often a necessity for robust control strategies. As a result, there has been a relatively recent emphasis from the controls community on friction models specifically amenable to implementation in control strategies. One key goal of the controls models is an integrated friction description which is *continuous* across operating regimes (ie, sticking and slipping) as much as possible, resulting in a model which is numerically non-stiff and provides reasonable controller frequency response.

Haessig and Friedland [75] propose two new friction laws for use in simulations, with an emphasis on control approaches. The *bristle* model consists of a statistical description of surface contact with bristle location and distance between bristles described by random variables. The authors use the bristle model as a physically-motivated representation of the microscopic details of surface contact, although the number of parameters in the model itself makes its use challenging. The second model, the *reset integrator* model, defines a position-dependent friction force which resists motion and represents bonding between surfaces during sticking. When compared with other friction models from the literature, these two new models perform reasonably well, although computational efficiency suffers in some cases. Each represents an attempt to smooth the inherently nonlinear (and discontinuous at zero relative velocity) friction force to make simulation more efficient.

Armstrong-Hélouvry [76,77] examines the role of system stiffness and PD control on stability of steady sliding, especially at low velocity. Plant and controller parameters are included in the stability analysis, and the friction model includes time lag, velocity dependence, dwell time dependence, and pre-slip displacement under sticking conditions. The result, based upon an energy argument, is a prediction for critical stiffness above which stick-slip is eliminated. This stiffness can be interpreted as either a physical stiffness (plant) or a controller parameter (displacement gain).

Dupont and Bapna [59] examine the role of variable normal force on stability of steady sliding in a single-dof system with general rate- and state-dependent friction behavior. The authors note that single-parameter friction laws (ie, those for which friction depends only upon instantaneous sliding velocity) cannot generate values of critical stiffness above which stick-slip oscillations are extinguished. The physical example is a single-dof system with inclined spring, such that effective normal load is a linear function of system displacement. A further comparison between quasi-static (ie, inertial forces neglected) and fully dynamic models is presented, with the conclusion that system mass does play a role in the existence of stick-slip.

Dupont [22] addresses the implications of state-dependent friction on stability of steady sliding from a controls perspective. By interpreting system stiffness and damping parameters as analogies to controller gains, design criteria for PD controllers can be developed. A critical stiffness, above which stick-slip oscillations are not possible, is predicted, and this result is contrasted with that of time delay friction models (of the form proposed in [14]) for which only *regions* of stiffness provide stable sliding.

Armstrong-Hélouvry, Dupont, and Canudas de Wit [78,79] review the general literature spanning the tribology and controls community, focusing specifically on control options for low-velocity friction-induced vibration problems. Stick-slip problems are examined in light of several modeling and analysis tools (describing functions, algebraic analysis, etc), and various compensation approaches (PD, integral, model-based, etc) are examined. The authors conclude with recommendations for future investigations, including physics-based friction models (instead of empirical models), adequate consideration of lubrication, and a more thorough understanding of the repeatability of friction data. The conflict, with regard to typical controls applications, relates to the fundamental trade-offs among model fidelity, physical relevance, and computational intensity. For controls problems, frequency response is often of prime importance, and high-fidelity models are simply not feasible. This theme reappears in Section 5.4.

Subsequently, another bristle model emerged for controls applications, and the so-called *LuGre* model was presented by Canudas de Wit, Olsson, Åström, and Lischinsky [80]. Stemming from a collaboration among researchers at the Lund Institute of Technology (Sweden) and in Grenoble France (Laboratoire d'Automatique de Grenoble), the LuGre model captures a variety of behaviors observed in experiments, from velocity and acceleration dependence of sliding friction, to hysteresis effects, to pre-slip displacement. The price paid for such a versatile model is that it is a *six parameter* model, and the friction force is defined as:

$$F_f = \left(\sigma_o z + \sigma_1 \frac{dz}{dt} + \sigma_2 V_{\text{rel}} \right) F_n \tag{8}$$

where σ_o is a characteristic bristle stiffness, σ_1 is a damping parameter, σ_2 is a viscous damping coefficient, z is the average bristle deflection, V_{rel} is the relative velocity, and F_n is the contact normal force. The bristle deflection is defined by:

Table 3. LuGre model parameters and limiting behaviors

Case	Condition	Relevant Equation	Controling Parameter
stiction	$V_{\text{rel}}=0$	$F_f=\mu_s z F_n$	stiffness σ_o
hysteresis	$V_{\text{rel}}\neq 0$	$F_f=\sigma_o z+\sigma_1\left[V_{\text{rel}}-\frac{\sigma_o\lvert V_{\text{rel}}\rvert}{g(V_{\text{rel}})}z\right]+\sigma_2 V_{\text{rel}}$	damping σ_1,σ_2
break-away stick-slip	$V_{\text{rel}}=0$ periodic response	$\sigma_o z=\mu_s$ equations (8), (9), (10)	stiffness σ_o, friction μ_s velocity function $g(V_{\text{rel}})$ friction μ_c, velocity v_s

$$\frac{dz}{dt}=V_{\text{rel}}-\frac{\sigma_o\lvert V_{\text{rel}}\rvert}{g(V_{\text{rel}})}z \tag{9}$$

where the function $g(V_{\text{rel}})$ contains information about the velocity dependence of friction. Several varieties of $g(V_{\text{rel}})$ have been proposed, all using the general form:

$$\sigma_o g(V_{\text{rel}})=\mu_c+(\mu_s-\mu_c)e^{-\lvert V_{\text{rel}}/v_s\rvert^{\alpha}} \tag{10}$$

where μ_c is the Coulomb friction coefficient, μ_s is the static friction coefficient, v_s is the Stribeck velocity (helping to define the velocity dependence of friction), and α is an application-dependent exponent which has been reported as $\alpha=2$ [80] or $\alpha=0.5$ [81]. The limiting cases for this model are worth exploring (See Table 3). Note here that each parameter plays a different role in determining system response under different operating conditions. This approach does present a unified model which, when coupled with an appropriate dynamic model and control scheme, models the system across the entire range of potential responses.

Previously, a seven-parameter friction model was developed for control applications by Armstrong-Hélouvry [76]. The model includes Coulomb, viscous, and Stribeck friction plus frictional memory, time-dependent sticking friction, and pre-slip displacement. It is an integrated model, in the same sense as the LuGre model, and it captures relevant behavior for a variety of sticking or slipping scenarios. Once again, the price paid for this versatility and robustness is the necessity for identifying seven different friction parameters. Nonetheless, the model has been used in the controls literature, and is expressed for sliding as:

$$F_f(V_{\text{rel}},t)=-\left[F_c+F_v\lvert V_{\text{rel}}\rvert+F_s(\gamma,t_2)\frac{1}{1+\left(\frac{\dot{V}_{\text{rel}}(t-\tau_L)}{v_s}\right)^2}\right]\text{sgn}(V_{\text{rel}}) \tag{11}$$

where these parameters are similar to those in the LuGre model:

$F_c=$ Coulomb friction force

$F_v=$ viscous friction force

$v_s=$ characteristic velocity in Stribeck curve

$\tau_L=$ time constant for frictional memory

In addition, other descriptions become appropriate for other sliding scenarios:

pre-sliding displacement $\quad F_f(x)=-k_t x$ (12)

static friction

$$F_s(t;t_\infty,\gamma)=F_{s,a}+(F_{s,\infty}-F_{s,a})\frac{t-t_\infty}{t-t_\infty+\gamma} \tag{13}$$

where $F_{s,a}$ is the magnitude of the Stribeck friction at the onset of sticking, $F_{s,\infty}$ is the long-time value for static friction, $t-t_\infty$ is the sticking time, and γ is a time constant for static friction evolution. The authors describe the typical parameter ranges for this model, as well as the physical situations which most closely influence each parameters.

Recently, a new modeling approach for so-called *hybrid* systems, those dynamical systems possessing time-domain discontinuities, has emerged, as have numerical tools for simulation of generic hybrid systems. Taylor has developed a suite of Matlab software for hybrid system simulation which takes advantage of the Hybrid Systems Modeling Language (HSML) [82–84]. The algorithm is designed to efficiently handle state-change events, including continuous-time, discrete-time, or logic-based alterations in model behavior; friction is one excellent example. Indeed, Taylor presents [85] simulation results for an electro-mechanical system with both saturation and stiction; the HSML implementation in Matlab shows clear advantages in capturing state (ie, stick-slip) transitions. In addition to advances in simulation approaches for hybrid systems, a stability theory for such systems is continuing to emerge (eg, Hou and Michel [86]).

The controls literature has emphasized computationally-efficient, multi-parameter friction models suitable for fast simulation and providing reasonable controller frequency response. The six-parameter LuGre model, for example, provides a well-integrated view of friction; using an appropriate calibration approach to identify the model parameters can result in a useful model for controls applications, and other applications for which the highly localized details of interface response (ie, interface partial slip, slip displacements, etc) are not required.

2.4 Friction and mechanics of materials

The mechanics of materials community has also examined the friction interface problem, again with various approaches to friction. The most common analysis approach seems to be

a constant coefficient of sliding friction, with multi-valued zero-velocity friction. This approach emerged as being very reasonable considering the small interfacial slip velocity and the analytical tractability of a constant friction coefficient problem. Key problem quantities are shown schematically in Fig. 3. The figure is based upon the classical result attributed to Mindlin [87], who showed that under constant normal-plus-tangential loading of Hertzian-type contacts, a region of slipping propagates inward from the contact edges with increasing tangential load. This is a *partial slip problem*, in which by definition part of the interface slips while part of the interface sticks. In the figure, the stick zone of the contact between two cylinders is defined for the region $|x|<c$, and the slip zone is defined by $c<|x|<a$. The contact radius a is derived from Hertz contact considerations, and the stick zone size is governed by:

$$\frac{c}{a}=\left(1-\frac{F_q}{\mu F_p}\right)^{1/2} \tag{14}$$

where F_p is the global normal load, F_q is the global tangential load (which may be reciprocating), and μ is the coefficient of friction corresponding to interfacial slip. Of course, for non-constant coefficient of friction, the formulation becomes analytically less tractable, and in this sense a constant friction coefficient seems to be a good choice. However, note that the slip displacements $u_x(x,t)$ in these partial slip problems tend to be quite small, certainly small compared to the slip zone size. As a result, in order for (say) velocity dependence of friction coefficient to play a significant role, tangential excitation frequency under harmonic input according to:

$$F_q(t)=F_{q,1}\sin\omega_q t \tag{15}$$

would need to be very large such that the steady-state slip velocity given by:

$$\dot{u}_x(x,t)=\omega_q u_x(x,t) \tag{16}$$

is significant compared to velocity dependence of $g(V_{\text{rel}})=\dot{u}_x$. Here we have assumed a steady-state harmonic interface response. For small-scale relative motion in cases like these, we might expect that typical forms of parameter dependence of friction coefficient would represent a second-order effect. These types of analyses have been pursued widely in the fretting fatigue community, and a variety of interesting observations have been made concerning friction modeling and the role of system dynamics.

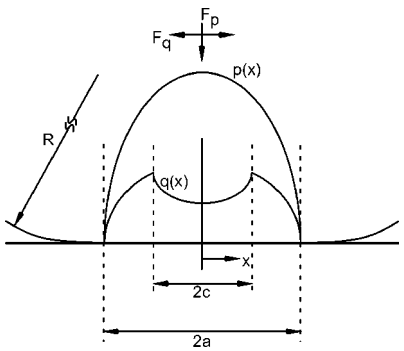

Fig. 3 Schematic of Mindlin (partial slip) result for nominal Hertzian contact: contact half-width a and stick zone half-width $c<a$

Oden and Pires [88] propose nonlinear and nonlocal friction laws for elastic contact problems, and present a variational formulation for the contact boundary-value problem. A *nonlocal* friction law is one which depends not only upon the contact conditions (ie, normal stress) at a point, but also upon contact conditions in the near-vicinity of that point. The value of these models lies in calculations for impending motion, and also as an interpretation of the partial slip problem discussed elsewhere in this paper. Solution techniques for the nonlinear and nonlocal laws are later reported in [89,90]. Further, these non-local interface laws have overlap with adhesive contact models such as the DMT model, which includes adhesion effects not only within the contact, but also just outside the contact where the surface separation remains small and the surface interaction is non-negligible–see Greenwood [91] for a thorough numerical analysis and Section 2.8 for a brief discussion.

In a series of articles, Adams has examined relative sliding of two elastic half-spaces, including extensive analytical work with the continuum elasto-dynamic equations of motion. Using a constant coefficient to describe the interface contact [92], he concludes that dynamic instabilities are promoted by mismatch of the elastic wave speeds in the materials. Next, separation wave pulses are investigated for their potential to induce relative motion in nominally sticking contacts [93]. Their existence can indeed produce relative surface sliding, under the condition that a small separation region propagates along the interface encouraging *local* relative motion. He further shows [94] that the observed coefficient of friction (far from the contact interface) can be different from the actual interface friction coefficient, and a mismatch of the shear wave speeds in the contacting materials is identified as the mechanism of this behavior. This conclusion is similar to the assertions of Oden, who previsouly indicated (Section 2.2.2) that the friction coefficient is not a fundamental surface property, but rather a composite function of surface interaction and system properties.

One of the most frequently-cited works in the fretting literature is the fundamental contribution of Ruiz and Chen [95,96]. They examined fretting fatigue in turbomachinery blade/disk dovetail joints, and their bench-scale experiments suggest a predictive criterion for fatigue crack initiation which depends not only upon normal and tangential contact stress, but also on frictional work:

$$k=\sigma_T\tau_f u_x \tag{17}$$

where σ_T is an in-plane tensile stress at the interface (responsible for driving any fatigue cracks which develop at the surface), τ_f is the interface friction shear stress, and u_x is the slip displacement. Here we see an important link between interface friction τ_f and interface response u_x, and it is proposed that *both* are critical in determining component fatigue life.

Nix and Lindley [97] provide indirect support for the Ruiz and Chen fretting criterion by showing a sensitivity of fa-

tigue strength to slip displacement, with a minimum observed for slip displacements on the order of 10–30 μm (Fig. 14 of their paper). However, the authors argue that an intermediate parameter, the plateau value of friction force during the experiment, provides the link between slip displacement and fatigue life, and that it may be the fundamental governing parameter. Changes in this plateau value determine fatigue life, and observed changes in slip displacement are simply consequences of the change in friction force.

Kuno, Waterhouse, Nowell, and Hills [98] provide further support for the Ruiz and Chen criterion by applying the theory to a geometry fundamentally different from that used in the original work [96]. A Hertzian contact is used to generate fretting parameter maps. The Ruiz and Chen parameter correctly predicts the location and shape of the cracks observed in experiments, and of course the slip displacement (calculated from a Mindlin-type analysis) plays an important role. Subsequent life calculations are based upon fracture mechanics approaches.

In addition to providing further experimental support for the Ruiz and Chen criterion, Nowell and Hills [99] also propose a further physical interpretation of the criterion. The composite criterion described by Eq. (17) is actually a bridge criterion which quantifies the following two components necessary for fretting fatigue to occur:

- fretting surface damage governed by frictional work $\tau_f u_x$ provides *nucleation sites* for fatigue cracks, and
- bulk tensile stress σ_T opens the crack and drives its propagation.

So, a sufficient combination of nucleation *and* propagation effects must be present, or else either i) a crack will not nucleate, or ii) it will self-arrest. Fretting fatigue predictions are therefore very sensitive to our knowledge of the interface stress state and displacements, and accurate predictions depend upon good contact models and appropriate friction models.

Waterhouse [100] comprehensively reviews the fretting literature and emphasizes the important role played by frictional work in fretting contacts, citing [95] and [96] and their proposed criterion of Eq. (17). To complement the discussion of analytical tools, the author cites a variety of experimental efforts which support the conclusion that interface slip displacement is a governing parameter in fretting fatigue crack initiation. Furthermore, the location of crack initiation is identified, under relatively low load conditions, as the stick-slip boundary—thus reinforcing the idea that accurate fretting fatigue behavior prediction relies upon a complete understanding of the interface response.

An interesting development in the fretting literature, and an important link to other friction modeling approaches, is the proposition of a critical length scale in fretting contacts. When the slip displacement exceeds the characteristic asperity spacing, then each asperity within the contact undergoes more than one loading cycle for each cycle of motion. This distinction between macro-scopic surface interaction (many asperity contact) and small-scale surface interaction (single asperity contact) has been examined in the fretting literature as described next. If this important fretting length scale is related to slip displacement u_x and asperity spacing, then it seems clear that performance and durability of large-scale fretting components is substantially influenced by interactions on much smaller length scales.

Hills, Nowell, and O'Connor [101] briefly review the literature and present new experimental results which demonstrate a distinct size effect in fretting contacts. The authors reproduce, using a slightly different test configuration, the results of Brumhall [102], who observed that below a critical contact size, fatigue life is infinite. They then put forth two hypotheses concerning the mechanism of this size dependence, and one, the *initiation-based* criterion, relates the critical contact size to the slip displacement u_x. For smaller contact size, the slip displacement remains small and the Ruiz and Chen initiation criterion falls below the critical crack initiation value. The work does not conclusively validate the initiation hypothesis, but once again interface slip displacement appears to play an important role in fretting contacts.

Hills [103] further pursues the length-scale question in fretting contacts by carefully examining the contact mechanics of fretting. Referring to the basic solutions of Mindlin [87] and Cattaneo [104], Hills analyzes the test rig itself and verifies the use of Hertz-type approach (accounting for partial slip). The slip displacement is linked to the size-dependent behavior by the following argument: if the slip displacement is larger than the characteristic spacing between asperities, then each asperity experiences more than one loading cycle for each cycle of motion. This behavior is then independent of the contact size, an observation supported by experiments. In addition, Nowell and Hills [105] previously examined the differences between typical fretting fatigue tests, and fretting fatigue modeling. They specifically compare the Mindlin-type solutions often used in fretting analysis with the actual prevailing stresses in the test components. They conclude that the bulk tension associated with the fretting test significantly affects the interface shear traction and stick-slip behavior, and that the Mindlin approach must be modified to account for bulk loading effects.

Szolwinski and Farris [106] present a new fatigue life parameter, the so-called Γ parameter, defined as the product of maximum normal stress and normal strain (and independent of slip displacement), derived from the assumptions of elastic, nominally Hertzian contact of isotropic components. The Γ parameter correctly predicts the crack origin location, the crack orientation, and (approximately) the nucleation life of fatigue cracks (as compared to published data [99]). However, the Γ parameter does not capture the observed size dependence reported previously [103], and the authors assert that their elastic analysis cannot model the apparently plastic effects associated with the size dependence. Recall that Hills [103] suggested that this plastic behavior is critically related to the ratio of slip displacement and characteristic asperity spacing, reinforcing the idea that slip displacement is a fundamentally important parameter.

A critical link between the mechanics literature and other friction-related areas is the apparent contact dynamics-

dependence of fretting test results. Söderberg, Bryggman, and McCullough [107] and Bryggman and Söderberg [108] both critically examine the contact conditions in fretting, with a keen eye on interface slip displacement, transition from pure stick to partial slip to pure slip, and on frequency effects in fretting contacts. In [108], critical displacement amplitudes indicating the transitions from stick to partial slip (Δ_1) and partial slip to pure slip (Δ_2) show a strong dependence on excitation frequency. The authors attribute this to the competing effects of temperature (which decreases surface hardness) and strain hardening (a plastic process which increases hardness), which combine in a complicated frequency-dependent way. In [107], high frequency fretting experiments reinforce the observation that at low fretting amplitudes (ie, partial slip conditions), fretting behavior is very sensitive to excitation frequency. However, high amplitude (ie, pure slip) fretting experiments are proposed for accelerated life tests, because the sensitivity of fretting fatigue life to frequency was small across a wide frequency range for this condition.

Subsequently [109,110], these researchers closely examined the roles of various test parameters on a number of measureable outputs. [109] details the effects of normal load, excitation frequency, and fretting amplitude on wear scar size, critical tangential displacement which governs transitions from stick to partial slip to pure slip (see [107,108]), and critical tangential force. The pronounced frequency effect indicates that accelerated fretting tests should not be used for low amplitude fretting applications. As frequency increases under constant fretting amplitude, different interface regimes (stick, partial slip, pure slip) are encountered; this calls into question the validity of the accelerated life test predictions. The work culminates in the development of fretting maps which plot regimes of behavior in a two-parameter space, one example of which is shown schematically in Fig. 4. Part *a* of the figure indicates that slip amplitude plays a primary role in i) determining the interface response regime, and ii) determining the fatigue life. The partial slip regime is the most deleterious. Figure 4*b* shows a fretting map in fatigue life-normal load space which again reinforces the criticality of partial interface slip in governing fatigue life. Schouterden, Blanpain, Çelis, and Vingsbo [111] again reinforced the frequency dependence of fretting results, indicating that extrapolation of results from one operating regime (eg, low amplitude, high frequency) to another (eg, high amplitude, low frequency) is difficult because the interface conditions change as well. Further support is provided by Rehbein and Wallaschek [112], who conclude that high frequency contact is dominated by dynamic parameters including time variation in both normal and tangential forces. They introduce a time-averaged *high frequency* friction coefficient which on average is smaller than the sliding or static coefficients. They invoke the essential argument of Tolstoi [26], proposing that the mean surface separation and, therefore, the real area of contact is smaller under the presence of normal vibrations, and therefore, the apparent coefficient of friction is smaller as well.

While at first the constant friction coefficient argument in fretting fatigue analysis is appealing, experimental results have been reported for which a constant coefficient cannot adequately explain the observed behavior. It seems that more complicated interface phenomena may be at work, including spatial and temporal variations in normal force, critical slip distance (ie, memory) effects, temperature-dependent friction coefficient (perhaps indirectly via material hardness), or simply operating in an interface response regime which is different from the application of interest (ie, operating in pure slip instead of partial slip). The conclusion is that even model geometries such as fretting contacts, which use nominal Hertzian contacts, must be approached with some caution, and a great deal of richness of response can be obtained by varying operating conditions, contact size, and other problem parameters.

2.5 Friction and geomechanics

Early work in the geomechanics area focused on earthquake understanding and prediction. One of the most prominent bodies of literature contains the work of Caughey and Iwan, who developed simplified models of friction mechanics and applied them to a variety of engineering systems within and outside of the earthquake area. Their focus was a family of *bilinear hysteresis* models for friction which were also applied to modeling elasto-plastic material behavior. The bilinear hysteresis models are attractive because they include finite material compliance as well as slip behavior. As such they can be used to model transitions from stick to slip, originating in elastic material response as the loading is initiated, to break-away when the load reaches a critical value. A number of articles on a variety of related subjects have appeared [113–119]. Figure 5*a* shows the standard bilinear hysteresis element composed of a single discrete spring and Coulomb damper in series. The single, massless contact point can either stick or slip, and because partial slip cannot be obtained it is sometimes called a *macroslip* element. [119] seems to be most frequently cited because in it the author describes a procedure for defining a pseudo-continuum model based upon a large number of bilinear hysteresis elements whose properties are distributed according to some statistical function; Fig. 5*b* shows the parallel-series (P-S) models, while Fig. 5*c* shows the series-parallel (S-P) models. Furthermore, Iwan's assertion that the parallel-series model

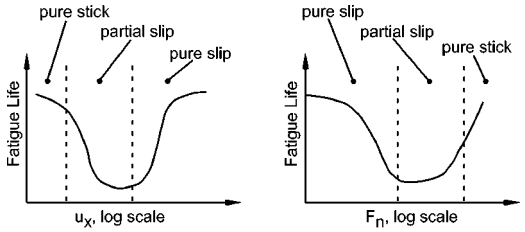

Fig. 4 Variation of fatigue life in fretting contacts as a function of *a*) interface slip displacement u_x and *b*) applied normal load F_n (after Vingsbo and Söderberg [110], Figs. 10 and 11 respectively)

(Fig. 5*b*) is more suitable for dynamic system modeling has been leveraged in much of the slip damping research referenced in Section 2.6. Note that this model was originally used by Masing [120], who applied it to material behavioral modeling, and in fact the so-called *Masing rules* have been invoked by a number of researchers cited later in extending the model from monotonic to cyclic loading scenarios.

Continuum mechanics approaches later emerged, including Byerlee and Brace [121] and Byerlee [122] which focused on stable fault slip as well as stick-slip events. Dieterich produced a series of rock-friction-related works in the late 1970s which introduced a friction constitutive modeling framework of general parameter dependence, specifically related to time-dependence of static friction [123]. Later, stick-slip simulations [124] and pre-seismic slip predictions [125] were undertaken, resulting in new insights concerning friction modeling and its effects on dynamic system performance.

Subsequently, Rice and Ruina [24] put forth a new friction consitutive law derived from their experiences in geomechanics research, and later extended it [25,126]. Related to the work done previously by Dieterich, the so-called rate- and state-dependent friction law has the following generic form:

$$\tau_f = \tau_f(V_{\text{rel}}, \theta_1, \theta_2, \ldots) \tag{18}$$

This model includes not only an instantaneous friction response to changes in system operating condition (ie, sliding velocity or normal load), but also an evolutionary part. The evolutionary portion of the response is governed by a critical slip distance d_c, which is related to the sliding distance required to make and break new populations of asperity contacts. With a continually and rapidly changing population of asperities in contact, the friction coefficient remains stable; with the same population of asperities in contact the time-dependence of sticking friction comes into play. Used primarily in large-scale geomechanics simulations of fault slip and earthquake events, this model's utility in forced response calculations has yet to be fully explored. Note also the similarity in the physical argument behind the existence of a critical slip displacement for the Rice friction model and contact size

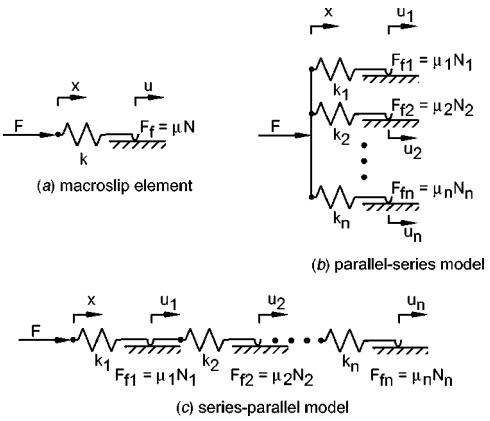

Fig. 5 Lumped-parameter models for friction contact: *a*) macroslip (bilinear hysteresis) element, *b*) Iwan parallel-series model, *c*) Iwan series-parallel model

effects in fretting contacts observed by Hills [103], among others. This notion is similar to Rabinowicz' memory-dependent friction in that it contains information about the current sliding condition and also previous sliding history. Rice's work reports critical slip displacements on the order of 10–100 μm, consistent with Rabinowics' assertions 25 years previous. Further work along these lines was summarized by Ruina [127], and reported by Linker and Dieterich [128].

Rice subsequently assembled very large scale simulations and linked the inherent friction length scale d_c to domain discretization requirements for numerical solutions. He shows [129] that under a general rate- and state-dependent friction law with weakening distance d_c, a critical cell size h^* can be derived for the discretized system, and h^* is an explicit function of the friction constitutive model parameters and scales with d_c. For discrete systems with cells of size $h<h^*$, the discrete model demonstrates a clear continuum limit (ie, as $h\rightarrow 0$). For larger cell sizes, the model may respond as what Rice calls an *inherently discrete* system, one with no well-defined continuum limit. The simulations show that for large cells, each cell may respond discretely—ie, independent of surrounding cells—unlike the continuum formulation for $h<h^*$. The outcome for $h>h^*$ is extremely rich nonlinear dynamic slip behavior resulting not from the fundamental elasto-dynamics of the original governing equations, but from the local dynamics of the discrete system. Rice demonstrates that this response complexity (in both time and length scales) is therefore not a fundamental property of the continuous system, but rather an artifact of a coarse discretization. This idea was further explored and supported in subsequent work [130], and discussed in the context of an *elastic coherence length* ξ (a characteristic length indicating the minimum size of a slipping region at an interface) by Persson [131]. In fact, Persson suggests that the relevant length scale governing discretization is in fact $\xi \gg d_c$, which relaxes the computational constraints somewhat, and presents a more practical guideline for domain discretization.

The geomechanics literature has favored continuum-mechanics-motivated models for friction, from Iwan's elasto-plastic material models using lumped-parameter elements, to Rice's general rate- and state-dependent friction. A key result here is the observation of a critical slip displacement d_c over which friction evolves. This is in support of the time lag observations made previously, and has important implications on both modeling formulation and appropriate discretization of continuous models.

2.6 Friction and energy dissipation

Dry friction as a mechanism for vibration control has been used successfully for many years. Indeed, dry friction provides an inexpensive, passive, environmentally-tolerant approach to energy dissipation, and across a wide range of applications friction damping has been explored. The dry friction damping problem is usually approached from a *forced response perspective*, for which the dynamic response of the structure under (usually) periodic forcing is obtained. This is fundamentally different from much of the literature

Table 4. Normal load effects on contact interface conditions

Normal Load F_n	Interface Condition	Friction Force F_f	Sliding Velocity V_{rel}	Energy Dissipation ΔW
Low	pure slip	low	high	low
Moderate	partial slip	moderate	moderate	high
High	pure stick	high	zero	zero

previously cited, which focuses on self-excited or unforced problems, for which steady-sliding stability or stick-slip limit cycles are predicted.

The early quantitative work in this area is attributed to Mindlin and Deresiewicz [132], who developed predictions for energy dissipation in model contacts as an extension to previous work [87]. The constant friction coefficient model is employed to describe interface behavior. They predict hysteresis loops under cyclic loading, and in general this theory has been corroborated through contact mechanics experiments. A key result is the dependence of energy dissipation on the *third power* of tangential load under light loads. The result is in fact independent of the mean loading, and sensitive only to the loading range. For a time-varying tangential load defined as $F_q(t) = F_{q,o} + F_{q,1} \sin \omega_q t$, the energy dissipation is functionally expressed as:

$$\Delta E = A \frac{(F_{q,1})^3}{F_{q,\max}} \tag{19}$$

where A is a collection of scalar parameters related to contact geometry and elastic constants, and $F_{q,\max}$ is the critical tangential load required to produce gross slip of the interface. Note that this result is independent of the mean tangential loading $F_{q,o}$. (This is in contrast to fretting experiments, where component life is the focus, for which bulk stresses related to $F_{q,o}$ are important, as described by Nowell and Hills [99].) This result has been scrutinized via careful experiments by Goodman and Brown [133], who report third-power dependence of energy dissipation on tangential load range, and present hysteresis loops to determine frictional work. Johnson [134] reports the results of fretting experiments essentially in support of the theory of Mindlin, showing energy dissipation calculations based upon log decrement measurements, as well as post-test wear scar examination. Johnson points out the role of elastic hysteresis effects, which, especially at light loads, can represent a significant portion of the total dissipation. He further notes the apparent variation in friction coefficient within the contact circle, and attributes this observation to break-down of surface oxide films within the slip annulus.

The key here is that the stick-slip nature of the interface response plays a crucial role in providing energy dissipation. Consider first a single-DOF problem with only one discrete contact point loaded by a constant normal force F_n and a cyclic tangential force $F_q(t)$. The steady-state motion of the mass may contain periods of stick and periods of slip, and for displacement of the system denoted by $x(t)$, a sticking condition is $\dot{x} = 0$. Keeping in mind the general expression for frictional work over one forcing period $T_q = 2\pi/\omega_q$

$$\Delta W = \int_{t_o}^{t_o + T_q} F_f \dot{x} \, dt \tag{20}$$

the general trends are summarized in Table 4.

It is then clear that careful consideration of the interface sticking and slipping state is required for accurate prediction of energy dissipation. den Hartog [61] provided the first complete solution for forced response with combined viscous and Coulomb damping, although he assumed a constant coefficient of friction. den Hartog solved explicitly for slipping and symmetric sticking motions, having two stops per forcing cycle, and he also observed a smaller resonant peak and a lower resonant frequency in the presence of friction. These combined effects of amplitude and frequency modulation in the presence of friction are characteristic and are observed with other structural and friction models. Shaw [135] augmented den Hartog's work with a distinction between static and kinetic friction, as well as an analysis of stability of steady-state motions. He also examines bifurcations in the forced response, including multiple stick events per forcing period, and develops sticking *maps* in position-time space (a concept later used and extended by Anderson and Ferri [57]).

2.6.1 Nominally-stationary joints

One of the key roles for friction at a contact interface is to provide passive damping to the structure, and this performance issue has serious implications in, for example, large space structures and other built-up structures whose inherent damping may be low. As such, the design of nominally-stationary joints—bolted or riveted connections, clamped boundaries, etc—requires careful consideration of friction modeling. Once again, the structural dynamics can be tuned to promote friction damping, although this requires robust friction models.

The use of controlled interfacial slip for vibration suppression has been pursued by Beards in a number of articles. He has periodically reviewed the relevant literature in this area (eg, [8]), and in fact returns to some general conclusions concerning the role of frictional slip damping. First, he surmises that roughly 90% of inherent damping in structures arises from structural joints, and this assertion is echoed in other areas including damping of turbine blades, in which blade attachment damping, inherent material damping, aerodynamic damping, and other potential sources are small compared to that of properly-designed friction dampers (this literature is reviewed more thoroughly later in this paper). Beards emphasizes the duality of joint clamp force which plays a critical role both in friction damping and static structural stiffness, and as described in Table 5. Further, Beards and Woohat [136] examined the influence of clamp force on

Table 5. Comparison of interface slip regime and normal load effects for fretting problems and interface energy dissipation problems; strong similarities exist despite vastly different applications.

Interface Regime	Normal Load	Energy Dissipation	Fretting Fatigue
pure slip	low	low frictional work due to low friction (despite large slip)	large slip wears away potential crack nucleation sites, improving fatigue life
partial slip	moderate	large friction work with moderate slip provides optimal energy dissipation	moderate slip does not wear away potential crack nucleation sites, therefore reducing fretting fatigue life
pure stick	high	high friction but zero slip results in no frictional work and no energy dissipation	zero slip provides for no frictional work and therefore no fretting surface damage, extending fatigue life

dynamic characteristics of a frame. They note that to a certain extent dynamic properties of the frame can be controlled, and that both natural frequencies and mode shapes can be substantially altered by varying the clamp force. The design trade-off is of course that optimal damping characteristics may undermine structural stiffness to an unsatisfactory degree.

Ferri has revisited the friction dynamics problem several times, and in addition to a recent review article [5], Ferri and Heck [137] present an interesting view of reduced-order friction damping models using singular perturbation theory. First, a one-mode turbomachinery blade structural model with friction damper *of non-zero mass* is presented. The limiting cases of infinite damper stiffness (studied originally by den Hartog) and zero damper mass (models such as those studied by Griffin [138], among many others) are easily extracted, but Ferri focuses more closely upon the general case for analysis. Zeroth-order and first-order perturbation solutions are compared with the classical solution of den Hartog and time integration of the full nonlinear model for frequency and amplitude changes with problem parameters. Ferri observes that the best agreement between the perturbation approximations and the full nonlinear solution is achieved for light, stiff dampers under relatively large response. This indicates that if the system truly does behave like a 1-dof system (and local damper dynamics are negligible), then a one-mode approximation and massless damper (or, at least, a system with damper natural frequency well above the excitation frequency) is justified and sufficiently accurate. However, the results also suggest that heavier dampers may provide excellent damping performance but undermine the predicative capability of lower-order models (as illustrated by Ferri's Fig. 11).

Previous work in this area includes Pierre, Ferri, and Dowell [139], who expand the solution to the nonlinear friction problem using multiple harmonics and an incremental harmonic balance method (HMB). The incremental HBM (IHBM) is capable of efficiently handling the *sgn* nonlinearity at zero relative velocity by making small increments in the argument (ie, performing successive linearization of the problem). The authors conclude that three harmonic terms are, in general, sufficient to capture the character of the solution (as Wang and Chen [140] also later reported), but detailed information about sticking and slipping response is not obtained. Furthermore, for problems in which the amount of sticking is substantial, the Fourier series representation of the response clearly requires many more than three harmonic terms, and the performance of the IHBM in such cases suffers.

Dowell [141] has examined the case of damping in the boundary supports of clamped beams and plates, with a primary emphasis on the case of pure slip (ie, no stick-slip is considered). He finds that for sufficiently large motion—that is, that the assumption of pure slip is essentially true—the problem becomes a *linear* one in which the friction damping is expressible as an equivalent viscous damping. Previously he examined the case of a cantilever beam with dry friction point contact damper attached [142,143]. Ferri and Bindemann [144] also examine the support damping problem for vibrating beams, and they consider a variety of physical configurations (in-plane slip, transverse slip, etc). In each case, the harmonic balance method is used to approximately determine the response to harmonic forcing, and in each case friction damping is found to be related to the response amplitude in a different way (ie, invariant, proportional, inversely proportional, etc). A key assumption for the analysis is that the response is substantially in pure slipping, and that a single harmonic term can adequately capture the response. The authors conclude that design changes which alter the geometry of contact interfaces (ie, in-plane vs transverse slip) may increase efficiency and overall damping of the joint.

In a two-part article, Makris and Constantinou demonstrate an exact solution for constant or linear Coulomb friction laws [145], and also that velocity-dependent friction can have a profound effect on the dynamic response [146]. They consider single and multiple stops per forcing cycle of a single-dof oscillator, and include rigorous treatment of the frequency cases for which no asymptotically stable periodic motions exist (under constant Coulomb friction). With velocity-dependent friction, the number of stops per forcing cycle was observed to be smaller than for constant Coulomb friction, and in addition the frequency content of the response was also different.

Finally, the recent contribution of Gaul, Nitsche, and colleagues has been substantial in our understanding of dynamic friction, particularly as it applies to mechanical joints. The review article [147] presents a comprehensive look at joint friction and includes specific aspects of various models described here relevant to friction joints. They also examine

issues such as the role of surface roughness in joints, computational approaches, and the randomness of friction forces. They further describe truss and frame structures, as well as semi-active joints, and the important role of friction in each case. The idea of active vibration control is explored [148], and maximal energy dissipation is achieved through joint normal force control. Nonlinear dynamics of friction joints have also been investigated [149], as has microslip behavior in joints [150] (see the next section).

2.6.2 *Microslip, partial slip, and passive damping*

The term *microslip* is often used interchangably with *partial slip*, although *microslip* leads to some confusion. A microslip interface response is one which has small regions of slipping while most of the interface is sticking. This term has been used in the mechanics literature (eg, [151]) as well as the slip damping literature. It may lead to some confusion because it is not clear whether *micro* refers to the size of the slip zone ($a-c$ from Eq. (14)) or the slip displacement amplitude (u_x from Eq. (17)). In this discussion, the term partial slip will be used consistently to describe contact situations with a part of the interface sticking while another part simulaneously slips.

A prominent body of work for partial slip friction damping has been developed by Griffin and colleagues in the gas turbine community over the past 20 years, although these approaches are equally relevant for any dynamic, partial slip contact situation. The initial work by Griffin [138] consisted of using a bilinear hysteresis element of the form shown in Fig. 5*a*. Griffin identifies two key design parameters: damper stiffness, and the force at which it slips. Note that the damper stiffness is a semi-physical parameter (see the discussion of Section 2.5 on Iwan models) which broadly indicates the pre-slip displacement behavior x_{pre} of the damper. The stiffness *does not* correlate to a structural property of the damping element itself (for example, an in-plane stiffness). Griffin is able to capture the amplitude and resonant frequency shift similar to den Hartog [61] for this airfoil damping application. Similar bilinear hysteresis models were employed later [152,153]. In addition, Menq and Griffin [154] investigate approximate solutions composed of a single harmonic for the blade damper problem using the macroslip element described above. They observe that the steady-state solutions for the approximate method correspond closely to those from time integration. Further, Menq, Griffin, and Bielak [155] use a displacement-dependent normal load (which is equivalent to using the gain $F_{n,1}$ in the friction law of [57] cited in Eq. (7)) along with the bilinear hystersis element to model blade damper performance. They conclude that the *coupling ratio* (ie, the gain $F_{n,1}$) plays an important role in determining the point of optimal energy dissipation and therefore optimal blade design.

Menq and Griffin published a series of articles in the mid-1980s related to the forced response of frictionally-damped structures. Their efforts produced an improved partial slip model which allows for spatially-distributed interface response, a feature which contrasts strongly with many previous analyses using point contact models. [156] and [58] introduce this improved partial slip model and exercise the model on various systems for comparison to experimental results. The model is motivated by a continuous system, including an elastic bar on an elasto-plastic shear layer foundation (or alternately two elastic bars connected in a lap joint with an elasto-plastic shear layer). When the shear layer is strained, regions of stick and slip can develop, and the authors derive various equations describing the system response. The elastic stiffness of the shear layer plays a strong role in determining the system dynamic response, just as it does for the bilinear spring model described above. Experimental evidence is given to support the model, although in each case agreement between model and experiment requires calibration of partial slip model parameters.

Despite the requirement for model tuning, the Griffin and Menq partial slip model provides insight where others had failed: the interface response is spatially distributed, the full range of interface responses is considered (pure stick, partial slip, and pure slip), and good quantitative agreement with experiments can usually be achieved. The biggest liability of this partial slip model lies in choosing the model parameters. Indeed, subsequent work [157,158] suggests a damper optimization procedure requiring model calibration via a test program or historical data. The procedure suggested is not sufficiently well defined to guarantee that the model parameters derived from experimental data are unique. Nonetheless, it is clear that the Griffin and Menq model provides good value to the design process, and if properly tuned it can be effective in blade damper design.

Muszynska and Jones [159] use a hysteresis friction model and single-harmonic solutions to examine the blade vibration problem for both tuned and mistuned bladed disk problems. They allow for both frictional and elastic coupling between adjacent blades, and conclude that the friction coupling itself may be the source of mistuning. Other work in this area includes the effort of Wang and Shieh [160] and Wang and Chen [140], who examine turbine blade vibrations under conditions of velocity-dependent friction coefficient and higher-order HBM approximations. Two key results are demonstrated. First, [160] shows that velocity-dependent friction may have a significant impact on damper performance predictions for the one-mode structural model similar to that proposed by Griffin. In particular, the resonant frequency shift for both stiff and flexible dampers can be substantially *overestimated*—especially in the near optimal preload range—if velocity dependence is neglected. This emphasizes the prominent role of friction model in predicting damper performance. Furthermore, resonant stress amplitude in the near-optimal preload range is only affected slightly by the inclusion of velocity-dependent friction. A second critical result reveals the strength of nonlinearity in many friction damper problems. [140] presents a multi-term HBM approximation to the nonlinear solution and shows that in cases of near-optimal preload, the linearized response using a one-term HBM solution is substantially in error as compared to the three-term solution (which itself is very close to the time integration solution for the full nonlinear equations of motion). Their conclusion is two-fold: *i*) one-

term HBM solutions may neglect critical system dynamics (ie, nonlinearities) for relevant physical situations of near-optimal preload, and *ii*) three-term HBM solutions seem to provide an acceptable result as compared to time integration solutions.

Other relevant work includes the contributions of the group at Imperial College led by Sanliturk and Ewins. Their efforts have also focused on HBM analyses of bilinear hysteresis elements. Sanliturk, Imregun, and Ewins [161] express the hysteresis element as a complex stiffness amenable to frequency-domain analysis, with the bilinear hysteresis element parameters fit directly from experimental data. This interpretation allows convenient analysis using the HBM, and the results again reinforce the computational efficiency and accuracy (compared to time integration) of HBM. Later, Sanliturk, and Ewins [162] extend the work to consider 2D friction contact and return to the HBM for approximate solution of the governing equations. The HBM solution accurately predicts response amplitude as compared to the time integration solutions.

Beyond the inclusion of damper dynamics lies the question of appropriateness of approximations to the full nonlinear solution of any dynamic model including friction. Consider a single-dof system as shown in Fig. 6*a*, excited by harmonic tangential force of the form $F_q(t) = F_{q,1} \sin \omega_q t$, and studied by den Hartog under *constant* sliding friction coefficient. Potential system response under two parameter sets is shown schematically in Figs. 6*b* and *c*, where part *b* shows a case of very short duration sticking per cycle, and case *c* shows longer-duration sticking per cycle (these diagrams are similar to den Hartog's Fig. 3). If we overlay on each part of the figure a one-term harmonic approximation to the velocity response, we see clearly with only two HBM response parameters to adjust (magnitude and phase), only case *b* under limited sticking can be adequately captured. If the discussion is resricted to cases of $F_f < F_{q,1}$, then case *b* is only *weakly nonlinear*, and in fact if sticking is precluded, den Hartog shows that the solution under pure slip conditions is nearly harmonic (his Figure 2). On the contrary, it is clear that for more strongly nonlinear cases, a one-term approximation will not adequately capture the true dynamics.

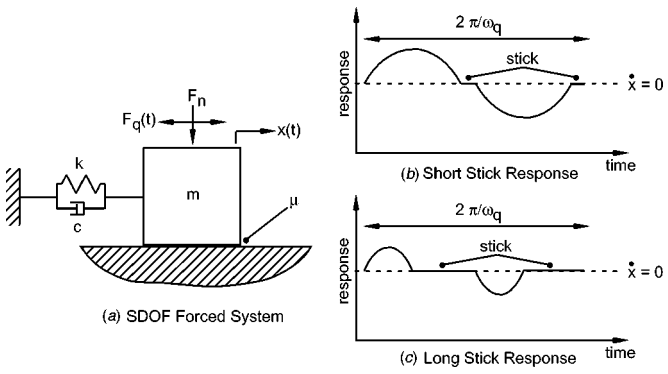

Fig. 6 Single-dof stick-slip oscillations, two possible cases: *a*) single-dof forced system, *b*) short stick response, *c*) long stick response

This issue becomes important for microslip analysis, because it has been reported that the optimal system damping is achieved under conditions of approximately 50% sticking per forcing cycle [138], ie, much closer to case *c* (strongly nonlinear) of Fig. 6 than to case *b* (weakly nonlinear). It is clear from Fig. 6 that a response with substantial sticking contains a great deal of high frequency information, and so it should not be surprising that single-term harmonic solutions do not capture the qualitative nature of the response—even if they do accurately predict the slip response amplitude. This is a critical feature of one-term solutions, because no energy is dissipated during the sticking segment of the response. As a result, the caveats in the literature seem relatively clear: *one-term HBM should be used with caution, particularly in parameter regions yielding substantial microslip (as opposed to almost pure slip or pure stick).*

However, there is an important distinction between the work of [138], and the work of den Hartog. In Griffin's work—and this is characteristic of bilinear hysteresis approaches—*the structural mass itself never experiences sticking*. Indeed, it is only the massless damper which may stick, and regardless of the kinematic state of the damper, the structural mass has a smooth response which is captured fairly accurately using a small number of harmonic functions. This is an important distinction which is explored more fully in Section 4.3.1.

The energy dissipation problem has been treated by both mechanics and dynamics researchers, with the recent emphasis lying on lumped-parameter models using bilinear hysteresis elements. In general, because damping in, for example, structural joints plays an important role in overall structural stiffness and vibration response, it is important to accurately represent friction energy dissipation. However, because the joint is one part in a much larger structure, computational demands favor the lowest model order possible for representing joint damping, and this usually leads to point-contact models with a limited number of friction parameters. As reported in Section 4, this low-order approach is reasonable, but not without its limitations.

2.7 Friction and stochastic processes

An important issue which has seen somewhat less attention in the friction and dynamic systems literature is the stochastic nature of dynamic surface interactions. The familiar static rough surface models proposed by Greenwood and Williamson [27] have been augmented and extended by many researchers, including Whitehouse and colleagues [163–165]. Whitehouse asserts that two important length parameters govern rough surface characterizations: the asperity rms height and the correlation length. The correlation length is on the order of (and perhaps slightly larger than) the asperity spacing—an important length scale which we have seen earlier. These analyses suggest, and our intuition supports, the notion that if the normal contact of rough surfaces is described non-deterministically, then certainly the sliding contact of rough surfaces will exhibit a similar non-deterministic nature. Indeed this is the case, as described by Kilburn [166] who shows that friction under nominally constant sliding

conditions can be described by a constant value plus broadband noise; the instantaneous coefficient of friction can be fit by a normal distribution. The suspicion that random normal contact vibrations play a critical role in friction's random nature has subsequently been examined by a number of authors who model or measure normal and/or tangential vibrations [28,29,37,39].

In itself, the observation that friction is a random process is important and helps us to explain and interpret experimental data. Certainly the random nature of friction will introduce some error into our quantitative predictions of friction behavior. But a more critical issue arises: does the randomness of the friction interface behavior play a *qualitative* role in the overall system response? A number of recent articles have examined this question, and we focus here on the work of Ibrahim and colleagues. Through their experimental work and modeling efforts [167–169], the authors have examined the stochastic dynamics of disc brake-type systems and they conclude that friction force probability density function is affected by normal load, becoming less Gaussian with increasing load. Moreover, they conclude that random friction force fluctuations of sufficient magnitude can indeed alter the qualitative character of the dynamic response, ie, change the stability of an equilibrium configuration. This is an important result which indicates the random component of friction force may be critical for successful modeling in some applications. This issue is also addressed by Hinrichs, Oestreigh, and Popp [73], who apply a bristle-type model to introduce random variation in friction force. They similarly conclude that random friction behavior has an important effect on (for example) bifurcation maps and other system response measures.

A related topic is that of response sensitivity. We have seen the role of random vibrations in dynamic system behavior, but the brake squeal literature also presents studies of general eigenvalue sensitivity and stability predictions. Primary contributions in this area include those of Brooks, Crolla, and colleagues, as well as Mottershead, Cartmell, and colleagues. First, Mottershead *et al* have examined the stability of elastic discs subject to friction loads on their surface, with either the disc stationary and the load rotating, or the disc rotating and load stationary [170–173]. These models include follower force approaches to friction (also found in [174]), as well as hybrid analytical/FE models for the rotor-pad-caliper system. The important results from these articles are the stability maps for variations in a number of problem parameters. A number of these maps—particularly those for friction and damping—show a striking sensitivity, with very small changes in system parameters resulting in qualitative response changes [170]. This aspect of the squeal problem is well established by experiments as well as everyday experience, and in large part explains why brake squeal remains an active, important research area. Further studies in sensitivity are more explicitly carried by Brooks *et al*, who use eigenvalue analysis to examine dynamic instabilities [175–177]. Sensitivity of squeal modes to important physical parameters such as contact locations, brake pad length, and brake pad material properties is explored. These studies illustrate that sensitivity of system response to not only friction parameters, but also operating conditions and physical properties, can be extreme in some cases. When coupled with the nonstationary nature of many friction-related problems, and the stochastic nature of friction itself, the sensitivity problem highlights the continued challenges of modeling systems with friction.

2.8 Friction and micro/nanoscale contacts

With the development over recent years of various micro- and nanoscale contact investigation tools, and the trend towards miniaturization in engineering and science, nano-scale science has become more accessible and better understood. Not surprisingly, friction has emerged as a dominant feature of small-scale contact which often limits performance, usability, fabrication, or other critical design criteria for small components. This is demonstrated dramatically in MEMS devices, where power requirements and failure (ie, stiction) are dominated by adhesive contact forces. This section is not intended as a comprehensive review of micro-scale or nanoscale developments; other excellent reviews have appeared over the past few years, and the interested reader is referred to them [178–180]. Rather, nano-scale observations of friction are examined here in light of their substantial similarity—on a qualitative level—to macro-scale friction experiments and models.

2.8.1 Adhesion in small-scale contacts

Small-scale contacts behave fundamentally different than their large-scale counterparts, and one of the most important reasons for this change in behavior is the importance of surface interactions (ie, adhesion). When surface energy approaches the same order of magnitude as other energy components of the system (elastic strain energy, kinetic energy), adhesive effects can become dominant, and this occurs readily at small-scale contacts. Close-range interactions between materials are governed by an interaction potential, the most well-known being the Lennard-Jones potential, which indicates the interaction strength as a function of separation distance. For very large distances, the interaction is very small, but for short distances on the order of a characteristic length z_o, the interaction can become substantial. This characteristic distance is related to the lattice spacing in the structure of the material, on the order of $1-10$ Å. So, by introducing an interaction potential into the problem, a new length scale is inherently integrated into the model. This is in stark contrast to traditional continuum mechanics, which possesses no inherent length scale. The usual approach to interaction modeling follows the Lennard-Jones (L-J) potential, given as:

$$\phi(z) = \frac{8w}{3z_o}\left[\left(\frac{z}{z_o}\right)^{-9} - \left(\frac{z}{z_o}\right)^{-3}\right] \tag{21}$$

where w is the work of adhesion, z_o is the equilibrium separation, and z is the actual separation. It is also customary to express the adhesion work in terms of surface energy γ, and L-J potential functions of this form are often encountered.

Early efforts toward integrating adhesion effects into contact mechanics solutions resulted in the well-known Johnson-Kendall-Roberts (JKR) model [181] for adhesion in normal contacts. Under Hertz-type elastic contact interactions, the JKR model predicts the role of adhesion snap-to-contact and pull-off force in small-scale contacts. JKR theory predicts only the role of adhesion in the contact pressure, and neglects contributions outside the Hertz contact zone (ie, where the surfaces are not in contact, but their separation is small enough that the interaction potential predicts a non-negligible force). This approach was later extended to include potential interactions outside the contact, and this view of adhesive contact was later unified by Tabor [182], who proposed a dimensionless parameter μ which compares the role of elastic energy and surface energy in contacts:

$$\mu = \left[\frac{Rw^2}{E^{*2} z_o^3} \right]^{1/3} \tag{22}$$

This parameter indicates regions of suitability of the various adhesion models developed and can be interpreted as the ratio of surface energy to elastic energy. Detailed *adhesion maps* have been constructed recently [183] to reveal the role of small-length-scale interactions in contact mechanics.

2.8.2 *Micro-scale measurements*

Micro-scale contact mechanics and friction measurements have been achieved using the surface force apparatus (SFA) (eg, [184]), shown schematically in Fig. 7. Thin sheets of mica, cleaved to be atomically smooth, are adhered to cylindrical glass substrates using epoxy; the cylinders are then brought into normal contact and tangential load is applied. The contact radius in SFA is on the order of 10–30 μm. Note that although the schematic shows the cylinders as being axially aligned, in general the cylinders contact in a crossed configuration, resulting in a general elliptical contact area. The surfaces are lubricated either by a liquid lubricant or by a pressure- and humidity-controlled ambient atmosphere. The SFA has been used to measure friction and lubrication properties of very thin luricant layers, down to a single Å, and can characterize sliding friction over several orders of magnitude of relative velocity. Further, a variety of interesting small-scale friction-related behavior have been observed, including atomic-scale stick-slip (Section 2.8.4) as well as a so-called *superkinetic* friction state [185].

2.8.3 *Nano-scale measurements*

Nano-scale contacts are relevant in the present discussion not for their fundamental nature and the interaction potential which governs attractive or repulsive forces, but rather for the measurement devices used to interrogate small-scale contacts. This discussion focuses on the atomic force microscope (AFM), but the spirit of the discussion is equally relevant to other apparatuses. AFM measurements are made using a cantilevered beam outfitted with a contact tip, typically of small radius on the order of 10–100 nm; see Fig. 8. By applying force at the root of the cantilever as shown, the tip contacts the specimen surface, and the tip can then be scanned across the surface at small sliding velocities V_o on the order of $10^2 - 10^4$ nm/s. Measurements are usually made using an optical system consisting of a laser which is reflected off the cantilever tip, with the light collected by a photodetector. The apparatus can be calibrated such that incident light on the photodetector can be correlated to cantilever motion, which in turn can be correlated to normal and tangential contact forces (see Fig. 8). Note that both bending and torsion of the cantilever occur as a result of the contact forces at the tip, F_n and F_t. Furthermore, the bending deflection u and the angular deflection θ are coupled through the geometry of the beam, and calibration and interpretation of the results can be challenging. Nonetheless, the AFM is a very versatile instrument which has been used for materials characterization, nanoscale friction testing, topology measurements, and a variety of other configurations. It has also been used to observe atomic-scale stick-slip behavior, which is the focus of the remainder of this discussion.

2.8.4 *Atomic-scale stick-slip*

Atomic-scale stick-slip behavior is shown schematically in Fig. 9; for concreteness, this discussion relates to AFM measurements, and atomic stick-slip is of interest here because: i) atomic-scale stick-slip response manifests itself as observable (ie, large scale) motion of the sensing cantilever; and ii) the cantilever structure can be treated with traditional continuum mechanics models. Measurement of stick-slip response in nano-contacts relies not only upon the details of the contact interactions, but also upon the measurement system, and in this sense atomic-scale stick-slip appears to be no different than macro-scale stick-slip. The sticking portion of the cycle allows elastic strain energy to build in the system, and in AFM measurements this includes deformation of the

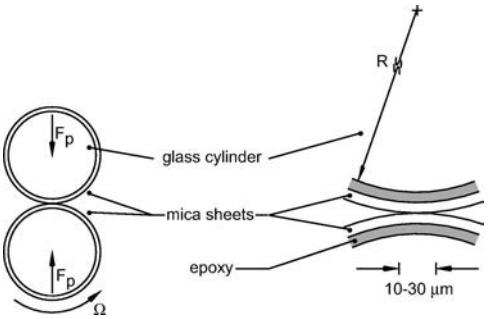

Fig. 7 SFA experiment schematic showing glass substrate, epoxy, and atomically-smooth mica sheets

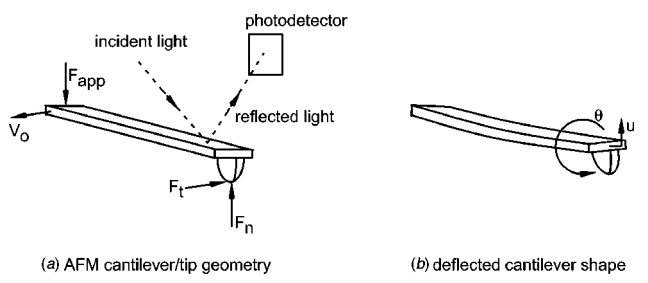

Fig. 8 AFM experiment schematic: *a*) AFM cantilever and tip, with incident light for displacement measurement, *b*) AFM cantilever deformed shape

cantilever and tip. During slipping the elastic energy is released and the displacement relaxes, and energy is dissipated due to contact dissipative mechanisms, heating, material hysteresis, etc. In this sense, atomic-scale stick-slip shares many similarities with macro-scale observations, and indeed Fig. 9 bears a resemblance to Fig. 18 for a macro-scale system.

Various observations in small-scale contact investigations reveal behavior conspicuously similar to that observed at the macro-scale. For example, it has been observed [186] that relatively compliant cantilevers in AFM experiments are more likely to result in atomic-scale stick-slip than stiffer cantilevers. This conclusion is supported by a large number of observations from the tribology, controls, and geomechanics literature. Further similarities to macro-scale observations relate to a critical slip velocity (scan rate in AFM experiments) above which stick-slip is extinguished, and this again is a well-known result from the tribology literature. On the macro-scale, the mechanism of this behavior is the velocity-dependence of friction, and for small-scale contact it might be suspected that some rate-dependent interaction is responsible, although this has yet to be proven.

Many researchers have noted the existence of a critical system velocity above which atomic stick-slip is extinguished (eg, [187,188]). Note further that a critical system stiffness (above which no stick-slip is observated) results from friction constitutive behavior *which possesses some inherent length scale* (see [24,76], others). Here, the length scale inherent in the friction law is the physical connection to macro-scale systems. As described above, the lattice spacing of the material is the important length scale in nano-scale contacts, as it directly influences the potential interaction of the tip-specimen interface. The lattice spacing, scan rate, and system stiffness have all been implicated in atomic stick-slip observations, and their synergy seems to produce observations not inconsistent with those made at the macro scale.

The key analogy to macro-scale systems is now more clear: stick-slip processes at the micro- and nano-scale are the build-up and subsequent relaxation of elastic strain energy in the structure, just as in macro-scale systems. Further, the observation of a critical system velocity and a critical system stiffness above which stick-slip is extinguished follows closely the macro-scale observations. Further, there is another important analogy to macro-scale systems. The friction observation in both SFA and AFM experiments is achieved using sensing elements which are large compared to the contact size, and therefore our interpretation of friction is critically dependent on interface interactions occurring on a length scale *much smaller than the length scale of the sensing element*. For example, the AFM cantilever is a micro-scale component, with a 10–100 nm tip radius, capturing variations in friction occurring over only 1–10 Å. Indeed, for reciprocating sliding in nano-scale experiments, hysteresis loops of the form shown in Fig. 24 can be observed with a short-wavelength stick-slip event superimposed [189]. The wavelength of this stick-slip event is the characteristic lattice spacing, roughly 1–5 Å. So, while the fundamental physics governing micro- and nano-scale component interactions are quite different than a traditional macro-scale Coulomb-type friction law (or even a length-scale law like general rate- and state-dependence) the qualitative character of many small-scale observations closely resembles those on a larger length scale. While this observation does not allow us to comment on the fundamental nature of small-scale surface interactions, we can draw some general conclusions about friction and simulation across diverse length scales.

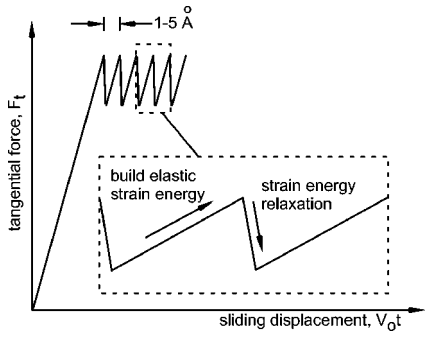

Fig. 9 Atomic-scale stick-slip response

2.9 Modeling summary

Despite the large variation in applications and interests across the tribology, controls, dynamics, geomechanics, contact mechanics, aeromechanics, and mechanics of materials communities, several common themes have emerged. First, velocity-dependent friction is almost universally used, and in fact this form of parameter dependence allows prediction of a key physical mechanism to controlling friction-excited oscillations: larger system damping promotes stability. Further, other physical mechanisms have been observed in different applications. The friction memory models and the general state- and rate-dependent friction laws possess the common feature of a critical length or time scale over which the sliding friction force evolves to a steady-state value. This length (time) scale has been linked to surface roughness characteristics including asperity spacing, which also has implications in low-amplitude fretting analyses and observations of contact-size-dependent fatigue life.

But the overwhelming theme in the literature presented here is that *friction response* is intimately related not only to interface descriptions, but also to system dynamics. Indeed, in each case listed above the interface friction constitutive behavior manifests itself in a variety of ways, but a *critical system dynamic parameter* could often be predicted to suppress unwanted friction-excited behavior. In this way, it becomes clear that the choice of system dynamic model and the choice of friction model are closely coupled. Furthermore, it seems that two fundamental varieties of system modeling approaches have emerged (see Table 6).

Each modeling option has implications on the dynamic system simulation, including both computational cost and formulation complexity. Indeed, a common theme across the literature seems to be that small-scale contact interactions play a very significant role in determining system performance or durability. Energy dissipation and fretting fatigue

Table 6. Low-order and high-order approaches to modeling dynamic systems with friction

Model	Low-Order	High-Order
structural friction	lumped model with <5 dof's point contact with simple parameters dependence	FEM or modal for continuous system dynamics sophisticated parameter dependence (eg, LuGre model with six friction parameters) or continuous contact model with partial slip

are both extremely sensitive to the highly localized details of contact interactions, including the stick zone size and slip displacement. Steady-sliding stability in engineering or geomechanics systems is sensitive to contact details over some critical slip displacement d_c which is on the order of the asperity spacing, or perhaps the elastic coherence length $\xi \gg d_c$. Control strategies and controller gains are influenced also by state- and rate-dependence of interface response. The challenge which has been recognized so far in the literature is that the dynamic model must be sufficiently sophisticated to capture surface interactions on the small length scale, and in the next section, some example results from a variety of applications are presented to illustrate the use and impact of various friction and dynamic models.

3 SELF-EXCITED VIBRATIONS OF SYSTEMS WITH FRICTION

In this section, a variety of friction models are introduced and applied to a simple one-dof friction-excited system as shown in Fig. 10. The general equation of motion for this system is given by:

$$m\ddot{x}+c\dot{x}+kx=F_f(\dot{x},x,t,F_n,\ldots) \tag{23}$$

where

$$F_f=\mu F_n \tag{24}$$

and both μ and F_n can possess general parameter dependence. The conclusions of this section are two-fold: *i*) dynamic system response is intimately tied to both the structural model and the interface model, and *ii*) a large variety of dynamic responses can be predicted using different combinations of structural and friction model.

First, steady-sliding stability calculations are introduced, beginning with low-order friction models and progressing to models with more sophisticated forms of parameter dependence. Then, self-excited, stick-slip oscillations are introduced and their characteristics examined. First, we define the notation for the sliding configurations in Fig. 10 as follows. For a reference velocity V_o of the moving surface, the relative velocity is defined as:

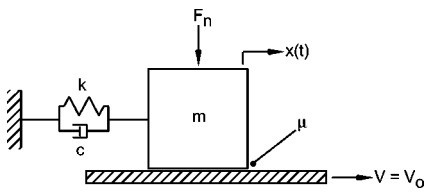

Fig. 10 Single-dof structural model for study of self-excited problems

$$V_{\text{rel}}=V_o-\dot{x} \tag{25}$$

with two special cases of motion possible:

$$\text{steady sliding:}\quad \dot{x}=0\Rightarrow V_{\text{rel}}=V_o \tag{26}$$

$$\text{sticking:}\quad \dot{x}=V_o\Rightarrow V_{\text{rel}}=0 \tag{27}$$

3.1 Constant and velocity-dependent friction coefficient

The most prominent friction model in the system dynamics literature is given by a simple velocity dependence, often assumed to be monotonically weakening with increasing velocity. In general a monotonic sliding friction coefficient can be described by a functional relationship to relative velocity and three independent friction parameters:

$$\mu(V_{\text{rel}};\mu_o,\mu_1,\alpha)=\mu_o+\mu_1\exp(-\alpha|V_{\text{rel}}|) \tag{28}$$

The parameter μ_o governs the large relative velocity behavior, μ_1 controls the low velocity behavior, and $\alpha>0$ controls the rate of change of friction with changes in relative velocity; this is shown schematically in Fig. 11. With a friction coefficient defined as in Eq. (28), the sign of μ_1 corresponds inversely to the sign of the friction curve slope (the importance of this will become apparent later).

When the friction law of Eq. (28) is applied to the single-DOF system with constant normal force, the following equation can be derived for sliding motion:

$$m\ddot{x}+c\dot{x}+kx=[\mu_o+\mu_1\exp(-\alpha|V_{\text{rel}}|)]F_n \tag{29}$$

It will be helpful to normalize this equation using the following scaling parameters:

$$\omega_n=\sqrt{\frac{k}{m}} \tag{30}$$

$$\tau=\omega_n t \tag{31}$$

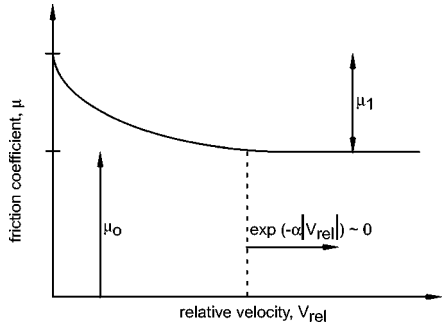

Fig. 11 Velocity-dependent friction curve showing dependence upon three independent parameters (μ_o,μ_1,α)

$$x_{\mathrm{st}}=\frac{\mu_o F_n}{k}\Rightarrow\hat{x}=\frac{x}{x_{\mathrm{st}}} \tag{32}$$

$$\frac{d}{dt}=\omega_n\frac{d}{d\tau}=\omega_n(\cdots)' \tag{33}$$

$$\frac{d^2}{dt^2}=\omega_n^2\frac{d^2}{d\tau^2}=\omega_n^2(\cdots)'' \tag{34}$$

$$\hat{V}_{\mathrm{rel}}=\frac{V_{\mathrm{rel}}}{\omega_n x_{st}} \tag{35}$$

which results in the following dimensionless equation:

$$\hat{x}''+2\xi\hat{x}'+\hat{x}=1+\hat{\mu}_1\exp(-\hat{\alpha}|\hat{V}_{\mathrm{rel}}|) \tag{36}$$

where $\xi=c/\sqrt{km}$ and $\hat{\mu}_1=\mu_1/\mu_o$ and the friction coefficient is a normalized function of $\hat{V}_{\mathrm{rel}}$.

3.1.1 Constant friction coefficient

The case of constant friction coefficient can be easily extracted from Eq. (36) by setting $\hat{\mu}_1=0$. The result is a linear, second-order differential equation with constant forcing whose homogeneous solution is stable for all $\xi>0$. The long-time solution is $\hat{x}\to 1$ as $t\to\infty$. For this structural model, which is linear with constant coefficients, an unstable response can *only* result from negative viscous damping of the structure, and the friction law *cannot* drive an unstable response. Furthermore, it is the homogeneous solution which becomes unstable under negative viscous damping, indicating a truly self-excited response.

3.1.2 Velocity-dependent friction

For the case of velocity-dependent friction, the question of steady sliding stability requires more analysis. The right-hand-side of Eq. (36) can be linearized via Taylor series about the steady sliding equilibrium point $\hat{V}_{\mathrm{rel}}=\hat{V}_o$, with the following result:

$$\hat{x}''+2\xi\hat{x}'+\hat{x}=1-\underbrace{(-\hat{\alpha})\hat{\mu}_1\exp(-\hat{\alpha}|\hat{V}_o|)}_{S}\hat{x}' \tag{37}$$

The linearized governing Eq. (37) can be mapped into a state space with two state variables: $(\hat{x},\hat{x}')\Rightarrow(a,b)$. The resulting first-order system equations are:

$$\begin{Bmatrix}a'\\b'\end{Bmatrix}=\begin{bmatrix}0 & 1\\ -1 & -(2\xi+S)\end{bmatrix}\begin{Bmatrix}a\\b\end{Bmatrix}+\begin{Bmatrix}0\\1\end{Bmatrix} \tag{38}$$

Eigenvalues of the coefficient matrix are:

$$\lambda_{1,2}=\frac{-(2\xi+S)\pm\sqrt{(2\xi+S)^2-4}}{2} \tag{39}$$

clearly indicating that the steady-sliding equilibrium point is stable for:

$$2\xi>-S\Rightarrow 2\xi>\hat{\alpha}\hat{\mu}_1\exp(-\hat{\alpha}|\hat{V}_o|) \tag{40}$$

This classical result shows that the *negative slope* of the friction curve (ie, $\hat{\mu}_1>0$) is a necessary, but not sufficient, condition for steady sliding instability of systems like this one. A stability map in the parameter space $(\hat{\mu}_1,\hat{\alpha})$ can be developed from Eq. (40). Figure 12 shows a map of the parameter space for the case $\xi=0.05$, with a family of curves indicating the stability boundary for a number of different reference velocities. Each line on the map corresponds to the marginal stability condition for which $2\xi+S=0$. Above each line, the equilibrium point is unstable, and below each line the equilibrium point is stable. Note that the steady sliding stability of single-dof systems with friction defined as in Eq. (28) is *independent* of the parameter $\hat{\mu}_o=1$.

3.2 Time- or displacement-dependent normal forces

It is difficult to envision a real engineering system in which the normal contact force is either temporally or spatially constant. Motion-dependent (ie, displacement-dependent) normal forces arise naturally as a result of the function of the component; in addition, a component may operate in an environment which exposes it to a variety of time-dependent external forces possibly unrelated to its motion. In fact, a number of researchers have examined the profound influence that normal force variations can have on steady sliding stability, due to either friction excitation or some form of dynamic coupling/internal resonance phenomena.

Berger, Krousgrill, and Sadeghi [60] have demonstrated an unstable steady sliding solution related to time-dependent normal forces. For the system shown in Fig. 10, we assume the normal force F_n is composed of two parts:

$$\hat{F}_n(\tau)=\hat{F}_{n,o}+\hat{F}_{n,1}\sin\Omega\tau \tag{41}$$

where $\hat{F}_{n,1}\sin\Omega\tau$ is possibly the result of external inputs or represents normal force fluctuations due to normal contact vibrations. The equation of motion for the system is:

$$\hat{x}''+2\xi\hat{x}'+\hat{x}=1+\hat{F}_{n,1}\sin(\Omega\tau)+\hat{\mu}_1\exp(-\hat{\alpha}|\hat{V}_{\mathrm{rel}}|)+\hat{\mu}_1\hat{F}_{n,1}\exp(-\hat{\alpha}|\hat{V}_{\mathrm{rel}}|)\sin(\Omega\tau) \tag{42}$$

which is similar in form to Eq. (36), with the addition of a dimensionless time-dependent normal force $\hat{F}_{n,1}(\tau)=F_{n,1}(\tau)/F_{n,o}$. The linearized form of Eq. (42), analogous to Eq. (37), is:

$$\hat{x}''+2\xi\hat{x}'+\hat{x}=1+\hat{F}_{n,1}\sin(\Omega\tau)-S[1+\hat{F}_{n,1}\sin(\Omega\tau)]\hat{x}' \tag{43}$$

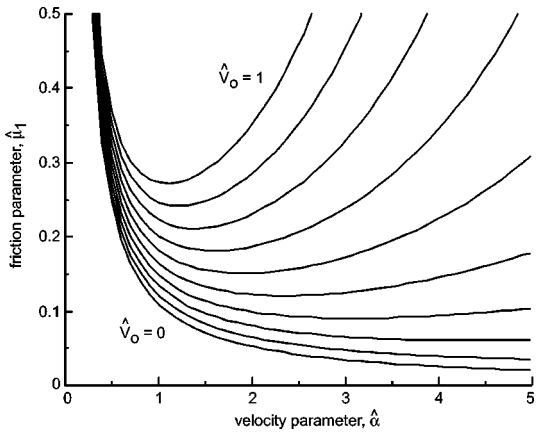

Fig. 12 Stability map for velocity-dependent friction and single-dof structural model

Table 7. Stability criteria for a single-dof system with time-dependent (harmonic) normal force

Frequency Tuning	Stability Criterion	Comment
$\Omega \approx \frac{1}{2}$	$\delta > 0$	negative slope instability only
$\Omega \approx 1$	$\delta > 0$	negative slope instability only
$\Omega \approx 2$	$\gamma < 2\sqrt{\delta^2 + (\Omega - 2)^2}$	parametric instability

where S has the same definition as in Eq. (37).

Another change of coordinates $y = \hat{x} - 1$, and isolating the y' terms on the left-hand-side, results in:

$$y'' + [\,\delta + \gamma \sin(\Omega\tau)\,]y' + y = \hat{F}_{n,1} \sin(\Omega\tau) \tag{44}$$

where $\delta = 2\xi + S$ and $\gamma = S\hat{F}_{n,1}$. Equation (44) is a linear, parametrically-excited second-order differential equation, and as such may exhibit (friction-excited) parametric dynamic instabilities. A steady-sliding stability analysis of this system can be carried out using the method of averaging. Using a coordinate transformation of the form $(y, y') \Rightarrow (a, b)$, the stability criteria of Table 7 can be developed for the three frequency tuning cases of interest, which are the primary (linear) resonance $\Omega \approx 1$, the 1/2-subharmonic resonance $\Omega \approx 1/2$, and the traditional parametric resonance $\Omega \approx 2$. The parameter ε indicates the tuning relationship for each resonance case; for example, the parametric resonance frequency tuning parameter is $\varepsilon = \Omega - 2$.

The information in Table 7 can be used to develop a stability equation in the parameter space including $[\xi, \hat{F}_{n,1}, \varepsilon, S]$. By substituting the definitions of the parameters γ and δ into the parametric resonance stability criterion, the following quadratic equation for the critical value of friction curve slope S_{crit} emerges:

$$(\hat{F}_{n,1}^2 - 4)S_{\text{crit}}^2 - 16\xi S_{\text{crit}} - 4(4\xi^2 + \varepsilon^2) = 0 \tag{45}$$

Figure 13 shows stability maps for two different values of frequency tuning $\varepsilon = \Omega - 2$ near the parametric resonance. Each contour represents that critical value of friction curve slope S for which the response in the $(\xi, \hat{F}_{n,1})$ parameter space becomes unstable. The stability map indicates that for a given damping value ξ, frequency tuning ε, and friction curve slope S, the oscillatory part of the normal force must lie within a specified envelope for a steady-sliding instability to appear. First, notice that there are two branches of each stability contour, corresponding to the two roots of the quadratic Eq. (45). Further, note that at the convergence of the two branches in the parameter space, both *real* solutions disappear in favor of complex solutions (and thus non-physical values for friction curve slope). Second, for a given frequency tuning (say, $\varepsilon = 0.001$), a higher system damping ξ requires a more negative friction curve slope to induce an instability; this is consistent with the conclusions from simple velocity-dependent friction. Next, as the frequency mistuning $|\varepsilon|$ increases, a more negative friction curve slope is required to promote an instability. The general characteristics of both parts of the figure—that is, the roughly parabolic nature of the stability boundary branches and the general decreasing trend indicated by the dashed line—are strongly reminscent of stability solutions for other parametrically-excited systems such as Mathieu's equation; see [190] for more details. In addition, parametric instability has been identified as a mechanism of disc brake squeal; see [170,171] for examples. Finally, note that in general the existence of a steady-sliding instability of this sort is restricted to a fairly small segment of the parameter space, including large friction curve slopes and good frequency tuning $\varepsilon \to 0$.

3.3 Rate- and state-dependent friction

The geomechanics community has developed a class of general friction constitutive laws for use in simulation of earthquake events, although these models have been applied to a variety of other problems as well. Earthquakes arise due to unstable steady sliding events, and Rice has devoted considerable research effort to their modeling and analysis. He formulated a general rate- and state-dependent friction law [24] of the form in Eq. (18), where τ_f is the frictional shear stress at the interface, V_{rel} is the relative sliding velocity, and the θ_i are interfacial *states* related to potentially time-evolving contact conditions. The characteristics of the friction model of Eq. (18) are shown schematically in Fig. 14. For a step change in the sliding velocity V_{rel} from V_o to $V_o + \Delta V$ at time $t = t'$, the corresponding change in friction shear stress is composed of an instantaneous reaction $(f\Delta V)$ and an evolutionary part $h(t - t')\Delta V$, which occurs over a critical slip distance d_c. The requirements for this model include:

$$\lim_{(t-t')\to\infty} \tau_f(V_{\text{rel}}, \theta_1, \theta_1, \ldots) \to \tau_{ss}(V_{\text{rel}}) \tag{46}$$

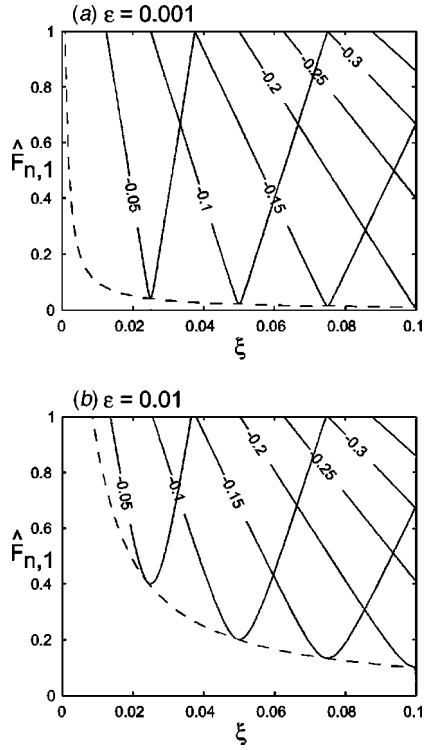

Fig. 13 Stability map for velocity-dependent friction and single-dof structural model, with time-dependent normal force: *a)* $\varepsilon = 0.001$, *b)* $\varepsilon = 0.01$

indicating that the friction shear stress evolves to a steady state value which is only a function of the sliding velocity V_{rel}. The instantaneous jump in friction shear stress generally follows:

$$\frac{\partial \tau_f}{\partial V_{\text{rel}}} > 0 \tag{47}$$

such that step increases in velocity induce increases in frictional shear. Furthermore, the steady-state frictional shear description is consistent with a large variety of other experimental observations, ie, it has a negative slope:

$$\frac{d\tau_{ss}}{dV_{\text{rel}}} < 0 \tag{48}$$

(where these are no longer partial derivatives because the steady-state frictional shear is a function of sliding velocity alone). Finally, $h(t)$ can be modeled as a monotonically decreasing function, often a first-order impulse response:

$$h(t) = h_o \exp(-\alpha t) \tag{49}$$

(where α is a characteristic decay time) and because $f > 0$

$$\int_0^\infty h(t)dt > f \tag{50}$$

to ensure the negative slope condition (48).

Rice then suggests a specific form of Eq. (49), namely $h_o = (1+\lambda) f\alpha$, which results in:

$$\frac{d\tau_{ss}}{dV_{\text{rel}}} = -\lambda f \tag{51}$$

which is independent of the decay time α and the size of the velocity perturbation ΔV. The resulting equation of motion for the sdof system governed by this sort of friction relation is a perturbation of Eq. (36):

$$\hat{x}'' + 2\xi\hat{x}' + \hat{x} + f\hat{x}' - \int_0^t (1+\lambda) f\alpha \times \exp[-\alpha(t-t')]\hat{x}'(t')dt' = \hat{q}(t) \tag{52}$$

where $\hat{q}(t)$ is an arbitrary small perturbing force applied at $t = 0$ which disturbs the equilibrium position and potentially triggers the steady-sliding instability. In Rice's original presentation [24], explicit damping of the form ξ in Eq. (52) was not considered. However, it is trivial to include it in the steady-sliding stability analysis because it manifests itself as a larger positive instantaneous damping in the friction constitutive relation; ie, $f' = f + 2\xi$. The result is that the steady-state friction curve slope required to overcome the combined effects of system damping ξ and positive viscous damping f must be *larger*—more negative—in order to promote a steady-sliding instability. In subsequent analysis, we assume that the parameter f includes such system damping. The stability analysis, presented by Rice as a root locus-type analysis, yields a characteristic equation in the s-domain which is *independent* of the perturbation function $\hat{q}(t)$ (which appears in the numerator of the system input-output relation). Roots of the characteristic equation with positive real parts indicate parameter combinations for which steady-sliding motion is unstable.

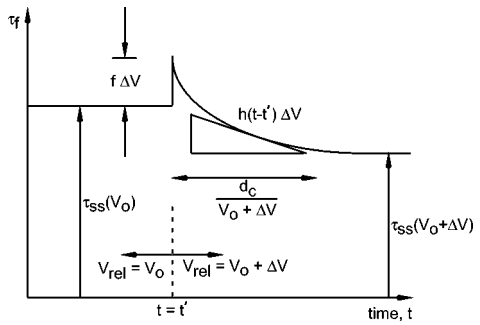

Fig. 14 Step-plus-evolutionary response of state-variable friction laws to step changes in sliding velocity

The resulting stability analysis predicts a critical stiffness above which steady sliding is stable; Rice's original equation can be written:

$$k_{cr} = -\frac{V_o}{d_c}\frac{d\tau_{ss}}{dV_{\text{rel}}}\left[1 + \frac{mV_o}{d_c\dfrac{\partial\tau}{\partial V_{\text{rel}}}}\right] \tag{53}$$

where d_c is the critical slip distance over which frictional shear stress evolution takes place; Rice notes that d_c is largely independent of V_o. It should be reinforced that this stability criterion, despite the presence of the linearized friction curve slope $S = \dfrac{d\tau_{ss}}{dV_{\text{rel}}}$ in the equation, is distinct from other negative-slope instabilities in that it also relies upon the slip history effects. The outcome is a prediction of critical system *stiffness* for steady sliding stability, where traditional analyses of negative-slope instabilities predicts a critical *damping* value.

This result can be rewritten in a dimensionless form by using a normalization procedure developed previously, except that in this case we choose the reference length for the problem x_{st} to be equal to the critical slip distance d_c. Then, several important dimensionless groups emerge:

$$\hat{V} = \frac{V_o}{d_c\omega_n} = \frac{V_o}{d_c}\sqrt{\frac{m}{k}} \qquad \text{dimensionless velocity} \tag{54}$$

$$\hat{f} = \frac{\partial\hat{\tau}}{\partial\hat{V}} = \frac{1}{m\omega_n}\frac{\partial\tau}{\partial V_{\text{rel}}} = \frac{1}{\sqrt{mk}}\frac{\partial\tau}{\partial V_{\text{rel}}} \quad \text{dimensionless instantaneous viscosity} \tag{55}$$

$$\hat{S} = \frac{d\hat{\tau}_{ss}}{d\hat{V}} = \frac{1}{m\omega_n}\frac{d\hat{\tau}_{ss}}{dV_{\text{rel}}} = \frac{1}{\sqrt{mk}}\frac{d\tau_{ss}}{dV} \quad \text{steady-state friction curve slope} \tag{56}$$

These equations introduce three composite friction-system dynamic parameters in a natural way, linking a critical friction length scale (d_c) to a system-dependent time scale (ω_n) and other friction parameters. Introducing this length scale into the problem has the most impact on the dimensionless velocity $\hat{V}$, which is now an expression of the sliding velocity, the critical slip distance, and the system natural frequency. The critical stiffness Eq. (53) can now be rewritten as:

$$\frac{k_{cr}}{k} = -\hat{V}\hat{S}\left[1+\frac{\hat{V}}{\hat{f}}\right] \tag{57}$$

We can now examine the three-parameter space $(\hat{V},\hat{S},\hat{f})$, which represents combinations of friction and system dynamic parameters for steady-sliding stability by recognizing the stability boundary in the parameter space is defined as $k_{cr}=k$:

$$-\hat{V}\hat{S}\left[1+\frac{\hat{V}}{\hat{f}}\right]=1 \Rightarrow \frac{1}{\hat{f}}\hat{V}^2+\hat{S}\hat{V}+1=0 \tag{58}$$

which has real solutions for $\hat{V}$ only if $\hat{S}^2>4/\hat{f}$. Figure 15 shows the stability boundary on the $(\hat{V},\hat{S})$ parameter plane as a solid line for various values of $\hat{f}$. Note that in the plot, no specific friction constitutive model has been considered, and the three parameters are considered to be *independent*. Nonetheless, the figure demonstrates the regions of the parameter space in which one of the parameters dominates the stability condition. First note that above each solid line on the plane, the values of $k_{cr}/k>1$, ie, the response is unstable. For points below each line, the response is stable. There also exists a region of the parameter space of *unconditional instability* corresponding to the region above the dashed line on the figure. This boundary can be defined by massaging Eq. (57) to show:

$$1+\frac{\hat{V}}{\hat{f}}=\frac{1}{-\hat{V}\hat{S}} \Rightarrow 1 \geqslant -\hat{V}\hat{S} \tag{59}$$

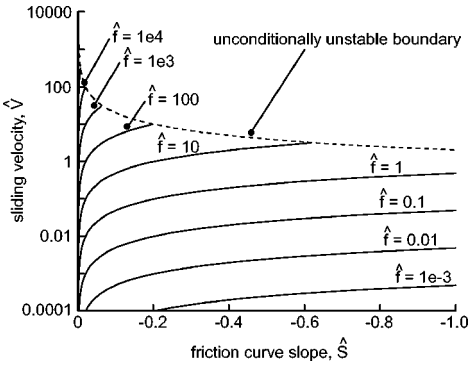

Fig. 15 Stability map in the $(\hat{S},\hat{V},\hat{f})$ parameter space: a family of stability boundaries (solid lines) above which the steady-sliding response is unstable; response is unconditionally unstable above dashed line

which can be derived by considering the underlying constraints $\hat{f}>0$, $\hat{V}>0$, and $\hat{S}<0$. The dashed line on the figure is the hyperbola $-\hat{V}\hat{S}=1$, and above this line $k_{cr}/k>1$ and the steady-sliding response is unstable, *regardless* of the instantaneous viscosity $\hat{f}$. The general trend of the result is that for a given sliding velocity, either a large instantaneous viscosity $\hat{f}$ or a large steady-state slope $(-\hat{S})$ is required to drive an unstable steady-sliding response.

The existence of a steady-sliding instability depends upon the evolution of the friction shear stress from the moment immediately after the velocity change, say t'^{+}, until it converges to the value $\tau_{ss}(V_o+\Delta V)$. Specifically, the total shear evolution must occur over a sufficiently short time scale, and the ratio of these (consider Fig. 14) is:

$$\frac{\Delta\tau_f}{\Delta t}=\frac{(f-S)\Delta V}{\dfrac{d_c}{V_o+\Delta V}} \tag{60}$$

which indicates that a large *evolutionary slope*—defined as $S_e=\Delta\tau_f/\Delta t$—can be achieved by having f large, $(-S)$ large, or d_c small. The evolutionary slope is a composite function of the instantaneous and steady-state viscosities, and therefore presents a picture of the contributions of each to steady-sliding instabilities. The key is that both larger shear evolution $(f-S)\Delta V$ and smaller critical slip distance d_c tend to be destabilizing mechanisms. Further consideration of the normalization scheme used here shows that increasing mass m tends to destabilize the system, a conclusion previously stated by Rice.

It should be noted that a wide variety of experiments from the geomechanics community support the state-dependent friction model discussed here. In addition, a number of experiments on engineering-scale systems have indicated the existence of a critical stiffness which suppresses friction-induced vibration (specifically stick-slip). Because a critical stiffness cannot be predicted from a simple velocity-dependent friction law, it seems clear the Rice model includes an important effect that other friction models neglect. Finally, it should be mentioned that similar instantaneous-plus-evolutionary friction behavior has been observed under step changes in normal load as well.

An interesting connection to other work in the friction area can be made by developing a *discrete analog* of the Rice model—that is, a lumped parameter model similar to the Iwan models discussed in Section 2.5. In order to capture the instantaneous-plus-evolutionary behavior of the friction relation of Fig. 14, a lumped model of the form shown in Fig. 16 is proposed. The nodes in the model are labeled a,b,c; the spring of stiffness k_v is in series with the Coulomb damper with friction force $F_f(\dot{u}_c)$ and a discrete viscous damping element described by the parameter c_v. The total reaction force provided by this collection of discrete elements is F_v. Consider a steady-sliding condition in which all components translate at a velocity V_o such that $\dot{u}_a=\dot{u}_b=\dot{u}_c=V_o$. For a step change in velocity ΔV at node a at time $t=t'$, the dashpot (ie, $\dot{u}_b-\dot{u}_a$) *will not* respond instantaneously, and therefore all instantaneous response results in compression of the spring and an increase in the spring force of $k_v\Delta u_{bc}$,

where $\Delta u_{bc} = u_c(t') - u_b(t')$. This corresponds to Rice's positive instantaneous viscosity term f. The spring force then relaxes over time as the dashpot responds, and if we postulate further that the Coulomb damper force is a weakening function of sliding velocity $F_f = F_f(\dot{u}_c)$, the friction force model can be described in terms of the lumped parameters as follows. For a step change in velocity ΔV at time $t = t'$,

$$F_v(t-t') = F_f(V_o + \Delta V) + h_o \exp\left[-\frac{(t-t')}{\tau_r}\right] \tag{61}$$

where

$$h_o = k_v \Delta u_{bc} - \left.\frac{dF_f}{dV_{\text{rel}}}\right|_{V_o} \Delta V \tag{62}$$

$$\tau_r = \frac{c_v}{k_v} \tag{63}$$

The critical slip displacement d_c of Fig. 14 manifests itself here in the relaxation time τ_r for the model, and therefore the equivalent dashpot parameter c_v is related to d_c and the sliding velocity V_o. This lumped model obeys all of the same criteria put forth by Rice:

instantaneous positive viscosity:	$\dfrac{\partial F_v}{\partial V_{\text{rel}}} > 0$
general rate weakening:	$\dfrac{dF_f}{dV_{\text{rel}}} < 0$
limiting behavior:	$F_v(V_o) \to F_f(V_o)$; $(t-t') \to \infty$

and of course the discrete model parameters have relationships to the continuous model. Note that this model actually has important physical appeal for situations other than steady sliding, ie, sticking. The spring and dashpot in parallel also allow nonlinear pre-slip displacement of a friction interface, similar to that observed in creep experiments under variations in applied stress. Although Iwan has proposed collections of simple spring-Coulomb damper elements for pre-slip displacement modeling, that approach develops a piecewise-linear fit to experimental data which requires a large number of bilinear hysteresis elements to yield a high-fidelity model. On the other hand, for changes in applied force at node a, the lumped-parameter model proposed above shows time-dependent strain response until the applied force overcomes the limiting friction value and slipping ensues.

This argument simply recasts the friction behavior as a viscoelastic material model (specifically a Maxwell model) with parameters k_v and c_v, although it differs slightly from traditional Maxwell models in that the parameters (including F_f) will in general be a function of the sliding velocity $\dot{u}_c$. This suggested model is highly nonlinear and no results are presented here. This interpretation does however provide a link to the seminal work of Iwan [119] who proposed spring-Coulomb damper series models for elasto-plastic material behavior. The so-called bilinear hysteresis element has enjoyed wide success in friction modeling (as described elsewhere in this article), and perhaps the Rice model of rate- and state-dependent friction can be viewed as an important extension to the Iwan family of models which implements a critical slip displacement d_c.

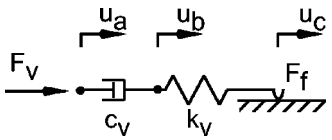

Fig. 16 Lumped-parameter (viscoelastic) model for rate- and state-dependent friction

Table 8. Summary of transition criteria for stick-slip oscillations

Transition	Criteria
slip-to-stick	(i) $\hat{x}' = 0$ (ii) $\hat{F}_f < \hat{F}_s$
stick-to-slip	$\hat{F}_f = \hat{F}_s$

3.4 Stick-slip oscillations

The steady-sliding stability calculations reported in the previous section rely largely upon linearization techniques and traditional stability analyses for response predictions. But linearization approaches predict time responses for the linearized, homogeneous system which exhibit one of three possible responses:

i) stable—response asymptotically approaches zero
ii) marginally stable—response neither grows nor decays
iii) unstable—response grows unbounded

However, the response of the nonlinear system is typically bounded by the nonlinearity itself, and one mechanism of this is for the system to achieve a stick-slip limit cycle.

We first consider the appropriate governing equations for stick-slip oscillations. For the single-dof system described above sliding against a surface moving at a constant reference velocity V_o, the equations of motion can be summarized:

$$\text{slipping:} \quad \hat{x}'' + 2\xi\hat{x}' + \hat{x} = \hat{F}_f; \quad \hat{F}_f = \mu\hat{F}_n \tag{64}$$

$$\text{sticking:} \quad \hat{x}' = \hat{V}_o \quad (\hat{x}'' = 0) \tag{65}$$

Note here that under slipping conditions, the motion of the system is unknown and is described by a second-order nonlinear differential equation, and the friction force is known. Under sticking conditions, the motion is prescribed by a kinematic constraint equation, and the friction force, which can be interpreted as a kinematic constraint force, is unknown. During sticking, the friction force must obey the inequality constraint:

$$\hat{F}_f \leqslant \hat{F}_s \tag{66}$$

where $\hat{F}_s$ is the limiting value of sticking friction. The largest challenge in the solution of stick-slip system response is determining the transition times from one system state (ie, sticking or slipping) to the other. Table 8 summarizes the requirements for transitions from one regime to the other.

Note that for a slip-to-stick transition, $\hat{x}' = 0$ is a necessary but not sufficient condition for sticking to occur. This is precisely the area in which Taylor's Hybrid Systems Modeling Language (eg, [82]), briefly described in Section 2.3, provides an excellent, general approach for capturing state transitions. Of course, the growing body of literature on analytical approaches to non-smooth dynamic systems [72] lends insight here as well.

With this background in mind, stick-slip oscillations can be examined from a more quantitative standpoint. Figure 17 shows an example time response [part *a*] and phase plane response [part *b*] for stick-slip oscillations. Several observations can be made. First, the oscillations are clearly bounded, indicating a qualitative difference between the linearized and nonlinear responses, as expected. Next, the response is periodic, indicated by a single closed trajectory in the phase plane; further, this response is an *isolated* closed trajectory, indicating that it is indeed a limit cycle oscillation. Stick-slip occurs even in the presence of non-zero system damping, as shown here. Finally, an energy argument can be made:

- system (potential) energy increases during sticking, as the spring is stretched, and
- system (kinetic) energy is dissipated during slipping through the viscous damper;
- therefore, the stick-slip limit cycle is the isolated, closed trajectory on the phase plane which balances energy input during the sticking portion and energy dissipation in the slipping portion of the cycle.

The frequency of the stick-slip oscillations is in general similar to, but not the same as, the damped natural frequency of the system.

Figure 18 shows the time history of the friction coefficient, which is defined here as:

$$\text{slipping:} \quad \mu = \mu(V_{\text{rel}}) \tag{67}$$

$$\text{sticking:} \quad \mu = \frac{2\xi\hat{V}_o + \hat{x}}{\hat{F}_n} \tag{68}$$

In this single-dof system, under the sticking constraint $\hat{x}' = 0$ defined above, the sticking friction coefficient can be explicitly defined in terms of the reference velocity $\hat{V}_o$, the displacement $\hat{x}$, and the normal load $\hat{F}_n$. Note a few features about the sticking friction coefficient:

- it grows at the rate $\mu' = \hat{V}_o / \hat{F}_n$, and
- at the slip-to-stick transition, the friction coefficient instantaneously drops from the limiting value $\mu(V_{\text{rel}} = 0)$ to a new value dependent only upon the position $\hat{x}$ of the mass when sticking commences.

The transition criteria described in Table 8 provide clear guidelines for transitions from one kinematic state to another, although implementing them in a computationally-efficient way is challenging. As a result, a number of approximation schemes have emerged to deal with this issue, including the low velocity tolerance band approach of Karnopp [191] and a variety of friction smoothing procedures using arctan-type functions. The result of these approaches is that *true sticking behavior* is precluded in favor of low-velocity creep. In these cases, the computational efficiency must be weighed against the goals of the simulation, ie, is error associated with using a friction smoothing approach too large a price for the increased computational efficiency?

In general, stick-slip oscillations present a very difficult nonlinear problem which has previously been analyzed using one of two usual methods: graphical tools (eg, [65]) or numerical tools as described above. Analytical tools for these types of non-smooth dynamical systems are also maturing [74]. Stick-slip response has been shown to play a primary role in many dynamics and controls problems, fretting fatigue, geomechanics, and friction damping. Further, implementing stick-slip algorithms on systems other than point contact models has historically been difficult, unless one of the friction approximation schemes described above has been used. In Section 4, two continuum-based partial slip/stick-slip formulations are presented, and their results contrasted against more traditional lumped-parameter models.

3.5 Summary

The literature on self-excited vibrations provides a broad view of the friction modeling approaches, and the key result is the close connection between friction parameters and system dynamics parameters. In each of the cases examined here—and this is generally true across the literature—a critical system dynamic parameter could be predicted for stability, and this system dynamic parameter is invariably a function of one or more of the friction parameters. A critical system stiffness or damping value can be derived based upon a critical slip displacement or velocity dependence of friction, respectively. Further, normal force variations are shown

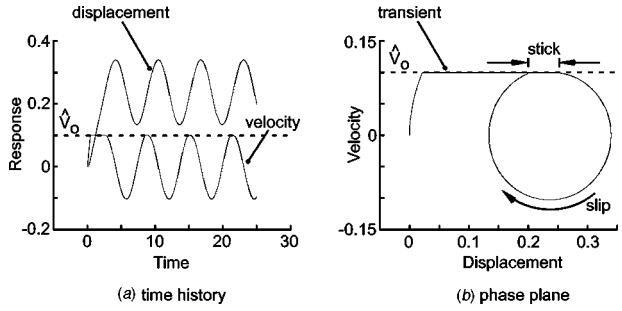

Fig. 17 Stick-slip response: *a*) time history, *b*) phase plane

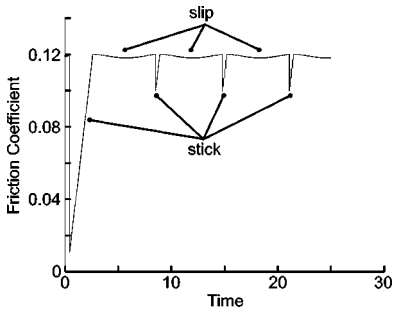

Fig. 18 Time response of friction coefficient in stick-slip oscillations

to be important in promoting self-excited response. A variety of other tangential-normal-angular coupling mechanisms have been implicated in self-excited vibrations as well. This literature points to the critical need to consider the system dynamics and friction model as an integrated unit which cannot be de-coupled in an easy way.

4 FORCED RESPONSE OF SYSTEMS WITH FRICTION

Forced response calculations using various friction models are considered in this section. Forced response under general friction conditions presents many obstacles, and the governing equations are often highly nonlinear, because of the discontinuous friction behavior at zero relative velocity. Two typical approaches to this problem are: *i*) detailed (usually numerical) stick-slip calculations which clearly delineate regions of sticking and slipping in the parameter space, and *ii*) friction approximations which smooth the discontinuity at zero relative velocity but still result in a nonlinear (but continuous) model. The second case above precludes a true *sticking* response, and therefore this simplification should be carefully considered in light of the specific application.

The general piecewise nonlinear equations of motion for a forced single-dof oscillator undergoing stick-slip response (Fig. 6) can be summarized based upon the normalized Eq. (36):

$$\hat{x}'' + 2\xi\hat{x}' + \hat{x} = \hat{F}_q(\tau) - \hat{F}_f(\hat{x}') \quad \hat{x}' \neq 0 \tag{69}$$

$$\hat{F}_f = \hat{F}(\tau) \quad \hat{x}' = 0 \tag{70}$$

where $\hat{F}_q(\tau)$ is a general time-dependent forcing function, and it is assumed that the sliding mass moves against a stationary countersurface such that $\hat{V}_{\text{rel}} = \hat{x}'$. Here, the slipping equation is a *nonlinear second-order differential equation*, while sticking is described by an *algebraic* equation. The piecewise nonlinear nature of the exact governing equations has inspired researchers to seek approximations to the governing equations and their solutions, although some analytical work has been completed, as described next.

4.1 Analytical analyses

The starting point for discussion on forced response calculations with friction is usually den Hartog [61], who developed an analytical solution explicitly considering stick-slip oscillations for a single-dof system with constant friction coefficient. He developed frequency response curves and a frequency-dependent stick-slip boundary which indicates the existence of sticking response. He focused on the analysis of symmetric system response, ie, two instances of sticking per forcing cycle. The exact solution in the presence of both viscous and friction damping is quite complicated, but can be written in closed form. Shaw [135] presents a thorough analysis and extension of den Hartog's work by including non-constant friction coefficient, and implementing stability analysis for the periodic oscillations. He develops bifurcation criteria which indicate the genesis of new (unsymmetric) motions under negative damping conditions. He also alludes to the existence of much more rich dynamic behavior of stick-slip oscillations, and in fact cites Pratt and Williams [192] who show numerically that the number of sticking instances per forcing cycle approaches ∞ as the forcing frequency goes to zero (this is the pure stick case). A typical result using Shaw's approach can be generated via iterative solution of the governing equations he presents, and is shown in Fig. 19 [Shaw's Fig. 5], where the frequency response curves show pure slip as well as stick-slip motions for various values of forcing amplitude ratio β and frequency tuning $\Omega = \omega_f/\omega_n$. β is the ratio of tangential forcing amplitude to limiting interface sticking friction, and Ω is the ratio of forcing frequency to natural frequency. Only response curves for $\Omega > 0.3$ are presented, because as Shaw points out, the low frequency stick-slip behavior is quite rich and complicated, and is not easily described via the analytical approach he pursues. Note that the response amplitude is continuous through the stick-slip boundary, indicating a smooth transition from non-sticking to two-sticking-instances per cycle solutions. While these analytical solutions provide significant insight into the stick-slip problem, they are limited to linear structural models and parameter-independent friction (ie, $F_f \neq F_f(V_{\text{rel}})$), although Shaw does analytically consider the case $\mu_s \neq \mu_k$, but with $\mu_k \neq \mu_k(V_{\text{rel}})$. More complicated structural models or general parameter dependence of the problem usually make analytical forced responsed calculations which explicitly include sticking largely intractable, and numerical methods are implemented. Nonetheless, these analytical solutions continue to be cited as important contributions with significant lasting value, because they represent various limiting cases of other friction/dynamic models cited in the literature.

4.2 Friction smoothing procedures

Owing to the analytical obstacles to examining discontinuous friction at zero sliding velocity, a number of friction smoothing procedures have been developed. There are two main classes of friction smoothing:

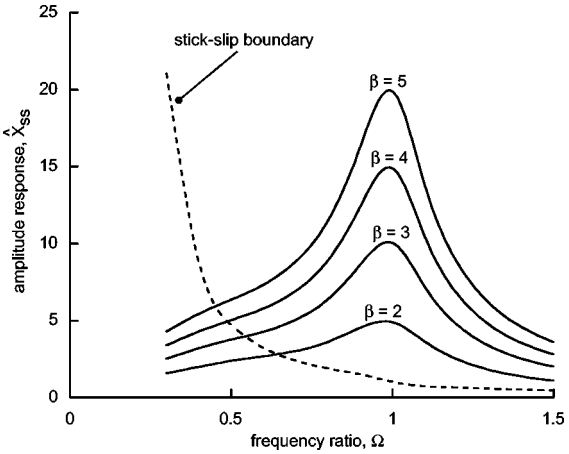

Fig. 19 Sample calculations from Shaw [135] showing frequency response of stick-slip oscillations with continuous amplitude curve through the stick-slip boundary

a) those which approximate the discontinuous friction force at zero relative velocity by a smooth function; for example using $F_f = F_{f,o} \arctan(cV_{\text{rel}})$

b) those which smooth the friction behavior using an assumed smooth solution to the nonlinear governing equation, as in harmonic balance method (HBM) solutions.

For case *a*), the governing equations remain nonlinear, and in fact in the vicinity of zero relative velocity the differential equations can be quite stiff; in case *b*) a harmonic solution is sought to represent the nonlinear, piecewise solution. The impact of these approaches will be considered next.

4.2.1 Case a): Friction force smoothing

In this case, a smoothing procedure is applied directly to the friction expression itself, and this idea has been implemented widely in the literature due to its simplicity and computational efficiency. Figure 20 shows a typical approach in which an arctan-type approximation is given for the friction behavior. A number of researchers have used this approach, including for example Oden and Martins [45]. The important features of this approach are the single-valued friction at zero relative velocity and the high friction gradients through $V_{\text{rel}} = 0$. The resulting numerical stiffness can be significant, and the choice here is between continuous, stiff differential equations, and piecewise, non-stiff equations. A further approach to smoothing the discontinuity at $V_{\text{rel}} = 0$ is to define a velocity tolerance $V_{\text{rel}}^{\text{tol}}$ within which very low relative velocity creep—although not true sticking—is permitted. This is the approach suggested by Karnopp [191].

4.2.2 Case b): Solution smoothing

Frequently in the literature, approximate solutions to the nonlinear governing equations have been pursued, and a common tool is the harmonic balance method. The HBM assumes the system responds with a harmonic solution to harmonic forcing; an assumed solution is substituted into the nonlinear governing equation, the nonlinear terms are expanded in Fourier series in the forcing frequency ω_q, and the coefficients of like terms (ie, $\sin \omega_q t$, $\cos \omega_q t$, $\sin 2\omega_q t$, $\cos 2\omega_q t$, etc) are collected and equated. A one-term harmonic balance includes only the first harmonic of the forcing frequency in the solution. Depending upon the type of nonlinearity in the solution, the HBM is a powerful and accurate tool for approximate analysis of nonlinear equations. In fact, the HBM can be shown to be equivalent to several perturbation approaches, including the method of multiple scales and the (first-order) method of averaging. The one-term HBM solution is most accurate when the full nonlinear solution is nearly harmonic, ie, when the nonlinearity is small. For friction problems, the effect of the friction nonlinearity is relatively small under conditions of near-pure slip or near-pure stick. So, for two extremes of system response, for which the governing equations are more weakly nonlinear, the HBM provides a reasonably accurate solution.

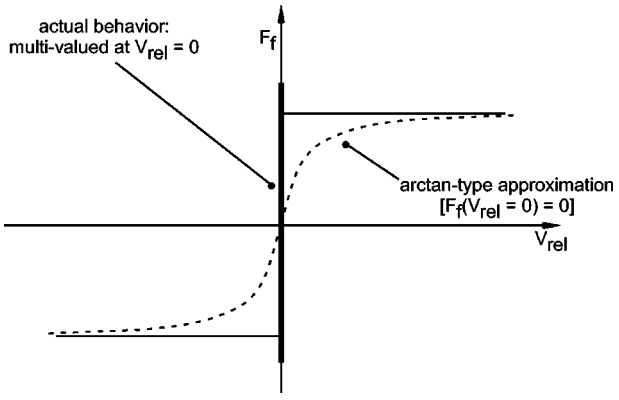

Fig. 20 Smoothing of friction discontinuity using an arctan-type approximation: mutli-valued friction at zero relative velocity (and therefore inclusion of true sticking) is neglected

A good example of this type of calculation is the work of Ferri, who has applied the HBM (or a modified version of it) to a variety of forced response calculations. Ferri and colleagues (eg, [144]) have developed much of the theory relating to displacement-dependent normal forces and other types of friction boundary conditions. They begin with a continuous system with end support whose clamp force is a function of system response (and whose contact is modeled as a discrete point), as shown in Fig. 21. Each case has a different support boundary condition, but in each case the solution to the continuous, elasto-dynamic governing equations can be approached using a one-term Galerkin expansion of the form:

$$w(x,t) = z(t)\,\phi(x) \tag{71}$$

where $w(x,t)$ is the transverse displacement, $z(t)$ is the modal amplitude time response, and $\phi(x)$ is the mode shape used in the expansion. $\phi(x)$ is chosen in each case according to appropriate boundary conditions on the beam, and the modal amplitude under harmonic forcing in each case can be approximated using a one-term harmonic expansion:

$$z(t) = A \cos \omega t \tag{72}$$

where A is the modal amplitude and ω is the forcing frequency. For each of the three cases shown in Fig. 21, the governing equation for the modal response can be written as a single, second-order nonlinear differential equation of the form:

$$m[\ddot{z} + \omega_n^2 z] = f(t) + F_f(t) \tag{73}$$

where $F_f(t)$ is the friction force at the support boundary, and is different in each case depending upon the mechanism of parameter dependence. m and ω_n are mass and natural frequency parameters related to beam geometry (L,I), material elastic and inertial properties (E,ρ), and the assumed mode shape $\phi(x)$. The governing equation of the form (73) can be expanded using the assumed HBM solution (72), and amplitude-frequency relationships can be derived. In addition, equivalent viscous damping ratio and damped natural frequency can be derived.

Within the discussion Ferri and Bindemann correctly point out that their one-term harmonic balance solution presupposes a response of nearly pure slipping, and they introduce constraint equations which define sticking boundaries

Table 9. Summary of results for equivalent damping under various support conditions in continuous systems (from Ferri and Bindemann [144])

Support Boundary Friction Condition	Damping Behavior	Comment
I. transverse slip	$\zeta_I = \frac{2\mu F_n \phi_L}{\pi A m \omega_n \omega}$	qualitatively the same as the classical result of [61]; standard dry friction behavior inversely proportional to response amplitude
II. in-plane displacement-dependent normal force	$\zeta_{II} = \frac{c_2 + c_3 A^2}{2m\omega\Omega_n}$	traditional hardening behavior of cubic-nonlinear systems, with damping related to response amplitude squared
III. out-of-plane displacement-dependent normal force	$\zeta_{III} = \frac{c_4 A}{2m\omega\Omega_n}$	damping linearly related to slip amplitude

in the (z,t)-space, along the lines of the previous work in this area [57,135]. Thus, sticking maps can be used to assess the validity of the harmonic balance solution. Within this context, Ferri and Bindemann present results for only those cases of pure slipping, and compare the HBM solution with time integration results. In light of the pure slip response, the comparison of HBM solution and time integration is excellent, and a schematic of the result for Case II (displacement-dependent normal force, with angle γ) is shown in Fig. 22 for various values of contact angle. Various features can be observed. First, increasing the contact angle γ is equivalent to increasing the magnitude of the normal force variations, and therefore increasing the friction force (and hence friction damping) over one forcing cycle. The peak amplitude for increasing values of γ decreases. Further, there is also a frequency shift, and indeed this type of boundary support condition introduces a nonlinear (hardening) stiffness term in the governing equation. Under sufficiently large γ, three HBM solutions can be found; two branches are stable and one branch (the middle branch) is unstable. As a result, this sort of support boundary condition can give rise to a jump phenomena for quasi-stationary variations in forcing frequency ω.

The damping results for all three cases are summarized in Table 9, where Ω_n is the damped natural frequency, and the c_i are scalars related to the mode chosen for the Galerkin expansion (the mode itself is denoted by $\phi(x)$ and $\phi(x = L) = \phi_L$), the friction coefficient, the normal contact stiffness k_n (for Cases II and III), the contact angle γ (Case II only), and the preload normal force $F_{n,o}$. The important result here is that friction manifests differently in each case, specifically the equivalent damping's dependence upon response amplitude and frequency. All cases have equivalent damping inversely proportional to frequency, but very different dependence upon response amplitude. The conclusion is that contact geometry, orientation of friction interface (with respect to the structure), and parameter dependence of normal force all play a significant role in the amount and type of friction damping. The authors emphasize the pure slip nature of the response, and indicate that under other conditions, the HBM solution may be suspect for its neglect of sticking conditions. However, they present a very thorough analysis of the structural response and provide clear guidelines for the appropriateness of their procedures, which amount to conditions under which an essentially pure slipping response can be expected.

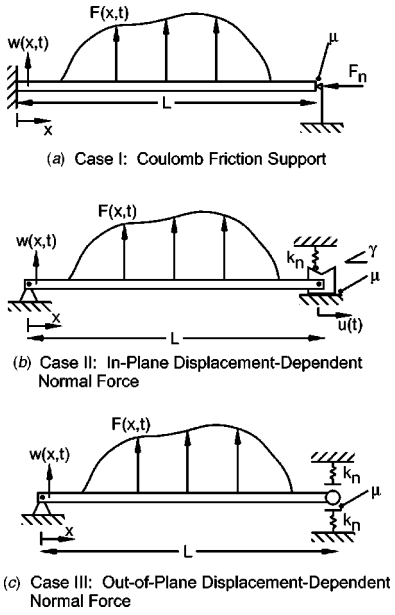

Fig. 21 Three continuous systems with different boundary friction conditions: *a*) coulomb friction support, *b*) in-plane displacement-dependent normal force, *c*) out-of-plane displacement-dependent normal force (schematic from Ferri and Bindemann [144])

4.3 Forced response of continuous contacts

Continuous contact systems present a special set of challenges for forced response calculations. If the contacting bodies are not assumed to respond as rigid bodies, then it is

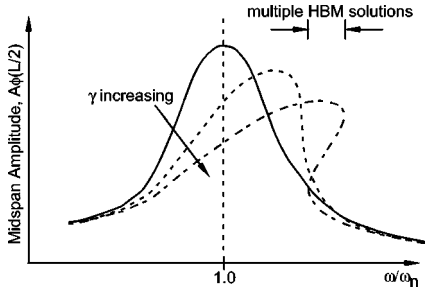

Fig. 22 Schematic of result from Ferri and Bindemann [144] showing hardening behavior with increasing contact angle (case II from Fig. 21*b*)

wholly unlikely that all points on the contact interface will stick or slip in unison. Rather, the more likely scenario is that a partial interface slip condition will prevail, and so forced response calculations must contain an accurate measure of the frictional energy dissipation which occurs only in the slipping regions. Such forced response problems are frequently encountered in a number of important engineering applications (bolted and riveted connections, turbine blade vibration damping, large space structures, etc), with implications on contact conditions in fretting as well.

4.3.1 Partial slip modeling: Lumped-parameter models

Partial slip modeling using bilinear hysteresis elements, or more sophisticated versions of them, dates back to the 1960s. Iwan [119] proposed a class of models for elasto-plastic material behavior modeling, and the simplest form is the familiar bilinear hysteresis model shown in Fig. 5*a*. Collections of macroslip elements, arranged as shown in Fig. 5*b* or *c* or other potential configurations, allow each contact point to stick and slip independently, and therefore allow for partial slipping of the interface. For a model with N macroslip elements, there are $2N$ independent parameters describing the model; they are k_i and $F_{f,i}$, $i=1,\ldots,N$. As a result, an efficient, accurate calibration process for partial slip model identification must be developed in order to completely specify the model parameters.

Model calibration can be achieved in the following way. Experimental measurements made under monotonically increasing loading indicate a force-displacement curve of the form shown in Fig. 23. The solid line (–) in the figure shows the experimental data, and the friction force increases toward a maximum value at which point break-away occurs and gross interface slipping ensues. All points previous to break-away represent pre-slip displacement. The model can be tuned by choosing $2N$ critical points along the loading curve, $x_{cr,i}$ for $i=1,\ldots,2N$, and noting the corresponding critical values of force $F_{cr,i}=F_f(x_{cr,i})$. Then, using an appropriate curve fitting procedure, the $2N$ model parameters can be identified. The corresponding behavior of the model under *cyclic* loading is shown in Fig. 24, where the pre-slip displacement is indicated. The actual behavior of a partial slip interface is therefore captured as a piecewise-linear fit of the actual data described by discrete springs and Coulomb dampers. The question of application of a model calibrated under *monotonic* loading to situations involving *cyclic* loading is addressed by several researchers who cite the so-called Masing rules (eg, [156]) which ensure validity of the model under cyclic loading. Several observations can be made about the modeling and calibration procedures:

- The fitting procedure is a collocation approach in which the model matches the experimental data at $2N$ discrete points, and approximates the model with linear interpolation elsewhere.
- A better fit to the experimental data can be achieved by increasing the model order N, or by concentrating critical points $x_{cr,i}$ in regions where dF_f/dx is large.
- Increasing the order of the model decreases the physical appeal of each individual parameter in the model, with each model parameter having mathematical significance for curve fitting experimental data, but limited physical relevance.

Figure 25 shows a single-DOF system with bilinear hysteresis friction damper attached to it. The damper itself is allowed to either stick or slip, and it is considered as a point contact. There is no friction between the mass m and ground, and the forcing function $F_q(t)$ excites the system in the tangential direction. Note that because the bilinear hysteresis element is massless, the system retains only one dof, and the damper displacement is denoted by the internal dof $u_d(t)$. A brief consideration of solutions of the sticking and slipping governing equations for the single-dof system with bilinear hysteresis friction element helps shed some light on the performance of such friction models. The equation of motion must use a piecewise friction definition, and for harmonic forcing of the form $F_q(t)=F_{q,1}\sin\omega_q t$ the normalized structural response equation of motion can be generically stated:

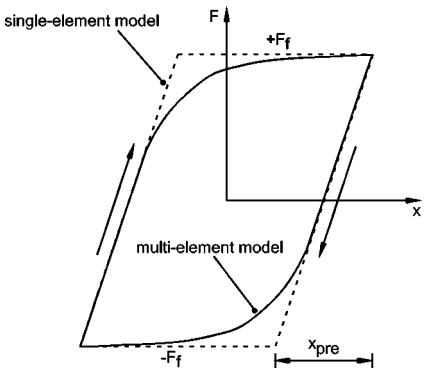

Fig. 24 Cyclic loading behavior of lumped-parameter partial slip models showing hysteresis (single-element model of Fig. 5*a*, multi-element model of Fig. 5*b*); pre-slip displacement for single-element model is shown

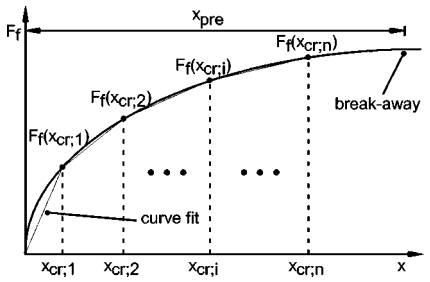

Fig. 23 Calibration of lumped-parameter partial slip models using monotonic loading and a collocation procedure at discrete points $x_{cr,i}$ (monotonic loading)

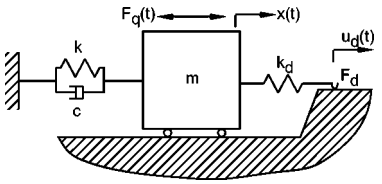

Fig. 25 Single-dof structural model with bilinear hysteresis friction damper

$$\hat{x}'' + 2\xi\hat{x}' + \Omega^2\hat{x} = \hat{F}_q(\tau) - \hat{F}_d(\hat{x}) \tag{74}$$

where for this forced response problem, the normalizations are slightly different than those for the self-excited problem:

$$\tau = \omega_q t \tag{75}$$

$$x_o = \frac{F_{q,1}}{k} \tag{76}$$

$$\xi = \frac{c}{2m\omega_q} \tag{77}$$

$$\Omega^2 = \frac{\omega_q^2}{\omega_n^2} \tag{78}$$

$$\hat{F}_q(\tau) = \frac{F_{q,1}}{m\omega_q^2 x_o}\sin\tau = \hat{F}_{q,1}\sin\tau \tag{79}$$

The piecewise nature of the equation is revealed by considering the friction damper force $\hat{F}_d$:

$$\hat{F}_d = \begin{cases} \hat{F}_f; & \text{slipping} \\ \gamma\Omega^2(\hat{x} - \hat{u}_s); & \text{sticking} \end{cases} \tag{80}$$

where $\hat{u}_s$ is the damper position at the onset of sticking, $\hat{F}_f = F_f/m\omega_q^2 x_o$, and $\gamma = k_d/k$ is a stiffness ratio which indicates the impact of the damper dynamics. Note that in Eq. (80), appropriate signs must be attached to the damper force, depending upon which branch of the hysteresis loop (Fig. 24) the slider operates on.

It is important to emphasize here that the structural model (ie, the mass m itself) never experiences sticking, and so the governing equation for this system is always a second-order differential equation—it is only the massless damper which can experience sticking. So in fact this approach is a type of friction smoothing procedure in the sense that the dynamics of the structure are never described by an algebraic equation of the form (70). Recall that the bilinear hysteresis element is a special case of Fig. 23 in which elastic-perfectly plastic behavior is exhibited (that is, only one collocation point x_{cr} is used to calibrate the model). Then, the friction element functions as a saturation element with the maximum restoring force equal to $\pm\hat{F}_f$. Under this normalization, the piecewise equations of motion can be written:

$$\hat{x}'' + 2\xi\hat{x}' + \Omega^2(1+\gamma)\hat{x} = \hat{F}_q(\tau) - \gamma\Omega^2\hat{u}_s \quad \text{sticking} \tag{81}$$

$$\hat{x}'' + 2\xi\hat{x}' + \Omega^2\hat{x} = \hat{F}_q(\tau) - \hat{F}_f\,\mathrm{sgn}(\hat{x}') \quad \text{slipping} \tag{82}$$

The limiting behavior of this system will be examined first. The fundamental dynamics of the system under sticking and slipping conditions are summarized in Table 10, which shows that sticking brings about an increased natural frequency, but a decreased effective damping. Both of these effects result from the damper spring stiffness being arranged in parallel with the system stiffness in Fig. 25. Furthermore, if the system is assumed to operate in a condition of pure slip (or nearly pure slip), then the HBM solution suggested earlier will likely be appropriate. Note that cases of substantial stick-slip *cannot* be approached using the procedures outlined by den Hartog or Shaw because at the stick-slip transition an instantaneous change in effective stiffness occurs (ie, in this case the dynamics at the stick-slip transition are not smooth). An exception to this is the limiting case $\gamma \to \infty$, which corresponds exactly to the analyses of den Hartog (constant friction coefficient) and Shaw (different static and kinetic friction coefficients).

Table 10. Comparison of slipping and sticking system parameters for a single-dof model with bilinear hysteresis friction element

Parameter	Slipping Eq. (82)	Sticking Eq. (81)
natural frequency	$\omega_n^{sl} = \Omega$	$\omega_n^{st} = \Omega\sqrt{(1+\gamma)}$
equivalent damping ratio	$\zeta^{sl} = \dfrac{\xi}{\Omega}$	$\zeta^{st} = \dfrac{\xi}{\Omega\sqrt{(1+\gamma)}}$
damper force	$\hat{F}_d^{sl} = \hat{F}_f$	$\hat{F}_d^{st} = \gamma\Omega^2(\hat{x} - \hat{u}_s)$

Harmonic excitation $\hat{F}_q(t) = \hat{F}_{q,1}\sin(\tau)$ produces a response $\hat{x}(t)$ which in general is not harmonic due to the nonlinearity of the friction damper. For a pure sticking case, in which the forcing amplitude $\hat{F}_{q,1}$ is insufficient to induce slipping, the equation of motion becomes linear (Eq. (81) with $\hat{u}_s = 0$ for all time τ), with solution of the form $\hat{x}_o(t) = \hat{X}_o\sin(\tau + \phi)$, with:

$$\hat{X}_o = \frac{\hat{F}_{q,1}}{\sqrt{\left[1 - \left(\dfrac{1}{\omega_n^{st}}\right)^2\right]^2 + \left[2\zeta^{st}\dfrac{1}{\omega_n^{st}}\right]^2}} \tag{83}$$

where ω_n^{st} and ζ^{st} are defined in Table 10, along with the phase angle ϕ. For a near-pure slipping case, the HBM can be used to approximate the response as a pure harmonic and the error of such an approach is likely to be small.

Because it is the *massless damper* which may respond in stick-slip, the structural response under mildly nonlinear conditions is likely to be *substantially harmonic*, regardless of the kinematic state of the damper. This is shown clearly in Fig. 26, which illustrates the response of the mass $\hat{x}(\tau)$ against time under single-frequency harmonic input. The dashed lines correspond to conditions of damper slipping while the solid lines correspond to damper sticking. We might estimate that the damper response $\hat{u}_d(\tau)$ sticks roughly 60% of the time over one forcing cycle in this simulation, yet fundamentally the response $\hat{x}(\tau)$ is single-frequency harmonic. This idea can be further investigated by varying the coupling parameter γ and examining the system response, as is shown in Fig. 27. $\hat{X}_{ss}$ is the steady-state response amplitude calculated from numerical simulation, and it is a non-monotonic function of the coupling parameter γ which peaks for small values of γ. Percent sticking *of the damper* per cycle is a monotonically-decreasing function of γ, with small γ corresponding to pure stick, and large γ corresponding to pure slip. From Table 10, the range of γ shown on the figure corresponds to a maximum resonant frequency shift of over 20%.

With reference to the hysteresis curve for a single-element model of Fig. 24, the relationship among the friction force, damper stiffness, and pre-slip displacement is:

$$k_d x_{\text{pre}} = 2F_f \tag{84}$$

which indicates that for large damper stiffness k_d, the potential sticking region becomes very small, and the parallelogram of Fig. 24 begins to look more like a rectangle with vertical sides. The physical implication is that as k_d increases, the pre-slip displacement (and therefore the amount of sticking per forcing cycle) decreases, and the problem becomes more weakly nonlinear with the damper force $F_d = \pm F_f$, depending upon the sign of the sliding velocity. Indeed, we can use $\gamma \to \infty$ and apply den Hartog's approach to predict an asymptote of $\hat{X}_{ss} \to 1.85$ for this case. The implication is that for moderately large γ, the steady-state response amplitude is very *insensitive* to the kinematic state of the damper; as such, an HBM solution for the response $\hat{x}(\tau)$ is likely to correctly predict the amplitude regardless of the kinematic state of the damper.

This is the key difference between implementing friction damping using massless Iwan-type models and non-zero mass contact models of the type considered originally by den Hartog. Indeed, under sticking, systems with bilinear hysteresis elements still retain a single dof, with the consequent changes in frequency and damping characteristics shown in Table 10. On the other hand, a single-dof point contact model similar to den Hartog's possesses kinematically constrained motion during sticking and therefore zero dofs; further, the concepts of natural frequency and damping ratio are essentially meaningless during sticking.

A key question, as yet not fully explored in the literature, is the effect of an Iwan-type model which has non-zero mass, equivalent to replacing the Coulomb damper in Fig. 25 with a mass m_d under normal load experiencing point contact with friction coefficient μ. The spirit of Iwan models indicates that the mass ratio $\beta = m_d/m$ should be small; if β assumes a larger value, then the damper dynamics begin to assert themselves, and it stops behaving like a damping element and starts behaving more like another structural dof. So, if the discussion is restricted to small values of β, the analysis lends itself well to perturbation approaches, and this is precisely the analysis used by Ferri and Heck [137], which indicates that damper mass m_d may have an important effect on overall damping characteristics. They used the singular perturbation theory to determine steady-state response of the mass m under various values of the parameter β, and the results (their Fig. 11) show that indeed mass can have a qualitative effect, particularly in situations where substantial stick-slip takes place. In operating regions of near-pure-slip or near-pure-stick, a variety of lower-order approaches is sufficient. As shown in the calculations presented in Fig. 28 (a partial result corresponding to Ferri and Heck's Fig. 11), damper mass can play a dramatic role, especially in the vicinity of resonance. These results correspond to $\beta = 0.2$ and demonstrate that a bilinear hysteresis approach significantly overestimates steady-state response under stick-slip conditions.

Finally, three performance issues for bilinear hysteresis elements should be recognized. First, these elements describe phenomenological models which are consistent with a key experimental observation—they allow for pre-slip displacement through stretching of the spring (see Fig. 1*d*)). Second, they are attractive for modeling systems with changing boundary conditions, such as turbine blades for which the

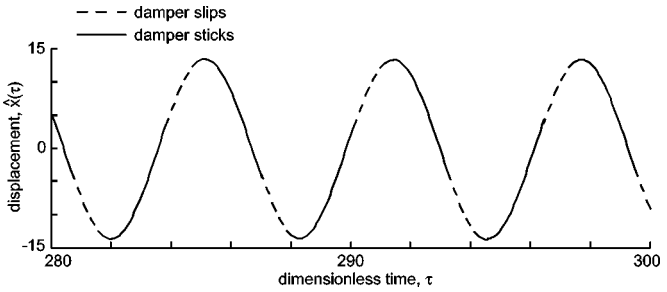

Fig. 26 Steady-state response $\hat{x}(\tau)$ under single-frequency excitation; damper sticks more than one-half of the time per forcing cycle yet $\hat{x}(\tau)$ is substantially harmonic

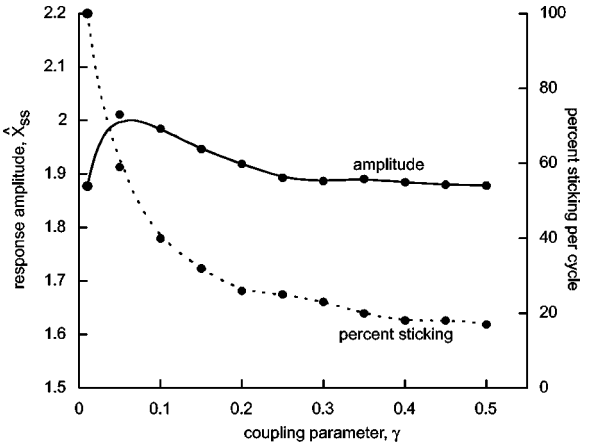

Fig. 27 Steady-state response amplitude $\hat{X}_{ss}$ and time-averaged percent sticking per forcing cycle variations with coupling parameter γ

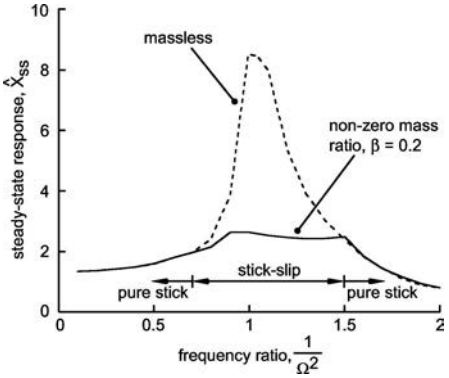

Fig. 28 Damper mass effects on steady-state forced response. An example result from Ferri and Heck [137] showing a qualitative difference in predictions for massless (bilinear hysteresis) and non-zero-mass models.

models have seen the most use. Indeed, if the single-dof system considered here is interpreted as a one-mode expansion for the response of a continuous system, then it is clear that the bilinear hysteresis elements allow for a change in natural frequency of that mode, by a factor of $\sqrt{(1+\gamma)}$ in Eq. (81), under a pure sticking boundary condition. This presents another means of calibrating the model as well: k_d can be chosen to match an experimentally-observed frequency shift as the boundary condition changes from pure slip to pure stick. Third, from a computational standpoint, the differential equations describing the structure only reflect the sticking or slipping state of the damper through F_d, and the structure itself is never described by a sticking algebraic constraint equation. This provides two attractive features: *i*) computational efficiency in that the response $x(t)$ is smooth and its derivatives are smooth, and *ii*) this lends itself to HBM-type solutions because the structure never undergoes sticking. The liabilities of these models include their only indirect access to interface response parameters, and the requirement for calibration of the models against a database of performance data.

4.3.2 Partial slip modeling: Continuum approaches

Several researchers have examined partial slip contact and forced response using continuum approaches. The most common procedure is to apply Hertz theory and Mindlin's approach to capture regions of slip and stick in the contact, slip displacement, energy dissipation, etc. These approaches assume quasi-static loading conditions and Coulomb friction. These models have enjoyed great success in the mechanics community and fretting fatigue in particular, and they work well for contacts which can be reasonably modeled using Hertz theory. Many large-scale FEM codes of today offer a computational framework within which partial slip calculations can be efficiently made for contact geometries other than Hertzian. However, they prove largely unsuitable for dynamic system simulation except in relatively simple cases, mainly because of the computationally intensive nature of contact mechanics solutions. As a result, dynamic system simulations have focused more closely on nominally flat contacts, or at least contacts for which variations in contact size can be neglected. Several approaches have emerged for detailed stick-slip investigations of continuous contacts.

Oden and colleagues have developed a continuum mechanics-motivated interface constitutive law (see Section 2.2). However, they use a friction regularization procedure to smooth the discontinuity at zero relative velocity, and so true interface sticking is never achieved in their models. Rice's rate- and state-dependent friction model (Section 2.5) also includes a continuum approach, but it has been applied either in self-excited response and steady-sliding stability problems, or to describe the forced response of a single-point contact.

Another partial slip model was proposed by Menq and Griffin in the mid-1980s [58,156]. Originally developed for turbine blade damping calculations, the model has since been applied to passive damping in joints of built-up structures, as well as a variety of other energy dissipation calculations. The model is based upon the schematic geometry shown in Fig. 29, which shows a lap joint of two elastic bars connected by an elasto-plastic shear layer. The length L interface, described by elastic parameter k and limiting shear stress τ_m, is sheared by the applied force F. The elastic bars are described by effective elastic moduli and cross sectional areas E_i and A_i, $i=1,2$. Two key dimensionless groups are formed:

$$\lambda_1^2 = \frac{kL^2}{E_1 A_1} \tag{85}$$

$$\rho = \frac{E_1 A_1}{E_2 A_2} \tag{86}$$

λ_1 indicates the relative stiffness of the shear layer to the top elastic bar, while ρ compares the effective stiffness of the two elastic bars.

The performance of the model is shown schematically in Fig. 30, which shows regions of sticking and slip, plus the distributed shear traction, at the elasto-plastic shear layer for four different values of applied load F. In the slipping regions, the shear traction is equal to the maximum shear, $\tau = \tau_m$. Note also that as F is increased, the slip zones propagate inward from the edges of contact; this is supported by many observation in the mechanics community (see [151]). Further, under monotonically increasing load, the force-displacement curve can be generated as shown in Fig. 31, and a comparison is made to the bilinear hysteresis model presented elsewhere in this article (see Fig. 5*a*)). Because of the continuous nature of the contact, it is not surprising that the loading curve contains more information than the simple bilinear hysteresis curve discussed earlier.

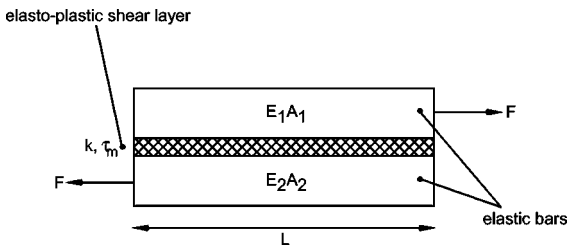

Fig. 29 The Menq-Griffin two elastic bar partial slip model

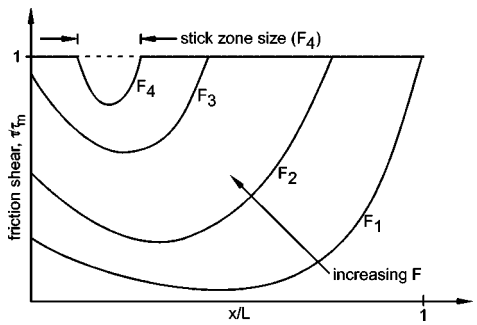

Fig. 30 Menq-Griffin partial slip model characteristics ($F_1 < F_2 < F_3 < F_4$)

This partial slip model, and various permutations, has been shown to qualitatively capture the relevant features of turbine blade vibration response across a wide range of operating conditions. The full range of possible interface conditions is considered (pure slip, partial slip, pure stick), and the consequent effect upon the system dynamics (ie, shifts of resonant frequencies or changes in mode shape) can be captured. Further, it is interesting to note that this model is analogous to the shear-lag models used for fiber pullout analyses in ceramic matrix composites (eg, [193]). The biggest liability of this model, and the extensions reported in the literature and used in the gas turbine industry, is the challenge of model calibration.

Another partial slip model has recently been proposed and applied to continuous contacts by Sextro. He proposes [194] that microslip arises from normal contact pressure variations related to surface roughness. Based upon a statistical roughness description, he derives a nonlinear normal contact law which is related to contact area and normal surface penetration. This is essentially a power law expression along the lines of those described in Section 2.2.2. From this, the tangential contact stiffness is derived, and it contains the familiar softening behavior expected of partial slip contacts. The result is a point contact model which captures the important normal pressure variations of a spatially-distributed rough contact. This is a useful low-order model which can again be analyzed using the HBM. The author reports good agreement with experiments in a turbine blade shroud damping application.

A new formulation for partial slip problems has recently been presented by the author [195]. This model uses a 2D elastic continuum approach to model the structure, with an interface description based upon contact normal stresses and Coulomb-type friction. The model couples the structural response to the interface response in a physically-motivated way, and interface sticking is explicitly allowed. The model uses straight-forward time integration to determine the time history of response. As a result, this model circumvents some of the obstacles described previously in the literature: *i*) the model does not use a friction regularization procedure, and sticking is explicitly accounted for at each interface node in the discretized model; and *ii*) the solution is not based upon a single harmonic, and the full richness of the interface response can be captured. Of course, the price paid for these features is increased computational intensity over other partial slip models and solution procedures. Nonetheless, the model does show promise in capturing energy dissipation in partial slip contacts, mainly because it substantially relieves the requirement for model calibration so critical for many other partial slip contact models. In addition, it captures the continuous variation in system dynamics as the boundary condition changes.

An example result using this approach is shown in Fig. 32, which demonstrates the break-away behavior of the friction force and clearly shows pre-slip displacement occuring over a finite time t_{pre}. An elastic block is pressed into a rigid, stationary countersurface by the uniform distributed load p_o such that $\int_0^L p_o dx = F_n$. The uniformly distributed tangential shear traction along the top surface of the block $q(t)$ increases monotonically from zero to a maximum value which is greater than $\mu_k F_n$, ie, the block will eventually experience pure slipping. The friction force F_f is given by:

$$F_f = \int_0^L \tau_f dx \tag{87}$$

where:

$$\tau_f = \begin{cases} \mu_k \sigma_n & \text{slipping} \\ \leqslant \mu_s \sigma_n & \text{sticking} \end{cases} \tag{88}$$

where no distinction has been made between static and kinetic friction (ie, $\mu_s = \mu_k$). The pre-slip displacement of each location in the elastic body will be different, and therefore the definition of x_{pre} in this case is not explicitly clear. Nonetheless, all points on the structure *away from the interface* experience displacement through this initial loading phase before gross slip. Further, sticking friction is truly multi-valued at zero relative velocity, in contrast to other friction regularization procedures detailed earlier in this paper. The model contains no non-physical parameters; the structural properties are determined using traditional FEM procedures and material and geometry parameters, while the interface constitutive behavior is defined by the interface friction coefficient and the contact normal force, which is explicitly determined at each step of the simulation. Despite the com-

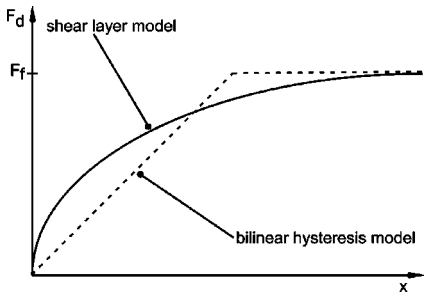

Fig. 31 Comparison of Menq-Griffin partial slip model and bilinear hystersis model under monotonic loading

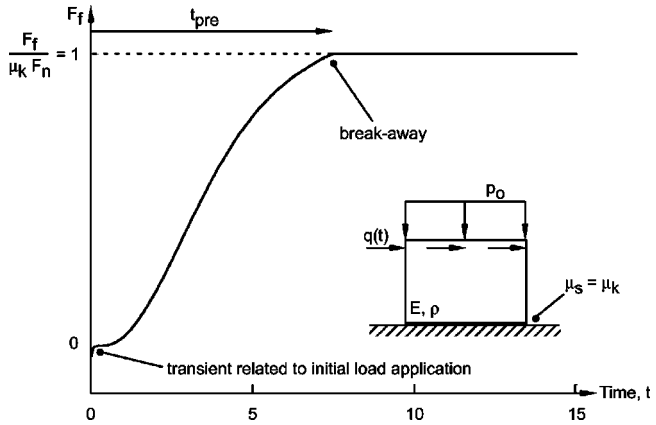

Fig. 32 Break-away behavior of elastic block on rigid support under monotonically-increasing tangential load; inset: schematic of system geometry and loading

putational intensity of this approach, it adds value to partial slip calculations because the only model tuning parameter is the friction coefficient itself.

4.4 Summary

Forced response calculations have traditionally relied upon lumped-parameter, point-contact models to describe friction, as it has been the *structural response* which is of primary interest. Indeed, using the simplest appropriate friction model presents a very attractive approach, and tuning the model against experimental data requires curve fitting of only a few friction parameters. However, even for low-order models of friction at structural supports, we have seen that contact details, including orientation of the slip direction with respect to the structure and parameter dependence of friction, can have a qualitative effect on the overall level of friction damping. Further, we have seen that bilinear hysteresis friction dampers perform well over some parameter ranges (ie, near-pure slip or near-pure stick), but they neglect potentially important effects under primarily stick-slip response. Finally, we have seen the emergence of several continuum-based partial slip contact formulations which provide improved access to interface response parameters, but require substantially more effort in model formulation and solution.

5 DISCUSSION

A wide body of literature has been examined throughout this article, and sources from a number of research communities have been cited. At first glance, the sheer number of friction modeling approaches, levels of sophistication, methods of coupling to system dynamics, approximation techniques for friction, and simulation frameworks is staggering. Making complete sense of the all the literature is quite a formidable task, which we will surely not achieve here. However, we can make some observations of broad truths, relevant across disciplines, which underlie the results presented here. The intent of this section is—to the extent possible—to unify our understanding of these diverse approaches and techniques, identify similarities and differences, and draw some conclusions about work which remains to be done.

5.1 Nature of friction observations

Friction and system dynamics cannot be decoupled because the act of measuring friction involves use of a sensing element with finite compliance. In addition, test components themselves are non-rigid (consider the disk of a pin-on-disk apparatus), their support frames are also non-rigid, and even when one goes to great lengths to achieve vibration isolation—as Tolstoi did over 30 years ago—the dynamic character of friction measurements always seems to assert itself. This being the case, we need to place more emphasis than ever on understanding test rig dynamics and how they affect friction measurements. This is not a new idea, and experimental observations made decades ago support this notion. It appears that *friction* between two contacting bodies is not strictly a function of the materials in contact and the contact conditions, but also of measurement approach. As such, velocity-dependence of friction measured in a pin-on-disk machine may not be an intrinsic property of the contact interface, but rather a property of the *structure-interface system*. We must recognize that there exists no canonical experiment which will provide, without error or misrepresentation, an *accurate and unique* picture of a contact interface behavior under dynamic conditions. The reason is that the interface response and the structural response are strongly coupled, and friction measurements are a complicated function of structural mechanical and thermal response, operating conditions, environment, material combination, surface chemical composition, and other factors. Uniqueness of friction description, it appears, will remain an elusive goal, and perhaps the best we can do is to recognize the role of non-interface factors in determining friction, and use them appropriately in simulation.

5.2 Friction similarities across disciplines

A key observation across the literature is the role of sliding distance (in point contacts) or slip displacement (in continuous contacts undergoing partial slip), which critically relate to memory-dependence, time lag, or a critical slip distance for friction. The memory-dependence and time lag approaches have both been used in the dynamics community to explain observations of friction *loops* in which friction is a function of sliding acceleration as well as sliding velocity. Further, Rice has shown the sensitivity of steady-sliding stability calculations to the critical slip displacement d_c, and derived a critical system stiffness above which steady-sliding is stable.

The mechanics community also has two important contributions in this area. First, the Ruiz and Chen fretting criteria relies closely upon interface slip displacement as a predictor of fatigue crack nucleation. Second, Nowell and Hills examine the observed size effect in fretting contacts and attribute it to the difference in slip displacements for large contact vs smaller contacts. In small contacts, the slip displacements are small—perhaps smaller than any inherent friction length scale in the problem. This is proposed as a difference between single-asperity sliding and multi-asperity sliding, and clearly the important parameter to examine is the ratio of slip displacement to characteristic asperity spacing. Further, the geomechanics community has identified this critical distance as something of a material parameter. Rice proposes the use of a critical slip displacement d_c over which friction evolves as a new population of asperities come into contact. For slip displacements well below the critical value, no significant evolution takes place because no new asperities were brought into contact. In micro-scale contacts, adhesion plays a significant role for component performance, and the characteristic material lattice spacing is the relevant parameter in this case. Similarly, for nano-scale contacts such as those in AFM or FFM experiments, a small-scale interaction potential plays an important role.

Another important theme across much of the literature is the role of out-of-plane response in friction oscillations. A variety of researchers have emphasized the critical role played by both the normal and angular dof in sliding friction

Table 11. Similarities in friction observations across length scale and problem type

Application	Length Scales (m)	Problem Type	Comments
earthquakes	$10^{4}-10^{-6}$	self-excited	stable sliding critically related to material parameter d_c
fretting fatigue	$10^{0}-10^{-6}$	forced	fretting fatigue strongly dependent upon small-scale interface response
joint damping	$10^{0}-10^{-6}$	forced	energy dissipation and structural response related to frictional work
controls	$10^{0}-10^{-6}$	forced	controller gains (ie, closed loop stiffness) related to critical slip displacement d_c or time lag of friction
MEMS	$10^{-5}-10^{-10}$	forced	stiction of MEMS components and adhesion effects
nano-mechanics	$10^{-6}-10^{-10}$	self-excited	AFM cantilever calibration and friction measurements sensitive to normal-angular-tangential coupling of deformation modes and atomic-scale potential interactions

problems, and the mechanism of coupling among the three dofs is a natural one—kinematic coupling related to problem asymmetry (Fig. 2). Further, contact normal vibrations may result from surface asperity interaction, and the observation of a normal contact resonance is common. The fundamental feature here is that any non-planar response—either rotational or normal translation—alters the contact conditions by changing the contact normal force F_n, and affects the real area of contact by changing the mean surface separation. The implications of this can be profound and have been observed in applications as diverse as brake squeal, fretting fatigue, joint damping, and others. Further, AFM measurements in nano-scale contacts show substantial coupling between tangential and torsional motions of the cantilever beam, and the coupling arises due to cantilever beam geometry. Even on the micro- and nano-scales, normal-angular-tangential coupling effects are important. A related issue is the variation of interface parameters with changes in system position, included either through one of the mechanisms proposed by Ferri, or through explicit time dependence of normal load. In any case, realistic contact scenarios across disciplines require careful consideration of out-of-plane vibration effects and their implications on observations and predictions of interface response.

5.3 Multiple scale effects

One of the more intriguing observations that can be extracted from the literature is the general dependence of friction on a critical length parameter *which is in general several orders of magnitude smaller than the length scale of the contacting components*. For example, Rice's work shows that unstable fault slip—with physical system size on the order of km—is critically dependent upon the critical slip distance d_c, which may be on the order of tens of μm. Recall that Rice presents two important implications: i) the critical system stiffness is related to the parameter d_c, and ii) appropriate discretization schemes rely upon cell sizes being smaller than the length parameter d_c. This is a remarkable result which links two length parameters over perhaps ten orders of magnitude in the same problem. But friction contact problems in general possess a number of length scales which fundamentally impact the problem.

For example, in contact mechanics and fretting fatigue scenarios, the components in contact are on the macro-scale, with dimensions on $O(\text{cm})$, while the contact size itself may be sub-mm in size. Further, the slip zone at the edge of contact will be even smaller, and the slip displacements within the slip zone smaller yet. If we revisit the Ruiz and Chen fatigue criterion, we see that the durability of macro-scale components is often linked to interface behavior (slip displacement) which occurs at the micro-scale. Energy dissipation in partial slip contact presents yet another case of multiple-scale effects. In partial slip contacts, such as those in joints of built-up structures or friction dampers in turbomachinery components, the structural response is controlled by contact interactions on the scale of microns or tens of microns—the frictional work at the interface is a function of the friction force and the slip displacement.

This argument scales down even further if we consider AFM measurements and nanomechanics. A micro-scale cantilever beam is used to measure nano-scale surface features or surface force interactions. The response of the beam is closely related to the interaction potential between the AFM tip and the surface being scanned; the critical length scale for the interaction potential is the atomic spacing, and clearly once again the structural response of the AFM cantilever is governed by contact interactions on a length scale three orders of magnitude smaller.

Table 11 presents a small overview of the length scale variations in some example problems. The common thread among each is the critical dependence of system performance/efficiency/durability on a contact interface parameter *with length scale several orders of magnitude smaller than the associated structural scale*. The two basic interface length scales which influence structural response are:

- $1-100$ μm: This includes a critical slip distance d_c in rate- and state-dependent friction laws, characteristic asperity spacing discussed in reciprocating sliding problems and memory-dependent friction, and interface slip displacement which partially governs fretting fatigue life and scale effects in fretting contacts.
- $0.1-10$ nm: Atomic spacing which governs small-scale contact interactions through potential function such as Eq. (21).

5.4 Implications for dynamic friction simulations

This variation in length scale presents substantial problems and requirements for capturing parameter dependence of friction in simulations: if the behavior of a system is dominated by response at a particular length scale, then any discretization schemes must be built around that length scale.

Again, this is precisely the result demonstrated by Rice, who indicates a qualitative difference between the response of an appropriately discretized system possessing a clear continuum limit, and one which is inherently discrete, with no continuum limit. The implication is that appropriately discretized dynamic systems quickly become computationally unwieldy, especially in light of the disparity between typical interface length scales and structural length scales. Rice discusses this issue in detail, and in many of his simulations he chooses an artificially large critical slip displacement d_c in order to make the computations reasonable. Berger, Begley, and Mahajani have also pursued such high-fidelity models with detailed structural and interface discretization, and the computational overhead of their simulations is also substantial. Further, the dynamic model used in the simulation must be capable of capturing the relevant interface response parameters, including macro-scale tangential-normal-angular coupling or micro-scale slip displacement at the interface, as appropriate for the problem.

The choice of friction and structural model can therefore be broken down into three broad categories.

i) *Low-order, lumped-parameter models:* The structure is described by a lumped model, and the contact is idealized as a single point, or at most a few contact points connected by collections of springs and dampers. Total number of dofs is low, on the order of 1–10.

ii) *High-fidelity continuum-based models:* The structure and interface descriptions are derived from continuum mechanics approaches, discretized with a cell size possibly related to a critical friction length scale. Total number of dofs is very high, and is dictated by the ratio of structure size to cell size.

iii) *Hybrid model with high-fidelity interface and modal structural models:* The structure is described by time-dependent modal amplitudes and spatial mode shapes, and the interface is discretized into appropriately sized cells; the interface model and structural modal can be coupled, resulting in a modest number of dofs governed by the interface cell size and the number of modes in the structural response.

Assets and liabilities of these approaches are listed in Fig. 33 as a function of eleven criteria for friction/structural model performance. The key trade-offs observed in the table are computational efficiency against solution details, including access to interface response parameters and contact geometry modeling.

In light of these observations, it is clear that choice of friction and structural models must then not only depend upon the application, but also upon the simulation objective. Each of the three approaches proposed above has assets and liabilities, and the decision about appropriate interface/structural modeling rests on the importance of the evaluation criteria of Fig. 33 for a specific application. For example, it seems likely that fretting fatigue calculations would emphasize physics and fidelity criteria because of life prediction dependence upon slip displacement, slip zone size, contact geometry, etc. However, the dynamic aspects of the problem may be de-emphasized, and therefore the ability to capture general parameter dependence may be of little consequence for a quasi-static problem. On the other hand, for controls applications, high-fidelity structural/interface models are inappropriate because of solution time constraints and the required controller frequency response. As a result, idealized lumped-parameter models which emphasize computational efficiency criteria take precedence.

But in some cases the choice of approach is not straight forward. For example, it is clear from Eq. (20) that energy dissipation in nominally stationary joints is very sensitive to friction force, slip zone size, and slip displacement. So, high fidelity models which emphasize direct access to interface response parameters seem the most promising for these applications. However, when simulating the dynamic response of a large structure with a number of joints, the simulations quickly become unreasonable, and the low-order models increase in attractiveness. In fact, with ample experimental data, Iwan-type models of the form in Fig. 5*b* can be quickly generated, calibrated, and applied to structural analysis applications. It is precisely this line of thinking which gives rise to non-parameterized methods of nonlinear structural identification which have been reported over the past 20 years (eg, [196]). Contact details in this case are sacrificed for a more global understanding of structural response in the presence of friction.

The key conclusions to be drawn concerning the sophistication of structural and friction models are two-fold:

- high-fidelity prediction of interface response usually requires resolving disparate length scales in numerical simulations, and this adds to the model formulation complexity as well as solution cost, although
- the required degree of sophistication of a friction model is highly application specific, and is dependent upon the sys-

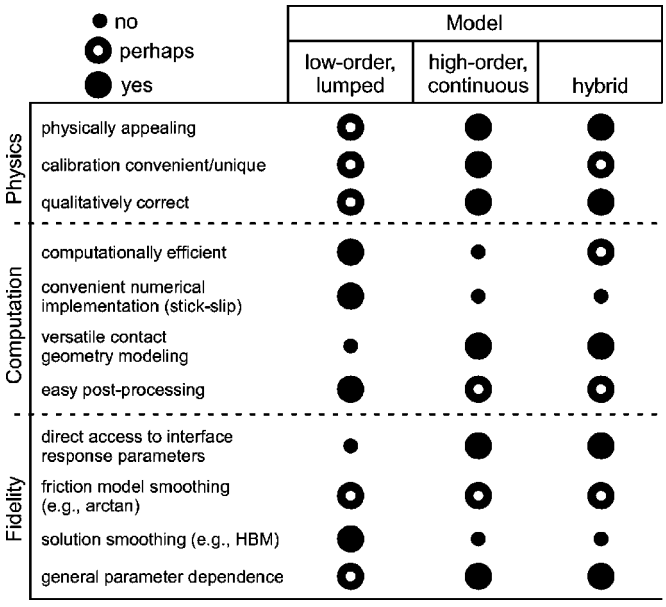

Fig. 33 Comparison of friction modeling approaches against key performance criteria: ability to capture relevant problem physics, computational efficiency, and model fidelity

tem dynamics, computational allowances (eg, frequency response for controllers), and acceptable level of spatial filtering of the interface response (ie, going from a high-order FEM model to a low-order, lumped parameter model).

By confronting these related issues, designers can appropriately choose a friction model which suits design and analysis needs.

6 CONCLUSIONS

Although the literature on friction modeling spans hundreds of years and multiple engineering and science disciplines, we can extract some common themes based upon the observations here. First, modeling of the four key experimental observations shown in Fig. 1 is very accessible, and researchers now have available a number of options and tools for each important behavior. Second, structural models which capture the contact kinematics using normal-angular-tangential coupling are also available, and they have applications across dynamics, controls, and other emerging micro- and nano-scale research areas. Third, there exists a wide variety of friction regularization and solution schemes, which typically seek to simplify the analytical formulation or reduce the numerical cost for the problem.

A key conclusion, drawn from consideration of the literature presented here, is the multiple-length-scale nature of friction modeling for system dynamics. In a huge variety of applications, the structural length scale is several orders of magnitude larger than the relevant friction/interface length scale. The implication is that system simulation approaches face a difficult multi-scale modeling problem in which the performance of the components is *governed by behavior occuring at a length scale much smaller than the overall dimensions of the parts*. This interface length scale drives appropriate discretization schemes, and computational efficiency quickly becomes unreasonably poor. Sections 5.3 and 5.4 present several potential approaches to this problem, although each approach possesses its own assets and liabilities. The conclusion is that friction and structural modeling for dynamic simulations must include careful consideration of not only the information required as output of the simulation, but also the simulation objectives themselves for computational efficiency, accuracy, and fidelity.

Although this conclusion may appear self-evident, it is not an understatement to say that a substantial amount of work remains in friction modeling on several fronts. The fundamental questions on the nature of friction and the science of surface interactions will be a vital research area for many years to come, especially in light of the trend toward engineering miniaturization and the role of friction/adhesion at small length scales. In addition, appropriate descriptions for parameter dependence, and their role in determining system response, will also continue as important research areas. Perhaps the most effort in friction simulation—especially in light of the continuing advancement of computational tools, parallel computing, etc—should be directed toward resolution of the diverse length scales required for high-fidelity simulations. Focused efforts toward developing hybrid models of the sort described in Section 5.4 may go a long way to easing the computational burden, and the result will be more convenient use of fundamental interface response calculations for slip zone size or slip displacement for overall component performance predictions.

This article has focused primarily on a discussion of experimentally-motived friction modeling tools, along with some examples of the types of information available from analysis using different friction and structural models. Further, it has emphasized the diversity of applications for which information about friction interface response is crucial. The intent is to provide researchers with an improved appreciation for the similarities in friction modeling approaches across disciplines, and to emphasize the obstacles to efficient and accurate friction simulation. Through continued interdisciplinary study and consideration of research across traditional disciplinary lines, progress in friction and dynamic simulations will continue, and many more options will be available to researchers in the future.

ACKNOWLEDGMENT

The author appreciates the help of a number of friends and colleagues in the preparation of this article. First, I thank the following people for their helpful conversations and their comments about various portions of the manuscript: M Begley, R Huston, C Krousgrill, F Sadeghi, and D Thompson. I also appreciate the encouragement of Editor-in-Chief A Leissa in my early writing efforts. I also thank two graduate students, H Govind and B Nawroth, for their help in obtaining copies of many of the references cited here, as well as the library staff of the University of Cincinnati for their help. Finally, the quality and completeness of this article was substantially enhanced through the efforts of the three anonymous reviewers and *AMR* Associate Editor R Ibrahim.

REFERENCES

[1] Coulomb CA (1785), Theorie des machines simples, *Memoirs de Mathematique et de Physique de l'Academie Royale*, 161–342.
[2] Kalker JJ (1990), *Three-Dimensional Elastic Bodies in Rolling Contact*. Dordrecht, Kluwer Academic Publishers, Boston.
[3] Ibrahim RA (1994), Friction-induced vibration, chatter, squeal, and chaos: Part I-Mechanics of contact and friction, *Appl. Mech. Rev.* **47**(7), 209–226.
[4] Ibrahim RA (1994), Friction-induced vibration, chatter, squeal, and chaos: Part II-Dynamics and modeling, *Appl. Mech. Rev.* **47**(7), 227–253.
[5] Ferri AA (1994), Friction damping and isolation systems, *ASME Special 50th Anniversary Design Issue* **117**, 196–206.
[6] Feeny B, Guran A, Hinrichs N, and Popp K (1998), A historical review on dry friction and stick-slip phenomena, *Appl. Mech. Rev.* **51**, 321–341.
[7] Back N, Burdekin M, and Cowley, A (1973), Review of the research on fixed and sliding joints, *Proc of 13th Int Machine Tool Design and Research Conf*, SA Tobias and F Koenigsberger (eds), MacMillan, London, 87–97.
[8] Beards CF (1983), The damping of structural vibration by controlled interfacial slip in joints, *ASME J. Vib., Acoust., Stress, Reliab. Des.* **105**, 369–373.
[9] Goodman LE (1959), A review of progress in analysis of interfacial slip damping, *Structural Damping*, JE Ruzicka (ed), ASME, 36–48.
[10] Ungar E (1973), The status of engineering knowledge concerning the damping of built-up structures, *J. Sound Vib.* **26**(1), 141–154.
[11] Sampson JB, Morgan F, Reed DW, and Muskat M (1943), Friction

behavior during the slip portion of the stick-slip process, *Journal of Applied Physics* **14**(12), 689–700.
[12] Rabinowicz E (1958), The intrinsic variables affecting the stick-slip process, *Proc of Physical Society of London*, **471**, 668–675.
[13] Bell R and Burdekin M (1969–1970), A study of the stick-slip motion of machine tool feed drives, *Proc. of Inst. of Mech. Eng.* **184**(1), 543–557.
[14] Hess DP and Soom A (1990), Friction at lubricated line contact operating at oscillating sliding velocities, *ASME J. Tribol.* **112**, 147–152.
[15] Hunt JB, Torbe I, and Spencer GC (1965), The phase-plane analysis of sliding motion, *Wear* **8**, 455–465.
[16] Pavelescu D and Tudor A (1987), The sliding friction coefficient-its evolution and usefulness, *Wear* **120**, 321–336.
[17] Lin Y-Q and Wang Y-H (1991), Stick-slip vibration in drill strings, *ASME J. Eng. Ind.* **113**, 38–43.
[18] Popp K (1992), Some model problems showing stick-slip motion and chaos, *Friction-Induced Vibration, Chatter, Squeal, and Chaos*, ASME, DE-Vol 49, 1–12.
[19] Bengisu MT and Akay A (1992), Stability of friction-induced vibrations in multi-degree-of-freedom systems, *Friction-Induced Vibration, Chatter, Squeal, and Chaos*, ASME, DE-Vol 49, 57–64.
[20] Bengisu MT and Akay A (1992), Interaction and stability of friction and vibrations, IL Singer and HM Pollock (eds), *Fundamentals of Friction: Macroscopic and Microscopic Processes*, Kluwer Academic Pub, 553–566.
[21] de Velde FV and Baets PD (1996), Mathematical approach of the influencing factors on stick-slip induced by decelerative motion, *Wear* **201**, 80–93.
[22] Dupont PE (1994), Avoiding stick-slip through pd control, *IEEE Trans. Autom. Control* **39**(5), 1094–1097.
[23] Lim YF and Chen K (1998), Dynamics of dry friction: A numerical investigation, *Phys. Rev. E* **58**(5), 5637–5642.
[24] Rice JR and Ruina AL (1983), Stability of steady frictional slipping, *ASME J. Appl. Mech.* **50**, 343–349.
[25] Gu J-C, Rice JR, Ruina AL, and Tse ST (1984), Slip motion and stability of a single degree of freedom elastic system with rate and state dependent friction, *J. Mech. Phys. Solids* **32**(3), 167–196.
[26] Tolstoi DM (1967), Significance of the normal degree of freedom and natural normal vibrations in contact friction, *Wear* **10**, 199–213.
[27] Greenwood JA and Williamson J (1966), Contact of nominally flat surfaces, *Proc. R. Soc. London, Ser. A* **A295**, 300–319.
[28] Nayak PR (1972), Contact vibrations, *J. Sound Vib.* **22**(3), 297–322.
[29] Gray GG, and Johnson KL (1972), The dynamic response of elastic bodies in rolling contact to random roughness of their surfaces, *J. Sound Vib.* **22**(3), 323–342.
[30] Godfrey D (1967), Vibration reduces metal-to-metal contact and causes an apparent reduction in friction, *ASLE Trans.* **10**, 183–192.
[31] Antoniou SS, Cameron A, and Gentle CR (1976), The friction-speed relation from stick-slip data, *Wear* **36**, 235–254.
[32] Sakamoto T (1987), Normal displacement and dynamic friction characteristics in a stick-slip process, *Tribol. Int.* **20**(1), 25–31.
[33] Bo LC and Pavelescu D (1982), The friction-speed relation and its influence on the critical velocity of stick-slip motion, *Wear* **82**, 277–289.
[34] D'Souza AF and Dweib AH (1990), Self-excited vibrations induced by dry friction, Part 1: Experimental study, *J. Sound Vib.* **137**(2), 163–175.
[35] D'Souza AF and Dweib AH (1990), Self-excited vibrations induced by dry friction, Part 2: Stability and limit-cycle analysis, *J. Sound Vib.* **137**(2), 177–190.
[36] Soom A and Kim C (1983), Interaction between dynamic normal and frictional forces during unlubricated sliding, *J. Lubr. Technol.* **105**, 221–229.
[37] Soom A and Kim C (1983), Roughness-induced dynamic loading at dry and boundary lubricated sliding contacts, *J. Lubr. Technol.* **105**, 514–517.
[38] Anand A and Soom A (1984), Roughness-induced transient loading at a sliding contact during start-up, *ASME J. Tribol.* **106**, 49–53.
[39] Soom A and Chen JW (1986), Simulation of random surface roughness-induced contact vibrations at hertzian contacts during steady sliding, *ASME J. Tribol.* **108**, 123–127.
[40] Polycarpou AA and Soom A (1995), Boundary and mixed friction in the presence of dynamic normal loads: Part I-System model, *ASME J. Tribol.* **117**, 255–260.
[41] Polycarpou AA and Soom A (1995), Boundary and mixed friction in the presence of dynamic normal loads: Part II-Friction transients, *ASME J. Tribol.* **117**, 261–266.
[42] Polycarpou AA and Soom A (1995), Two-dimensional models of boundary and mixed friction at a line contact, *ASME J. Tribol.* **117**, 178–184.
[43] Rice SL, Moslehy FA, and Elmi S (1993), Tribodynamic modeling, *19th Leeds-Lyon Symp-Thin Films in Tribology*, D Dowson *et al* (eds), Elsevier, New York, 641–648.
[44] Streator JL and Bogy DB (1992), Accounting for transducer dynamics in the measurement of friction, *ASME J. Tribol.* **114**, 86–94.
[45] Oden JT and Martins JAC (1985), Models and computational methods for dynamic friction phenomena, *Comput. Methods Appl. Mech. Eng.* **52**, 527–634.
[46] Hess DP and Soom A (1992), Normal and angular motions at rough planar contacts during sliding with friction, *ASME J. Tribol.* **114**, 567–578.
[47] Jarvis RP and Mills B (1963–64), Vibrations induced by dry friction, *Proc. of Inst. of Mech. Eng.* **178**(32), 847–866.
[48] Earles SWE and Lee CK (1976), Instabilities arising from the frictional interaction of a pin-disk system resulting in noise generation, *ASME J. Eng. Ind.* **98**(1), 81–86.
[49] Earles SWE and Soar GB (1971), Squeal noise in disk brakes, *Proc of Inst of Mech Eng, Vibration and Noise in Motor Vehicles*, 61–69.
[50] Earles SWE and Badi MNM (1984), Oscillatory instabilities generated in a double-pin and disc undamped system: A mechanism of disc-brake squeal, *Proc. Inst. Mech. Eng., Part C: Mech. Eng. Sci.* **198C**, 43–50.
[51] Swayze JL and Akay A (1992), Effects of systems dynamics on friction-induced oscillations, *Friction-Induced Vibration, Chatter, Squeal, and Chaos*, ASME, DE-Vol 49, 49–55.
[52] Martins JAC, Oden JT, and Simoes FMF (1990), A study of static and kinetic friction, *Int. J. Eng. Sci.* **28**, 29–92.
[53] Tworzydlo WW, Becker EB, and Oden JT (1994), Numerical modeling of friction-induced vibrations and dynamic instabilities, *Appl. Mech. Rev.* **47**(7), 255–274.
[54] Tworzydlo WW and Becker E (1991), Influence of forced vibrations on the static coefficient of friction-numerical analysis, *Wear* **43**, 175–196.
[55] Madakson PB (1983), The frictional behavior of materials, *Wear* **87**, 191–206.
[56] Froslie LE, Milek T, and Smith EW (1973), Automatic transmission friction elements, *Design Practices-Passenger Car Automatic Transmissions*, Soc of Autom Eng, 535–552.
[57] Anderson JR, and Ferri AA (1990), Behavior of a single-degree-of-freedom system with a generalized friction law, *J. Sound Vib.* **140**(2), 287–304.
[58] Menq C-H, Griffin JH, and Bielak J (1986), The influence of microslip on vibratory response, part ii: A comparison with experimental results, *J. Sound Vib.* **107**(2), 295–307.
[59] Dupont PE, and Bapna D (1994), Stability of sliding frictional surfaces with varying normal forces, *ASME J. Vibr. Acoust.* **116**, 237–242.
[60] Berger EJ, Krousgrill CM, and Sadeghi F (1997), Stability of sliding in a system excited by a rough moving surface, *ASME J. Tribol.* **119**(4), 672–680.
[61] den Hartog JP (1931), Forced vibrations with combined coulomb and viscous damping, *ASME J. Appl. Mech.* **APM-53-9**, 107–115.
[62] Blok H (1940), Fundamental aspects of boundary friction, *J. Soc. Autom. Eng.* **46**, 275–279.
[63] Derjaguin BV, Push VE, and Tolstoi DM (1957), A theory of stick-slip sliding in solids, *Proc Conf on Lubrication and Wear*, 257–268.
[64] Brockley CA, Cameron R, and Potter AF (1967), Friction-induced vibration, *J. Lubr. Technol.* **89**, 101–108.
[65] Brockley CA and Ko PL (1970), Quasi-harmonic friction-induced vibration, *J. Lubr. Technol.* **92**, 550–556.
[66] Pfeiffer F and Glocker C (1996), *Multibody Dynamics with Unilateral Contacts*, Wiley Series in Nonlinear Science, John Wiley and Sons, New York.
[67] Guran A, Pfeiffer F, and Popp K (1996), *Dynamics with Friction-Modeling, Analysis, and Experiment, Part I*, World Sc, Singapore.
[68] Popp K (1995), Dynamical behaviour of a friction oscillator with simultaneous self and external excitation, *Sadhana: Proc., Indian Acad. Sci.* **20**(2–4), 627–654.
[69] Budd C and Dux F (1994), Chattering and related behavior in impact oscillators, *Philos. Trans. R. Soc. London, Ser. A* **A347**(1683), 365–389.
[70] Foale S and Bishop SR (1992), Dynamical complexities of forced impacting systems, *Philos. Trans. R. Soc. London, Ser. A* **A338**(1651), 547–556.
[71] Bishop SR (1994), Impact oscillators, *Philos. Trans. R. Soc. London, Ser. A* **A347**(1683), 347–351.
[72] Hinrichs N, Oestreich M, and Popp K (1997), Dynamics of oscillators

with impact and friction, *Chaos, Solitons, Fractals* **8**(4), 535–558.
[73] Hinrichs N, Oestreich M, and Popp K (1998), On the modeling of friction oscillators, *J. Sound Vib.* **216**(3), 435–459.
[74] Popp K (1998), Non-smooth mechanical systems-an overview, *Forschung im Ingenieurwesen* **64**, 223–239.
[75] Haessig DA and Friedland B (1991), On the modeling and simulation of friction, *ASME J. Dyn. Syst., Meas., Control* **113**, 354–362.
[76] Armstrong-Hélouvry B (1991), *Control of Machines with Friction*, Kluwer Academic Publ, Boston.
[77] Armstrong-Hélouvry B (1993), Stick slip and control in low-speed motion, *IEEE Trans. Autom. Control* **38**(10), 1483–1496.
[78] Armstrong-Hélouvry B, Dupont P, and Canudas de Wit C (1994), Friction in servo machines: Analysis and control methods, *Appl. Mech. Rev.* **47**(7), 275–305.
[79] Armstrong-Hélouvry B, Dupont P, and Canudas de Wit C (1994), A survey of models, analysis tools and compensation methods for control of machines with friction, *Automatica* **30**(7), 1083–1138.
[80] Canudas de Wit C, Olsson H, Åström KJ, and Lischinsky P (1995), A new model for control of systems with friction, *IEEE Trans. Autom. Control* **40**(3), 419–425.
[81] Canudas de Wit C and Tsiotras P (1999), Dynamic tire friction model for vehicle traction control, *Proc of 38th Conf on Decision and Control*, 3746–3751.
[82] Taylor JH (1994), A modeling language for hybrid systems, *Proc of the Joint Symp of Computer-Aided Control System Design*, 337–344.
[83] Taylor JH (1995), Rigorous handling of state events in matlab, *Proc of IEEE Conf on Control Applications*, 156–161.
[84] Taylor JH and Kebede D (1995), Modeling and simulation of hybrid system, *Proc of IEEE Conf on Decision and Control*, 2685–2687.
[85] Taylor JH (1999), *Tools for Modeling and Simulation of Hybrid Systems-A Tutorial Guide*, Univ of New Brunswick, available at http://www.unb.edu.ca/jtaylor/HS_software.html.
[86] Hou L and Michel AN (1998), Stability theory for hybrid dynamical systems, *IEEE Trans. Autom. Control* **43**(4), 461–474.
[87] Mindlin RD (1949), Compliance of elastic bodies in contact, *ASME J. Appl. Mech.* **16**, 259–268.
[88] Oden JT and Pires EB (1983), Nonlocal and nonlinear friction laws and variational principles for contact problems in elasticity, *ASME J. Appl. Mech.* **50**, 67–76.
[89] Oden JT and Pires EB (1983), Numerical analysis of certain contact problems with non-classical friction laws, *Comput. Struct.* **16**, 471–478.
[90] Oden JT and Pires EB (1984), Algorithms and numerical results for finite element approximations of contact problems with non-classical friction laws, *Comput. Struct.* **19**(1-2), 137–147.
[91] Greenwood JA (1997), Adhesion of elastic solids, *Proc. R. Soc. London, Ser. A* **A453**, 1277–1297.
[92] Adams GG (1995), Self-excited oscillations of two elastic half-spaces sliding with a constant coefficient of friction, *ASME J. Appl. Mech.* **62**, 867–872.
[93] Adams GG (1999), Dynamic motion of two elastic half-spaces in relative sliding without slipping, *ASME J. Tribol.* **121**(3), 455–461.
[94] Adams GG (1998), Steady sliding of two elastic half-spaces with friction reduction due to interface stick-slip, *ASME J. Appl. Mech.* **65**, 470–475.
[95] Ruiz C, Boddington PHB, and Chen KC (1984), An investigation of fatigue and fretting in a dovetail joint, *Exp. Mech.* **24**, 208–217.
[96] Ruiz C and Chen KC (1986), Life assessment of dovetail joints between blades and disks in aero-engines, *Proc of Int Conf on Fatigue: Fatigue of Engineering Materials and Structures*, Inst of Mech Eng, 187–194.
[97] Nix KJ and Lindley TC (1988), The influence of relative slip range and contact material on the fretting fatigue properties of 3.5nicrmov rotor steel, *Wear* **125**, 147–162.
[98] Kuno M, Waterhouse RB, Nowell D, and Hills DA (1989), Initiation and growth of fretting fatigue cracks in the partial slip regime, *Fatigue Fract. Eng. Mater. Struct.* **12**(5), 387–398.
[99] Nowell D and Hills DA (1990), Crack initiation criteria in fretting contact, *Wear* **136**, 329–343.
[100] Waterhouse RB (1992), Fretting fatigue, *Int. Mater. Rev.* **37**(2), 77–97.
[101] Hills DA, Nowell D, and O'Connor JJ (1988), On the mechanics of fretting fatigue, *Wear* **125**, 129–146.
[102] Bramhall R (1973), Studies in Fretting Fatigue, PhD thesis, Oxford Univ.
[103] Hills DA (1994), Mechanics of fretting fatigue, *Wear* **175**, 107–113.
[104] Cattaneo C (1938), Sul contatto di due corpi elastici: Distribuzione locale degli sforzi, *Rendiconti dell'Accademia Nazionale dei Lincei* **27**, 342–348, 434–436, 474–478.
[105] Nowell D and Hills DA (1987), Mechanics of fretting fatigue tests, *Int. J. Mech. Sci.* **29**(5), 355–365.
[106] Szolwinski MP and Farris TN (1996), Mechanics of fretting fatigue crack formation, *Wear* **198**, 93–107.
[107] Söderberg S, Bryggman U, and McCullough T (1986), Frequency effects in fretting wear, *Wear* **110**, 19–34.
[108] Bryggman U and Söderberg S (1986), Contact conditions in fretting, *Wear* **110**, 1–17.
[109] Bryggman U and Söderberg S (1988), Contact conditions and surface degradation mechanisms in low amplitude fretting, *Wear* **125**, 39–52.
[110] Vingsbo O and Söderberg S (1988), On fretting maps, *Wear* **126**, 131–147.
[111] Schouterden K, Blanpain B, Çelis JP, and Vingsbo O (1995), Fretting of titanium nitride and diamond-like carbon coatings at high frequencies and low amplitude, *Wear* **181–183**, 86–93.
[112] Rehbein P and Wallaschek J (1998), Friction and wear behavior of polymer/steel and alumina/alumina under high-frequency fretting conditions, *Wear* **216**, 97–105.
[113] Caughey TK (1960), Sinusoidal excitation of a system with bilinear hysteresis, *ASME J. Appl. Mech.* **27**, 640–643.
[114] Caughey TK (1960), Random excitation of a system with bilinear hysteresis, *ASME J. Appl. Mech.* **27**, 649–652.
[115] Iwan WD (1965), The steady-state response of a two-degree-of-freedom bilinear hysteretic system, *ASME J. Appl. Mech.* **32**, 151–156.
[116] Iwan WD (1965), The steady-state response of a double bilinear hysteretic model, *ASME J. Appl. Mech.* **32**, 921–925.
[117] Iwan WD (1965), The dynamic response of the one-degree-of-freedom bilinear hysteretic system, *Proc of 3rd World Congress on Earthquake Engineering*, **2**, 783–796.
[118] Iwan WD (1966), A distributed-element model for hysteresis and its steady-state dynamic response, *ASME J. Appl. Mech.* **33**, 893–900.
[119] Iwan WD (1967), On a class of models for the yielding behavior of continuous and composite systems, *ASME J. Appl. Mech.* **34**, 612–617.
[120] Masing G (1923–1924), Zur hevnschen theorie der verfestigung der metalle durch verborgene elastische spannungen, (in German), *Wiss. Veröffent. aus dem Siemens Konzern* **3**, 135–141.
[121] Byerlee JD and Brace WF (1968), Stick-slip, stable sliding, and earthquakes-effect of rock type, pressure, strain rate and stiffness, *J. Geophys. Res.* **73**, 6031–6037.
[122] Byerlee JD (1970), The mechanics of stick-slip, *Tectonophysics* **9**, 475–486.
[123] Dieterich JH (1978), Time-dependent friction and the mechanisms of stick-slip, *Pure Appl. Geophys.* **116**, 790–806.
[124] Dieterich JH (1979), Modeling of rock friction 1: Experimental results and constitutive equations, *J. Geophys. Res.* **84**, 2161–2168.
[125] Dieterich JH (1979), Modeling of rock friction 2: Simulation of preseismic slip, *J. Geophys. Res.* **84**, 2169–2175.
[126] Ruina AL (1983), Slip instability and state variable friction laws, *J. Geophys. Res.* **88**, 10359–10370.
[127] Ruina AL (1986), Unsteady motions between sliding surfaces, *Wear* **113**, 83–86.
[128] Linker M and Dieterich JH (1992), Effects of variable normal stress on rock friction: Observations and constitutive equations, *J. Geophys. Res., [Solid Earth]* **97**, 4923–4940.
[129] Rice JR (1993), Spatio-temporal complexity of slip on a fault, *J. Geophys. Res., [Solid Earth]* **98**(B6), 9885–9907.
[130] Ben-Zion Y and Rice JR (1997), Dynamic simulations of slip on a smooth fault in an elastic solid, *J. Geophys. Res., [Solid Earth]* **102**(B8), 17771–17784.
[131] Persson BNJ (2000), *Sliding Friction: Physical Principles and Applications, Second Edition*, Springer-Verlag.
[132] Mindlin RD and Dereciewicz H (1953), Elastic spheres in contact under varying oblique forces, *ASME J. Appl. Mech.* **20**, 327–344.
[133] Goodman LE and Brown CB (1962), Energy dissipation in contact friction: Constant normal and cyclic tangential loading, *ASME J. Appl. Mech.* **29**, 17–22.
[134] Johnson KL (1961), Energy dissipation at spherical surfaces in contact transmitting oscillating forces, *J. Mech. Eng. Sci.* **3**(4), 362–368.
[135] Shaw SW (1986), On the dynamic response of a system with dry friction, *J. Sound Vib.* **108**(2), 305–325.
[136] Beards CF and Woohat A (1985), The control of frame vibrations by friction damping in joints, *ASME J. Vib., Acoust., Stress, Reliab. Des.* **106**, 26–32.
[137] Ferri AA and Heck BS (1995), Vibration analysis of dry friction damped turbine blades using singular perturbation theory, *Proc of ASME Int Mech Eng Congress and Exposition, AMD-Vol 192*, ASME, New York, 47–56.

[138] Griffin JH (1980), Friction damping of resonant stresses in gas turbine engine airfoils, *ASME J. Eng. Power* **102**, 329–333.
[139] Pierre C, Ferri AA, and Dowell EH (1985), Multi-harmonic analysis of dry friction damped systems using an incremental harmonic balance method, *ASME J. Appl. Mech.* **52**, 958–964.
[140] Wang JH and Chen WK (1993), Investigation of the vibration of a blade with friction damper by hbm, *ASME J. Eng. Gas Turbines Power* **115**, 294–299.
[141] Dowell EH (1986), Damping in beams and plates due to slipping at the support boundaries, *J. Sound Vib.* **105**(2), 243–253.
[142] Dowell EH and Schwartz HB (1983), Forced response of a cantilever beam with dry friction damper attached, Part I: Theory, *J. Sound Vib.* **91**(2), 255–267.
[143] Dowell EH and Schwartz HB (1983), Forced response of a cantilever beam with dry friction damper attached, Part II: Experiment, *J. Sound Vib.* **91**(2), 269–291.
[144] Ferri AA and Bindemann AC (1992), Damping and vibration of beams with various types of frictional support conditions, *ASME J. Vibr. Acoust.* **114**, 289–296.
[145] Makris N and Constantinou MC (1991), Analysis of motion resisted by friction, I. constant coulomb and linear/coulomb friction, *Mech. Struct. Mach.* **19**(4), 477–500.
[146] Makris N and Constantinou MC (1991), Analysis of motion resisted by friction, II. Velocity-dependent friction, *Mech. Struct. Mach.* **19**(4), 501–526.
[147] Gaul L and Nitsche R (2001), The role of friction in mechanical joints, *Appl. Mech. Rev.* **54**(2), 93–105.
[148] Gaul L and Nitsche R (2000), Friction control for vibration suppression, *Mech. Syst. Signal Process.* **14**(2), 139–150.
[149] Gaul L and Lenz J (1997), Nonlinear dynamics of structures assembled by bolted joints, *Acta Mech.* **125**(1–4), 169–181.
[150] Lenz J and Gaul L (1995), The influence of microslip on the dynamic behavior of bolted joints, *Proc of 13th Int Modal Analysis Conf*, Nashville, TN, 248–254.
[151] Johnson KL (1985), *Contact Mechanics*, Cambridge Univ Press, Great Britain.
[152] Sinha A and Griffin JH (1984), Effects of static friction on the forced response of frictionally damped turbine blades, *ASME J. Eng. Gas Turbines Power* **106**, 65–69.
[153] Griffin JH and Sinha A (1985), The interaction between mistuning and friction in the forced response of bladed disk assemblies, *ASME J. Eng. Gas Turbines Power* **107**, 205–211.
[154] Menq C-H and Griffin JH (1985), A comparison of transient and steady state finite element analyses of the forced response of a frictionally damped beam, *ASME J. Vib., Acoust., Stress, Reliab. Des.* **107**, 19–25.
[155] Menq C-H, Griffin JH, and Bielak J (1986), The influence of a variable normal load on the forced vibration of a frictionally damped structure, *ASME J. Eng. Gas Turbines Power* **108**, 300–305.
[156] Menq C-H, Bielak J, and Griffin JH (1986), The influence of microslip on vibratory response, part i: A new microslip model, *J. Sound Vib.* **107**(2), 279–293.
[157] Cameron TM, Griffin JH, Kielb RE, and Hoosac TM (1987), An integrated approach for friction damper design, *ASME Design Booklet, The Role of Damping in Vibration and Noise Control*, ASME DE-Vol 5, 205–211.
[158] Kielb RE, Griffin JH, and Menq C-H (1988), Evaluation of a turbine blade damper using an integral approach, *AIAA/ASME/ASCE/AHS* 29th *Structures, Structural Dynamics and Materials Conf (AIAA 88-2400)*, 1495–1500.
[159] Muszynska A and Jones DIG (1983), A parametric study of dynamic response of a discrete model of turbomachinery bladed disk, *ASME J. Vib., Acoust., Stress, Reliab. Des.* **105**, 434–443.
[160] Wang JH and Shieh WL (1991), The influence of variable friction coefficient on the dynamic behavior of a blade with friction damper, *J. Sound Vib.* **149**, 137–145.
[161] Sanliturk KY, Imregun M, and Ewins DJ (1997), Harmonic balance vibration analysis of turbine blades with friction dampers, *ASME J. Vibr. Acoust.* **119**, 96–103.
[162] Sanliturk KY and Ewins DJ (1996), Modeling two-dimensional friction contact and its application using harmonic balance method, *J. Sound Vib.* **193**, 511–523.
[163] Whitehouse DJ and Archard JF (1970), The properties of random surfaces of significance in their contact, *Proc. R. Soc. London, Ser. A* **A316**(1524), 97–121.
[164] Whitehouse DJ and Phillips MJ (1978), Discrete properties of random surfaces, *Philos. Trans. R. Soc. London, Ser. A* **A290**(1369), 267–298.
[165] Whitehouse DJ and Phillips MJ (1982), Two-dimensional discrete properties of random surfaces, *Philos. Trans. R. Soc. London, Ser. A* **A305**(1490), 441–468.
[166] Kilburn RF (1974), Friction viewed as a random process, *J. Lubr. Technol.* **96**, 291–299.
[167] Qiao SL and Ibrahim RA (1999), Stochastic dynamics of systems with friction-induced vibration, *J. Sound Vib.* **223**(1), 115–140.
[168] Ibrahim RA, Zielke SA, and Popp K (1999), Characterization of interfacial forces in metal-to-metal contact under harmonic excitation, *J. Sound Vib.* **220**(2), 365–377.
[169] Ibrahim RA, Madhavan S, Qiao SL, and Chang WK (2000), Experimental investigation of friction-induced noise in disc brake systems, *Int. J. Veh. Des.* **23**(3/4), 218–240.
[170] Mottershead JE, Ouyang H, Cartmell MP, and Friswell MI (1997), Parametric resonances in an annular disc, with a rotating system of distributed mass and elasticity; and the effects of friction and damping, *Proc. R. Soc. London, Ser. A* **A453**(1956), 1–19.
[171] Ouyang H, Mottershead JE, Cartmell MP, and Friswell MI (1998), Friction-induced parametric resonances in discs: Effect of a negative friction-velocity relationship, *J. Sound Vib.* **209**(2), 251–264.
[172] Ouyang H, Mottershead JE, Cartmell MP, and Brookfield DJ (1999), Friction-induced vibration of an elastic slider on a vibrating disc, *Int. J. Mech. Sci.* **41**, 325–336.
[173] Ouyang H, Mottershead JE, Brookfield DJ, and James S (2000), A methodology for the determination of dynamic instabilities in a car disc brake, *Int. J. Veh. Des.* **23**(3/4), 241–262.
[174] Lee D and Waas AM (1997), Stability analysis of a rotating multilayer annular plate with a stationary frictional follower load, *Int. J. Mech. Sci.* **39(10)**, 1117–1138.
[175] Brooks PC, Crolla DA, and Lang AM (1992), Sensitivity analysis of disc brake squeal, *Proc of Int Symp on Advanced Vehicle Control*, (*AVEC'92*), Yokohama, Japan, Paper No. 923005, 28–36.
[176] Brooks PC, Crolla DA, Lang AM, and Schafer DR (1993), Eigenvalue sensitivity analysis applied to disc brake squeal, *Braking of Road Vehicles*, Paper C444/004/93, Inst of Mech Eng, 135–143.
[177] Lang AM, Schafer DR, Newcomb TP, and Brooks PC (1993), Brake squeal-the influence of rotor geometry, *Braking of Road Vehicles*, Paper C444/016/93, Inst of Mech Eng, 161–171.
[178] Carpick RW and Salmeron M (1997), Scratching the surface: Fundamental investigations of tribology with atomic force microscopy, *Chem. Rev.* **97**, 1163–1194.
[179] Bhushan B, Isrealachvili JN, and Landman U (1995), Nanotribology: Friction, wear and lubrication at the atomic scale, *Nature (London)* **374**, 607–616.
[180] Bhushan B (1999), Nanoscale tribophysics and tribomechanics, *Wear* **225–229**, 465–492.
[181] Johnson KL, Kendall K, and Roberts AD (1971), Surface energy and the contact of elastic solids, *Proc. R. Soc. London, Ser. A* **A324**, 301–313.
[182] Tabor D (1977), Surface forces and surface interactions, *J. Colloid Interface Sci.* **58**, 2–13.
[183] Johnson KL and Greenwood JA (1997), An adhesion map for the contact of elastic spheres, *J. Colloid Interface Sci.* **192**, 326–333.
[184] Israelachvili JN (1992), Adhesion forces between surfaces in liquids and condensable vapours, *Surf. Sci. Rep.* **14**(3), 109–159.
[185] Yoshizawa H, McGuiggan P, and Israelachvili JN (1993), Identification of a second dynamic state during stick-slip motion, *Science* **259**, 1305–1308.
[186] McClelland GM (1989), *Adhesion and Friction*, Springer Series in Surface Science, Springer, New York.
[187] Yoshizawa H, Chen Y-L, and Israelachvili JN (1993), Recent advances in molecular level understanding of adhesion, friction and lubrication, *Wear* **168**, 161–166.
[188] Yoshizawa H and Israelachvili JN (1993), Fundamental mechanisms of interfacial friction; stick-slip friction of spherical and chain molecules, *J. Phys. Chem.* **97**, 11300–11313.
[189] Mate CM, McClelland GM, Erlandsson R, and Chiang S (1987), Atomic-scale friction of a tungsten tip on a graphite surface, *Phys. Rev. Lett.* **59**(17), 1942–1945.
[190] Nayfeh AH (1981), *Introduction to Perturbation Techniques*, John Wiley and Sons, New York.
[191] Karnopp D (1985), Computer simulation of stick-slip friction in mechanical dynamic systems, *ASME J. Dyn. Syst., Meas., Control* **107**(1), 100–103.
[192] Pratt TK and Williams R (1981), Non-linear analysis of stick-slip motion, *J. Sound Vib.* **74**, 531–542.
[193] Hutchinson JW and Jensen HM (1990), Models of fiber debonding and pullout in brittle composites with friction, *Mech. Mater.* **9**(2), 139–163.
[194] Sextro W (1999), Forced vibration of elastic structures with friction

contacts, *Proc of ASME Design Eng Tech Conf*, DETC/VIB-8180, ASME, New York.

[195] Berger EJ, Begley MR, and Mahajani M (2000), Structural dynamic effects on interface response—Formulation and simulation under partial slipping conditions, *J. Appl. Mech.* **67**, 785–792.

[196] Masri SF, Chassiakos AG, and Caughey TK (1993), Identification of nonlinear dynamic systems using neural networks, *J. Appl. Mech.* **60**(2), 123–133.